Sup'Biotech *projects*

Volume 3 • January 2019

Applied Transversal Projects – « Fil Rouge »

2018-2019 edition

- Endocrine disruptors
- Antifungal compounds
- Antitumoral activity of Curcumin
- Characterization of peptones
- Hydroponic culture
- Synthetic biology
- Epigenetics and regeneration
- 3D imaging
- Pharmacogenetics
- Analysis of wine composition

EDITORIAL

Project work is the foundation of teaching biotech engineering at Sup'Biotech. Throughout their curriculum, students are continually working on interdisciplinary projects in a broad range of research and development areas, spanning R&D, Production and Communication.

The "Fil Rouge" Project is dedicated to the students having chosen the R&D major in 4th year of their academic track. During 5 full weeks, placed between January and December, students are given a subject to develop, from beginning to end, with as much autonomy as possible.

At first, students have to research the subject, using the bibliographical tools that they were taught to use, and prepare specific aims, compatible with the constraints of time, finance and laboratory equipment at their disposal. The students then have to plan experiments accordingly, including the ordering of the material, and the setting up of the protocols. They then have to perform the experiments, either in the Sup'Biotech laboratories or in host laboratories, depending on their subject.

Of note, this year, four projects were tutored by mentors outside the school. Organotechnie, a company specialized in protein hydrolysates, Aeromate, an urban agriculture venture, and the Institut Jacques Monod. One of the projects was also coordinated by the iGEM coordination team of the Institut Pasteur in Paris, and another was tutored by the coordinator of the Sup'Biotech 3D Imaging platform, a new and very innovative laboratory equipment purchased by Sup'Biotech.

Every year, the students gather all the results from their project and write an article under the supervision of their tutor. This article is then peer-reviewed by the other teams before being published in the Sup'Biotech Projects Journal.

Frank Yates, PhD
Estelle Mogensen, PhD

Coordinators of the « Fil Rouge" Program

PROJECT TUTORS

Session 2018-2019

Agnès Saint-Pol

Elise Delage

Louise Douillet

Rafika Jarray

Chloe Lezin

Estelle Mogensen

Jacqueline Bert

Jean-Yves Trosset

Frank Yates

Anabelle Planques

Alexandre Ismail

Sarah Rakotosaimbola

Nicolas Rebergue

All articles published in Sup'Biotech Projects Journal are written by students, under the supervision of tutors. Articles are peer-reviewed by students before publication.

CONTENTS

Tests assessing the efficacy of natural antifungal compounds and their efficient dosage with *Aspergillus Oryzae*

Camille Beaulier*†, Constance Dollet, Victoria Launay†, Justine Marie dit Calais†
Sup'Biotech, Villejuif, France
*Corresponding author: Camille.beaulier@gmail.com
† These authors equally contributed to this work

Abstract - **Aspergillosis is the name that gathers all the different diseases caused by *Aspergillus fumigatus*. Nowadays, it can be treated with drugs, which have a high toxicity for the human body.**
Essential oils are known to have active compounds that can have antifungal properties. To investigate their efficacy, *Aspergillus oryzae,* which belongs to the same family as *A. fumigatus,* has been used.
Different methods using Sabouraud medium were tested. Drugs were added either in a liquid medium, in a solid medium, or on diffusion discs which were disposed on the solid medium. In a second phase, the fungicide or fungistatic effect of essential oils was investigated with a subculturing on solid Sabouraud medium. To go further, different times of exposition have also been tested.
The test with the drugs in the liquid medium was the one used for the identification of the antifungic essential oils. It appears that only two have a real efficacy: *Melaleuca alternifolia* and *Thymus vulgaris linaloliferum*. At the highest concentration tested, a reduction of the development is observed but it does not inhibit the fungal growth.

Index Terms - *Aspergillus oryzae*, essential oils, fungicide, fungistatic

INTRODUCTION

Fungi can be responsible for different human diseases like aspergillosis. This disease is caused by *A. fumigatus'* conidia that reach the lung alveoli after being spread in the atmosphere. *A. fumigatus* has become the most important airborne pathogen in developed countries, causing a significant increase in fatal pulmonary invasive aspergillosis especially in immunodepressed patients [1]. Today, the only treatments available are chemicals. Among them, amphotericin B [2] and fluconazole [3] have proven their efficacy against fungi from the *Aspergillus* family (*A. fumigatus* in particular). However, they induce side effects and a high nephrotoxicity [4] and hepatotoxicity [5]. That is why more natural compounds are being studied like essential oils, produced from plants, to fight against fungi. According to the literature, three different methods were used to investigate the efficiency of essential oils and to determine the best methods. Antifungigram has been described in the past decade as a screening of essential oils. This method is known to determine antimicrobial activity of compounds. The liquid medium method consists of testing different concentrations of antifungal substances which are incubated with fungal strain in broth medium. For the solid medium method, the antifungal substances are trapped in it [6]. Five different essential oils have been tested: *Thymus vulgaris linaloliferum, Melaleuca alternifolia, Citrus limon, Citrus reticula*ta and *Citrus paradisi* [6], [7], [8]. Such essential oils have already been studied in the literature as antifungal compounds against a large scale of fungi including *Aspergillus* family. They have been considered as efficient by having a large inhibitory rate (*Melaleuca alternifolia* oil MIC = 0-12 on *A. fumigatus*). In a second phase, the type of antifungal effects has been investigated. It can be either a fungicide agent, which kills fungi or a fungistatic agent, which unables the growth [9]. Amphotericin B has been used as the fungicide control and fluconazole has been used as the fungistatic control. For safety reasons, *A. oryzae* was used. This is a fungus from the same family as the pathological one (*A. fumigatus*) but without risk for humans as it is used for food processing. The aim of this project was to develop a test to assess the efficacy of antifungal compounds on *A. oryzae*, and to find an accurate dosage for them.

MATERIALS AND METHODS

Conidia material
Conidia are asexually produced spores. *A. oryzae* conidia came from the Laboratoire de Recherche Partenariale en Ingénierie Agroalimentaire (LRPIA). The sample has been stored at 4 °C for future experimentations. Conidia have been counted thanks to Malassez cell. For these experiments, we used a concentration of 10^4 conidia/mL.

Drug materials
Thymus vulgaris linaloliferum, Citrus limon, Citrus reticulata Citrus paradisi and *Melaleuca alternifolia* are essential oils known to have antifungal activities and have been tested at different concentrations (from $0.1 \cdot 10^{-3}$ to 50 mg/mL). To

solubilize the oils in the media, they were previously diluted with 0.05 % of Tween 20.
Positive controls were performed with amphotericin B at 240 µg/mL and fluconazole at 200 µg/mL, which are respectively fongicide and fongistatic agents.

Antifungigram
Conidia were inoculated in 55 mm diameter petri dishes containing solid Sabouraud medium (10 g/L peptone, 20 g/L glucose, 10 g/L agar). 20µL of different concentrations of drugs were poured on cellulose disks. Four cellulose disks were then put in each petri dish. Finally, one petri dish contained four caps of the same drug, with four different concentrations (for each essential oil, the concentrations used were 0.1, 0.2, 0.5 and 1 µg/mL as used in the literature [7]).

Conidia survival using drugs in solid medium
First, *A.oryzae* was inoculated on solid Sabouraud medium and disks of cellulose were added in the petri dishes and incubated at 30°C during three days.
In a second phase, solid Sabouraud medium was kept in its liquid form in Falcon® tubes and put in a water bath at 55° to avoid fusion. The different drugs were then added in the medium, homogenized by manual shaking and immediately poured into petri dishes.
To inoculate *A. oryzae*, cellulose caps previously prepared were used as fungi grew on them. They were taken from gelose in sterile conditions and one cap was put on each petri dish.
Petri dishes were incubated at 30 °C for 24h.

Conidia survival using drugs in liquid medium
In a 24-wells plate, solutions have been performed in a 1 mL final volume containing 800 µL of Sabouraud liquid medium (10 g/L peptone and 20 g/L glucose), 100 µL of drugs and 100 µL of *A. oryzae* conidia (10^4 conidia/mL final concentration). The plate has been incubated at 30 °C during 24 and 48 hours. Results were obtained thanks to ZOE microscope (ZOE™ Fluorescent Cell imager, BIO-RAD). Drug concentrations used are summarized in Appendix 1. Concentrations are from $0.1 \cdot 10^{-3}$ mg/mL to 50 mg/mL for *Citrus limon*, *Citrus reticulata* and *Citrus paradisi* and from 1 mg/mL to 50 mg/mL for *Thymus vulgaris linaloliferum and Melaleuca alternifolia*.

Subculturing
After performing the experiment "*Conidia survival using drugs in liquid medium*", the contents of each well were collected and put in 1.5 mL Eppendorf tubes. To check if any conidia stayed in the bottom of the wells, a verification has been performed with ZOE™ microscope.
Collected solution was vortexed and 100µL were inoculated in petri dishes containing solid Sabouraud medium and incubated at 30 °C for 24 to 72 hours.

RESULTS

Identification of the appropriate testing method
The antifungigram technique is considered as inefficient as fungi grew with amphotericin B (Figure 1) or fluconazole soaked caps.

The tests on solid medium containing drugs showed a difference between the different oils. Nevertheless, the control with amphotericin B showed a fungi growth (Figure 2) while it is a fungicide substance. This method has not been kept for the following experiments because the controls are not relevant.

In the liquid medium, in the controls with fungicide and fungistatic substances showed no growth of fungi as expected. Thus, the presence of fungi can be estimated. It has been decided that the experiment method "*Conidia survival using drugs in liquid medium"* will be kept for the following experiments.

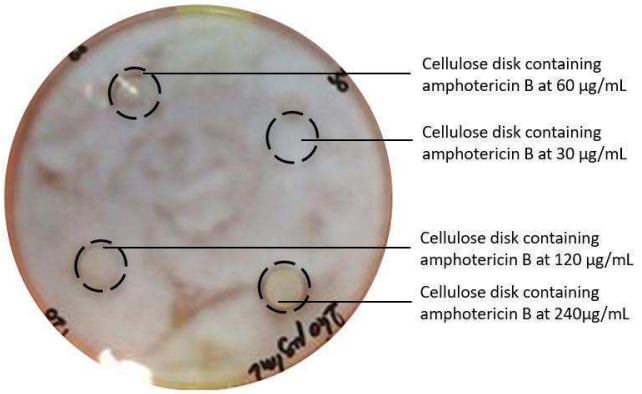

Figure 1: *A. oryzae* growth in presence of diffusion disks containing amphotericin B at different concentrations and incubated for 24h
There is no "inhibition zone" around the disks containing antifungal product

Figure 2: *A. oryzae* growth on a solid Sabouraud medium containing Amphotericin B (240µg/mL) after 24h of incubation
Growth has 2cm diameter around the cellulose disks ued for inoculation

Efficacy of oils

Well plates were observed at different times (24h, 48h and 120h). It has been notified that *Citrus limon*, *Citrus reticulata* and *Citrus paradise* did not inhibit fungi growth after 24h, even at the highest concentration (Figure 3C-E). However, *Melaleuca alternifolia* and *Thymus vulgaris linaloliferum* oils did show an inhibition of fungi growth at 24h (Figure 3 A-B) at concentrations between 50 mg/mL & 5 mg/mL and between 50 mg/mL & 1.5 mg/mL respectively (Appendix A). This test worked, since fungi did not grow with the presence of fluconazole and amphotericin B either (Figure 4A-B). Tween 20 did not interfere the oils action (Figure 4C-D). Results at 48h and 120h showed the same inhibition.

Thus, *Melaleuca alternifolia* and *Thymus vulgaris linaloliferum* oils having antifungal effects at a final concentration of 50 mg/mL. Those concentrations were used for the last experiment "*fungistatic or fungicide drugs"*.

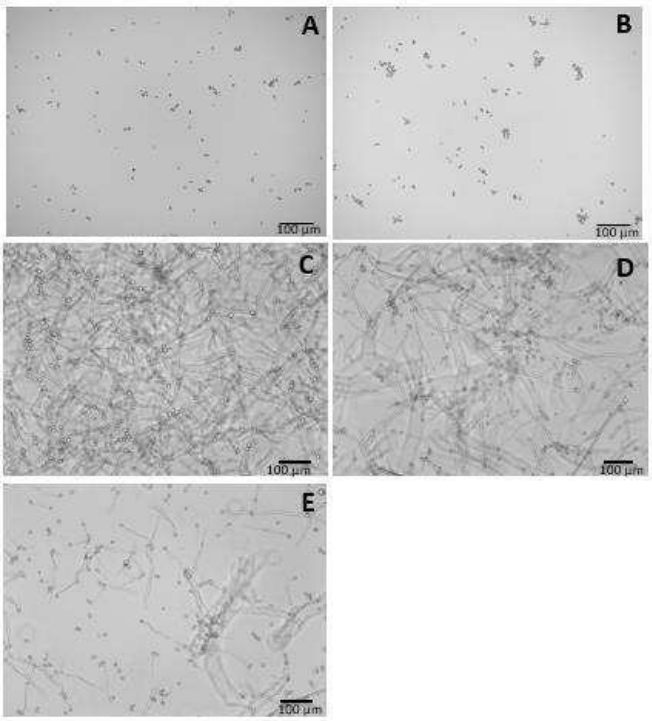

Figure 3: Observation of fungi growth when exposed to different essential oils after 24 hours of incubation. Photos taken with ZOE microscope, Zoom*100.

***A** – with Thymus vulgaris linaloliferum oil (50 mg/mL), only conidia are present, **B** - with Melaleuca alternifolia oil (50 mg/mL), only conidia are present, **C** - with Citrus paradisi oil (50 mg/mL), high and dense mycelium in observed, **D** - with Citrus reticulata oil (50 mg/mL), mycelium is observed, **E** – with Citrus limon oil (50 mg/mL), conidia and only a few mycelium is observed*

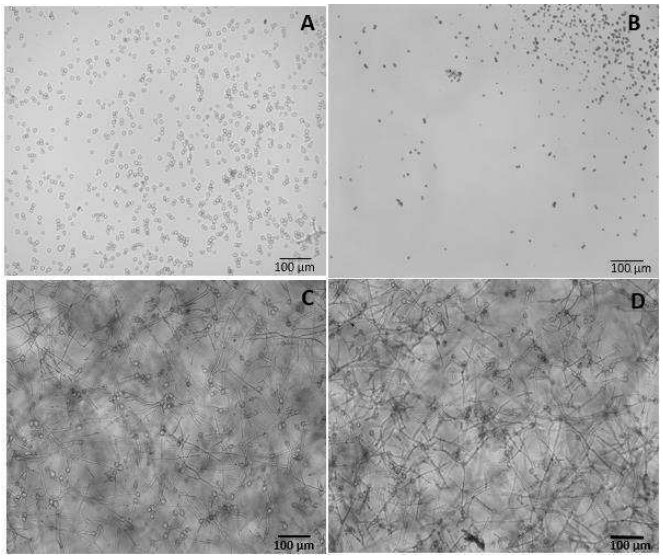

Figure 4 Positive and negative controls of fungi growth after 24 hours of incubation. Photos taken with ZOE microscope, Zoom*100.

***A** – in presence of fluconazole (200µg/mL), we observed only condia and absence of mycelium, **B** - in presence of amphotericin B (240 µg/mL), we observed only condia and absence of mycelium, **C** – in presence of Tween 20 (0.05%), we observed a development of the mycelium, **D** - in presence of pure water, we observed a development of the mycelium*

Fungistatic or fungicide drugs

After 24 hours of incubation, fungistatic effects have been observed. At a concentration of 50 µg/mL of *Melaleuca alternifolia* and *Thymus vulgaris linaloliferum* essential oils, mycelium development slightly began. At a concentration of 25 µg/mL of *Melaleuca alternifolia* essential oils, mycelium growth is observed, but less than the control. For the *Thymus vulgaris linaloliferum* oil, mycelium grew more than for *Melaleuca alternifolia* oil, but less than the control.

In order to find out if a longer exposition to essential oils has a fungicide effect, fungi and essential oils have been incubated in liquid medium for 5 days. Then, the wells plate has been stored at 4°C for one month. Fungicide effects have been observed with Tween 20 control, and all the oils. Therefore, the type of antifungal effect cannot be determined with these results

Data for these results are not shown.

DISCUSSION

In this project, different methods were used to determine the best one to observe the efficiency of essential oils in the fungal substance. A screening test was required to find a range of efficient dosage of the drugs: the fungi survival assessment allowed the determination of drug efficacy on fungi.

The antifungigram method were not used for the rest of the experiment because the control with fungicide substances showed fungi growth. It could be a consequence of an absence of direct contact between the drug compound and the fungi.

Concerning the test with drugs included in solid medium, it required a high temperature of the medium to avoid the

solidification. Due to this high temperature, the antifungal substances could have been altered [10].

It has also been determined if essential oils were either able to kill or inhibit fungi growth. Several tests were performed in order to find the appropriate dose, which was higher than what the ones found in the literature [6], [7]. The *Thymus vulgaris linaloliferum* and the *Melaleuca alternifolia* essential oils were the most efficient. For the other oils, results were insignificant compared to the ones with *Thymus vulgaris linaloliferum* and *Melaleuca alternifolia* with *A. oryzae*.

Nevertheless, cold might have interfered with our results. Indeed, our experiments could not be continued all at once and our samples had to be stored at 4°C for a long time and cold temperature might have a role in fungi survival.

Further studies are required to evaluate the fungistatic or fungicide properties. Moreover, *A. fumigatus* should be tested as it might react differently with the essential oils. For further applications as a treatment for humans or animals, the toxicity of essential oils must be taken into account. [11], [12], [13].

ACKNOWLEDGMENT

We would like to sincerely thank Jacqueline Bert for her availability, her kindness, and her trust to let us a lot of independence during this project.
We are grateful to thank Mrs. Mogensen and Mrs. Saint-Pol for their help and their advices reading this article.
We would like to thank Sup'Biotech for providing us the lab and all the materials required for these labworks.

REFERENCES

[1] Jean-Paul Latge, Aspergillus fumigatus and Aspergillosis, Clinical microbiology reviews, Vol. 12, No. 2, Apr. 1999, pp. 310–350

[2] Janna Brajtburg et al., Amphotericin B: Current understanding of mechanisms of action, Antimicrobial Angents and Chemotherapy, 34(2), 1990, pp. 183-188

[3] James S. Lewis II and John R. Graybill, Fungicidal versus fungistatic: what's in a world?, Expert Opin. Pharmacother, 9(6), 2008, pp.927-935.

[4] Deray G. et al., Nephrotoxicité de l'amphotéricine B, Néphrologie, 23, 2002, pp.119-122.

[5] Khoza S. et al., Comparative hepatotoxicity of fluconazole, ketoconazole, itraconazole, terbinafine, and griseofulvin in rats. J. Toxicol. 2017.

[6] Li Jing et al., Antifungal activity of *Citrus* essential oils, Journal of Agricultural and Food Chemistry, 62, 2014, pp. 3011-3033

[7] Laila Tabti et al., Antioxidant and antifungal activity of extracts of the aerial parts of *Thymus Capitatus* (L.) Hoffmanns against four phytopathogenic fungi of Citrus Sinensis, Jundishapur J Nat Pharm Prod., 9(1), 2014.

[8] K.A. Hammer C.F. Carson T.V. Riley, Antifungal activity of the components of Melaleuca alternifolia (tea tree) oil, journal of applied microbiology, Volume95, Issue4, October 2003, pp. 853-860.

[9] Kyle AA et al., Topical therapy for fungal infections. Am J Clin Dermatol. 2004;5(6):443–451

[10] Hamilton-Miller, J. M., The effect of pH and of temperature on the stability and bioactivity of nystatin and amphotericin B. Journal of Pharmacy and Pharmacology, 1993, 25: 401-407.

[11] Hartnoll G et al., Near fatal ingestion of oil of cloves. Arch Dis Child 1993; 69:392—3.

[12] Riordan M et al., Poisoning in children 4: household products, plants, and mushrooms. Arch Dis Child 2002; 87 : 403—6.

[13] Lane BW et al., Clove oil ingestion in an infant. Hum Exp Toxicol 1991;10:291—4

APPENDIX

[A] Appendix A: Table showing all the different essential oils used with all the concentrations tested on A. oryzae. From "-"to "+++" mean from the complete inhibition of the fungus from no antifungal effect on the fungus.

[A] Appendix A: Table showing all the different essential oils used with all the concentrations tested on A. oryzae. From "-" to "+++" mean from the complete inhibition of the fungus from no antifungal effect on the fungus.

Final concentrations (mg/mL)	***Thymus vulgaris linaloliferum***	***Melaleuca alternifolia***	***Citrus limon***	***Citrus reticulata***	***Citrus paradisi***	***Control: Tween 20***	***Control: Water***
$0.1.10^{-3}$	N/A	N/A	+++	+++	+++	+++	+++
$0,2.10^{-3}$	N/A	N/A	+++	+++	+++	+++	+++
$0.5.10^{-3}$	N/A	N/A	+++	+++	+++	+++	+++
1.10^{-3}	N/A	N/A	+++	+++	+++	+++	+++
10.10^{-3}	N/A	N/A	+++	+++	+++	+++	+++
20.10^{-3}	N/A	N/A	+++	+++	+++	+++	+++
50.10^{-3}	N/A	N/A	+++	+++	+++	+++	+++
0.1	N/A	N/A	+++	+++	+++	+++	+++
1	+	++	N/A	N/A	N/A	+++	+++
1.5	-	+	N/A	N/A	N/A	+++	+++
2	-	+	N/A	N/A	N/A	+++	+++
3.3	-	+	N/A	N/A	N/A	+++	+++
5	-	-	N/A	N/A	N/A	+++	+++
10	-	-	N/A	N/A	N/A	+++	+++
12.5	-	-	N/A	N/A	N/A	+++	+++
20	-	-	N/A	N/A	N/A	+++	+++
25	-	-	+	++	+++	+++	+++
50	-	-	+	++	+++	+++	+++

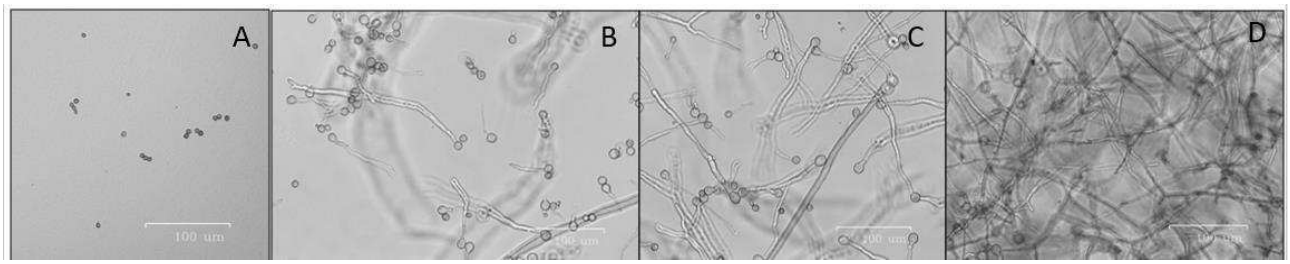

Legend of appendix A: Fungi growth after 48h of incubation of ***A-*** *Thymus vulgaris linaloliferum at 50 mg/mL considered as « - »;* ***B-*** *Citrus limon at 50 mg/mL considered as « + »;* ***C-*** *Citrus reticulata at 50 mg/mL considered as « ++ »;* ***D-*** *Negative water control considered as « +++ »*

Wine or water? … a mineral point of view

Alexandre Tan-Lhernould*, Adèle Alloin, Etienne Lallemand, Noé Legrelle, Julien Morin, Damien Lemaire
Sup'Biotech, Villejuif, France
*Corresponding author: alexandre.tan-lhernould@supbiotech.fr

Abstract

Wine is the end-result of a human-constrained geobiological process. In this study, we set up the statistical tools and the identification of relevant physicochemical descriptors to capture in an indirect manner the mineral component of wine, often called the terroir effect. Statistical workflow was developed and validated using a large-scale wine analysis data carried out on a few thousand different wines. As standard chemical descriptors used in this large-scale study do not discriminate high from low-quality wines as defined by referent oenologists, we propose in this paper a set of three descriptors inspired from soil science which relates to three main actors of biomineralization: protons, electrons and ions. The corresponding descriptors are pH, redox potential, and ionic conductivity. These descriptors also inform on the hydration forces of water, a central and forgotten player of wine quality.

INTRODUCTION

From street science, water is considered as the molecule of life. From their mineral contents, wine and water share three main constituents: O_2, CO_2 and ions, which also play a key role in nearly all ecological systems. For plants and especially grape variety, soil and primary rocks are the main reservoirs of minerals. Thanks to a powerful microbiological "Wood Wild Web" [1] made of mycorrhizae, a symbiotic consortium between roots, fungus and autotrophic and heterotrophic bacteria makes the biomineralization possible. A liana of interest was forced by human intervention to search for deep water, and grape varieties were selected to optimize biomineralization, an oxidoreductive process which is highly dependent on the type of soil. As such, wine is the result of the interactions between biological and mineral kingdom, between the terroir and the grape variety.

To understand which gustative factors influence wine taste, we carried out a statistical analysis on large scale wine data-set from a study realized by Cortez et al [2]. The authors measured 11 standard wine descriptors (fixed acidity, volatile acidity, citric acid, residual sugar, chlorides, free sulfur dioxide, total sulfur dioxide, density, pH, sulphates and alcohol) and provided a consensus quality score for each of the 4898 white wines and 1600 red wines from Portugal considered in the study. This score (from 1 to 10) is a consensus of the individual notes given by a consortium of professional wine tasters. This study gives the opportunity to the scientific community to analyze the underlying molecular criteria that contributes to wine quality and how pertinent these 11 standard chemical descriptors are to capture the holistic global human perceptions of wine, independently of the wine variety or the terroir.

As physicochemical descriptors of minerality were poorly represented in Cortez study, we carried out an exploratory characterization of white wines using bioindicators which are commonly used in soil science: redox potential, pH and resistivity or conductivity. A preliminary small set of 9 white wines was used to assess the pertinence of these three descriptors. A major difficulty in training Artificial Intelligence system for wine quality, is that taste is a personal matter which depends on a person's saliva, its olfactive gustative receptors profile, etc. However, there is still some universal wine quality criteria that distinguish wines. One of them is related to the quality of water, especially its drying or astringent effect on the mouth, which is one of the obvious defects of low-quality wines.

The first section describes the statistical workflow that was developed for general wine analysis and applied here to decipher the discriminant factors between various classes of wine. This is a quantitative analysis as wine descriptors can be related with wine quality consensus score given by oenologists. Three statistical techniques were implemented: Principal Component Analysis (PCA), Multiple Regression, Discriminant Analysis and various Clustering algorithms. Standard statistical validation techniques from the Quantitative Structure Activity Relationship techniques from pharmacological sciences were implemented. This involved data randomization and the splitting of the dataset into two training and test sets, the first one to construct the model and the second to validate the model. The second section describes an exploratory study to identify pertinent physicochemical descriptors that could differentiate small sample of 9 wines into two groups: with or without a stringent or drying impression during wine tasting. This two groups were provided by a professional oenologist, Bruno Quenioux from PhiloVino. The experiments were blinded, and results were revealed at the end of the study. We conclude on the pertinence of these descriptors to capture the mineral aspect of wine, a criterion under increasing consideration.

RESULTS

I. State of the art of statistical wine data analysis

Our construction of an in silico statistical tool for wine data analysis was guided by the problems that can be raised from the study by Cortez et al [2].

They carried out a large-scale physicochemical analysis on a few thousands of red and white wines, which relates measured

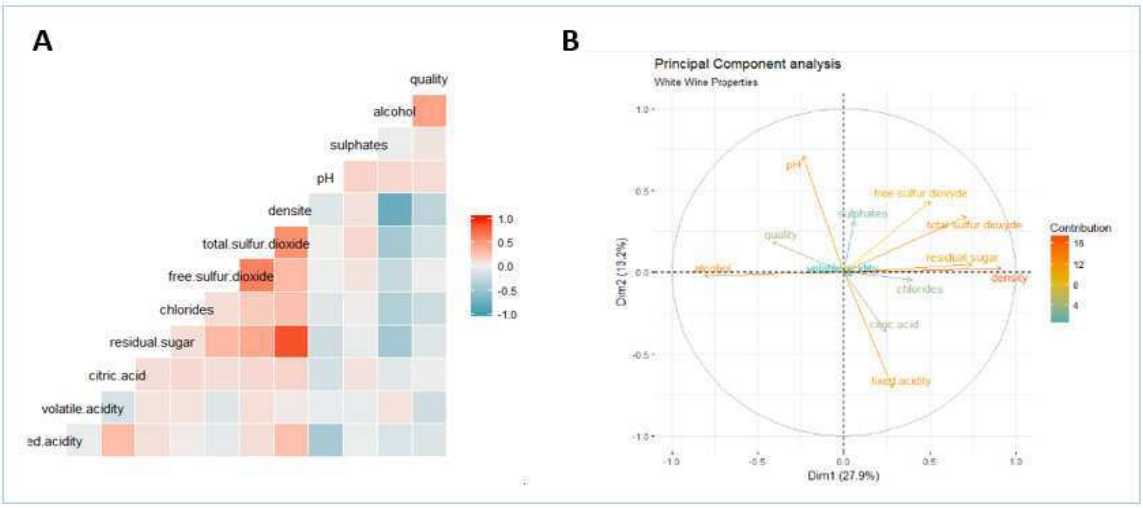

Figure 1. pairwise descriptors correlation (A) and Principal Component Analysis of eleven physicochemical descriptors (from 4898 white wines) (B).

physicochemical descriptors that are typically measured in oenology such as acidity, small volatiles molecules as well as the main secondary metabolites such as alcohol, malic acid, tartaric acid, etc. The goal of this study was to study the relation between those descriptors and the note given to each wine by a consortium of oenologist and professional on wine testing. The average score is given by a number between 0 and 10, the maximum score being given to the wine that best match the olfactory-gustatory wine criteria for this group of people. The sample is made of 4898 white wines and 1599 different red wines from Portugal.

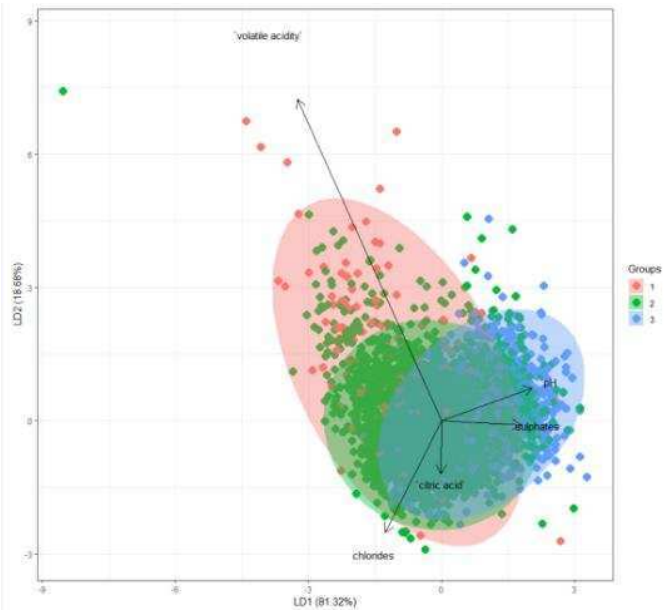

Figure 2. Projection of the 4898 white wines on LD1 & 2. Color code represents the 3 quality classes: group 1 (in red) represents the low-quality wines, group 2 (in green) the middle-quality wines, and group 3 (in blue) the high-quality wines. Physicochemical descriptors (from 4898 white wines).

A first answer can be captured by a principal component analysis (Figure 1). The x-axis (Dim1) explains about 28% of the variance of the data. It corresponds to the density of the liquid. Due to the high solubility of sugar, its high content makes liquid density increases. A reverse effect is given by alcohol that behave like lipid with a density less than 1 (density of water). Here alcohol and sugar can be understood as carbon source, i.e. carrier of electron for yeast metabolism. The alignment of SO_2 with sugar is somehow contradicting the assimilation of the x-axis with electron carrier. The y-axis (Dim2) instead seems to be better associated with pH, i.e. proton potential of the solution. Electron, proton and carbon sources seem to be the main three actors of this global view of wine physicochemical descriptors. Even if quality vector is correlated with alcohol descriptor, concluding that alcohol is the main quality of wine remains not satisfactory. Further insights can be captured by differentiating between various classes of wine: low, medium and high quality.

We, therefore, carried out a discriminant analysis to characterize three arbitrary classes of wine quality: low for score ranging from 0 to 4, medium for score ranging from 5 to 7 and high-quality wine for score greater than 7. If strong overlap remains between these three classes, two tendencies emerge: high quality wine seems to be associated with acidity criteria and low-quality wines are correlated with sugar content (Figure 2).

II. New tendency on wine descriptors

The goal of this study is not to validate statistically the quality of its judgement, but to select some potential physicochemical descriptors that could be used for future large-scale study on wine quality.

In order to estimate the quality of our 3 selected descriptors (pH, redox potential and ionic conductivity) as bioindicators of minerality, we used as statistical criteria the intrinsic coherency of the classification given by B. Quenioux.

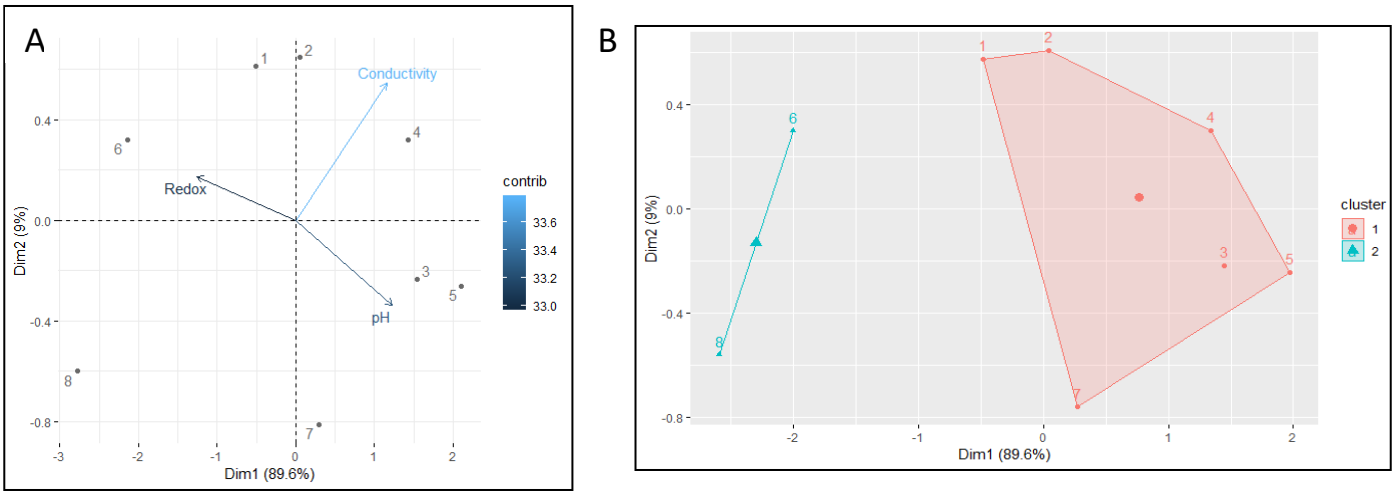

Figure 3. (A) Principal Component Analysis of three physicochemical descriptors: pH, Redox, conductivity (from 8 white wines). The contributions for each descriptor are respectively (Dim1/Dim2): pH (34% / 26%), Redox (36% / 7%) and Conductivity (30% / 67%) (B) Cluster analysis of 8 white wines with the k-mean algorithm.

The introduction of two Grand Crus from Bourgogne and Pays de Loire in the sample were used also as additional coherency criteria.

Figure 3, the x-axis (Dim1) explains most of the dataset variations (89.6%). Each descriptor has a similar contribution to the data variation, suggesting that these descriptors are good candidates to discriminate the wines. Thus, we conducted a cluster analysis with the k-mean algorithm [3] to verify whether it is possible to identify different categories of wine based on the pH, Redox and Conductivity.

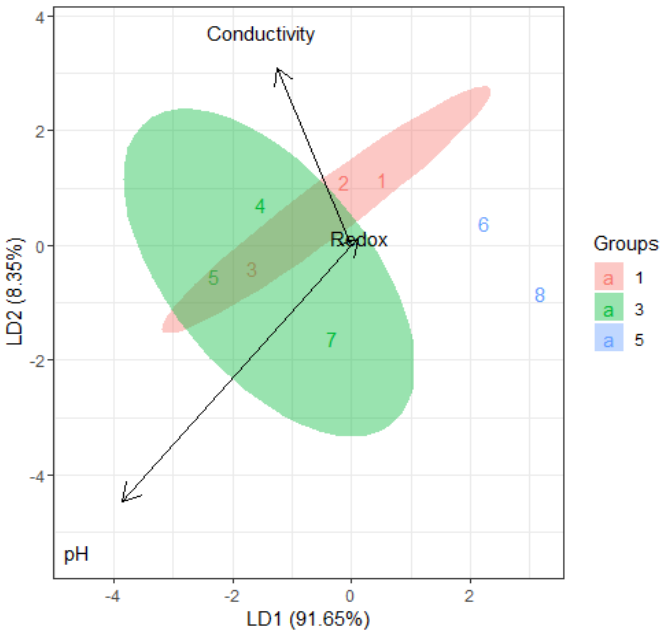

Figure 4. Discriminant Analysis based on the 'quality' score given by Bruno Quenioux. Each group correspond to the wine activity based on minerality (from 1 to 3).

Indeed, we can clearly see that the wines 6 and 8 are dissociated from the rest of the sample.

Once the previous analyses were done, the quality of the wines was revealed and a LDA was conducted based on these quality score. In Figure 4, the Redox is minimally represented in the graph suggesting low relevance of this descriptor compared to Conductivity and pH.

The distribution in the LDA space, dissociates clearly the wine of class 5 (in blue) from the other wines while the class 3 and 1 are overlapping.

DISCUSSION

Based on the state-of-the-art, we could infer that sugar and alcohol were important contributors to the wine appreciation. But the statistical discrimination was not precise enough to predict the quality based on the descriptors. Therefore, we investigated new descriptors (Redox and Conductivity) and kept the pH. From a statistical point of view, we determined that these 3 descriptors are good candidates in determining the wine's water activity. And when validating our results with a LDA based on quality, the results were similar to our cluster analysis, the wine samples 6 and 8 being largely dissociated from the wine sample. Also, the Redox seemed to be not as deterministic as the other descriptors.

From this study, we were not able to clearly differentiate the class 3 from the class 1.

CONCLUSION

The three descriptors chosen in this study are related to fundamental principle of aquatic chemistry and are well used in pedology and marine biotechnology. As mineral chemistry is concerned, similarity may be found in the wine composition since the terroir is an important criterion to differentiate wine types. As the classification of food and beverages on their appreciation (taste) is subjective, we used unsupervised method to assess the wine potential based on physicochemical

properties. pH and Conductivity appear to be good candidates for discriminating different wines. To support these observations, the increase of the sample size is required, and it would be a good perspective to investigate more specific descriptors related to mineral content such as potassium.

MATERIAL AND METHODS

I. Laboratory experiments

Wine samples. In order to get some significant representation of wine with and without this mineral quality, we asked Bruno Quenioux, from PhiloVino in Paris to prepare a diverse sample of 9 wines including one white "Grand Cru" from Bourgogne together with less prestigious wines (price of the bottle higher than 10€ at today's market price). It was a blind testing as the wine names were not known during the study. Care has also been made to not define an absolute criterion concerning wine taste has no one has the same saliva neither the same profile of gustatory receptors in the mouth. The classification given by Bruno Quenioux was based on minerality and water activity: each wine was attributed a quality of either 1 (low quality) or 2 (high quality). The samples were then put in 25mL Falcon and randomized to avoid any bias during their analysis. On these samples, we then performed the following measurements.

Physicochemical descriptors measurement. For this experiment, HANNA Instrument material were used.
The pH-meter was calibrated first using pH buffer 7.0 and then pH buffer 4.0. For the conductivity and Redox potential measurements, no calibration was needed. The measurements were taken after stabilization of the values. The measurements were repeated for each sample, and the electrode was rinsed with distilled water between each measurement.
The conductivity results were given in mS.

II. In Silico Analysis

This study relies on unsupervised learning approaches. The goal was to deduce a class of wine without a priori knowledge as for wine quality. The data collected from the experiments were stored in a matrix D (n, m) in which columns represent the n wine descriptors and rows represents the m types of wines. The data stored in the matrix were extracted using the language R, to perform several statistical Analysis, including Principal Component Analysis, Linear Discriminant Analysis and clustering.

Principal Component Analysis (PCA). For this study the PCA was used to get a global view of the repartition or the diversity of the descriptors and type of wines. PCA is an unsupervised method that gives a new set of variables called principal components, which are linear combinations of the data given for the analysis (here the descriptors) and can explain the maximum variance and summarize the most information in the data [4], [5].

Linear Discriminant Analysis (LDA). LDA is a similar technique to PCA, but as a supervised method it takes the quality score as a discriminant factor to categorize the sample based on the descriptors [6]. To assess the validity of the analysis of this technique, a randomization technique was used: the analysis was conducted on every possible subset (size of: 7, 6 and 5) of the individual sample.

Cluster Analysis. The cluster analysis is an approach in which we determine clusters while minimizing the distances between the individuals within a cluster and maximizing the distances between the clusters (Dunn Index). It allows to identify cluster based on the descriptors profiles [7], [8]. The k-means algorithm was used for partioning the dataset into 3 clusters**.** The validation of the cluster analysis was done by ranking different algorithm based on their Dunn index.

ACKNOWLEDGMENT

We would like to thank Bruno Quenioux, from PhiloVino for collecting the wine samples and providing us with their quality scores. We also thank Jean-Yves Trosset for his supervision and all the insights he provided during the project.

REFERENCES

[1] M. Giovannetti, L. Avio, P. Fortuna, E. Pellegrino, C. Sbrana, and P. Strani, "At the Root of the Wood Wide Web," *Plant Signal. Behav.*, vol. 1, no. 1, pp. 1–5, 2006.

[2] P. Cortez, A. Cerdeira, F. Almeida, T. Matos, and J. Reis, "Modeling wine preferences by data mining from physicochemical properties," *Decis. Support Syst.*, vol. 47, no. 4, pp. 547–553, 2009.

[3] A. Likas, N. Vlassis, and J. J. Verbeek, "The global k-means clustering algorithm," *Pattern Recognit.*, vol. 36, no. 2, pp. 451–461, 2003.

[4] H. Abdi and L. J. Williams, "Principal component analysis - Abdi - 2010 - Wiley Interdisciplinary Reviews: Computational Statistics - Wiley Online Library," *Wiley Interdisciplinary Reviews: …*. 2010.

[5] I. T. Joliffe, "Principal Component," *Princ. Compon. Anal. SE - 7*, vol. 36, no. 4, p. 432, 2002.

[6] J. H. Friedman, "Regularized discriminant analysis," *J. Am. Stat. Assoc.*, vol. 84, no. 405, pp. 165–175, 1989.

[7] J. Gareth, W. Daniela, H. Trevor, and T. Rober, *An Introduction to Statistical Learning with Applications in R*, vol. 7, no. 10. 2000.

[8] M. Charrad, N. Ghazzali, V. Boiteau, and A. Niknafs, "**NbClust** : An *R* Package for Determining the Relevant Number of Clusters in a Data Set," *J. Stat. Softw.*, vol. 61, no. 6, 2014.

AUTHOR INFORMATION

Alexandre Tan-Lhernould, Student, Sup'Biotech.
Adèle Alloin, Student, Sup'Biotech.
Etienne Lallemand, Student, Sup'Biotech.
Noé Legrelle, Student, Sup'Biotech.
Julien Morin, Student, Sup'Biotech.
Damien Lemaire, Student, Sup'Biotech.

Effect of curcumin, lomustine and berberine on the glioblastoma tumor

Alliaume Antoine, Bitton Odelia, Diallo Bilguissou, Lacombe Robin, Mota de Jesus Carine*

Sup'Biotech, Engineering school, 66 rue Guy Möquet, 94800, Villejuif, France

ARTICLE INFO

Article history:
Received 9 December 2018
Received in revised form January 00
Accepted 00 February 00

Keywords:
Curcumin, glioblastoma, berberine, cancer, synergy, lomustine, chemotherapy treatment.

ABSTRACT

Glioblastoma tumors are usually treated with alkylating agents, such as lomustine, inducing many side effects. Alternative medicine using natural substances such as curcumin or berberine could be used to treat cancer. This study shows the interest of molecules combination to improve therapeutic efficiency and lead to treatments less aggressive for the patient. Cancerous cells of glioblastoma U87MG were treated with combinations of curcumin, lomustine, and berberine for 24h and 48h. Given the fact that the 3 drugs show the decrease of cell viability and that combinations involved a higher toxicity, it could induce a potential synergistic effect between them.

1. Introduction

Glioblastoma multiform (GBM) is widely considered to be the most common high-grade cancer within the brain with an annual incidence of 5.26 per 100 000 population **[1].** It is also the most aggressive and incurable malignancy of the central nervous system. Patients diagnosed with glioblastoma have a median survival of approximately 14 months and only a very small percentage (3-5%) of patients survive for more than 3 years. GBM is characterized by an uncontrolled cell proliferation and a significant angiogenesis **[2].** GBM is generally diagnosed using magnetic resonance imaging (MRI) and treated with surgery followed by radiotherapy and chemotherapy. Chemotherapy treatments use DNA alkylating agents such as temozolomide (TMZ) or lomustine to cause cancerous cell apoptosis and to reduce cell proliferation. However, the efficiency is compromised by the high recurrence rate and the development of resistance against the different alkylating agent used. Moreover, treatments of malignant brain tumors are most of the time unsuccessful because of the difficulty for certain molecules to pass through the blood-brain barriers.

Lomustine is a lipid-soluble alkylating agent used in chemotherapy treatments to cure brain tumors for its ability to cross the blood-brain barrier and to cause DNA interstrand cross-links. It acts nonspecifically and can have toxic effect on normal cells at high doses. Lomustine induces apoptosis mainly. To reduce the toxicity, investigators have used nanoparticles to deliver more efficiently the drug to the tumor site **[3]**. Nevertheless, treatments with lomustine are aggressive for the patient and induce a lot of secondary side effects such as temporary hair loss or nausea. Due to the highly resistant and aggressive nature of GBM, new treatments are required.

Alternative medicine using medicinal herbs such as curcumin and berberine have shown to have anti-cancer properties. Curcumin is a curcuminoid highly lipophilic found in turmeric, an Indian spice, and that can cross the blood-brain barrier. Curcumin has been shown to have antioxidant, anti-inflammatory and anticancer properties which make a potential candidate to cure cancers. Recent finding regarding curcumin have led to the opportunities to treat cancer with this natural product. Curcumin has several

mechanisms of action including the suppression of inflammatory cytokines such as tumor necrosis factor alpha, interleukin IL1, IL6, IL8 and affects multiple signaling pathways **[5]**. Potential benefits of curcumin to treat glioblastomas have been studied by different laboratories and Aoki et al showed that it induced autophagy by suppression of the protein kinase B (AKT)/mammalian target of rapamycin (mTor)/p70S6K and activation of the extracellular-signal-regulated kinase (ERK1/2) pathways in U87MG human cells via ERK and c-JUN N-terminal protein kinase signaling. However, the way curcumin acts on cancerous cells still need to be clarified. Nevertheless, combination of curcumin with paclitaxel or with temozolomide has been proved to be efficient. In this study, we wanted to evaluate if the combination of curcumin and berberine could provide a synergistic effect on glioblastomas cells.

Berberine is an isoquinoline alkaloid present in many medicinal herbs. It possesses anti-inflammatory and anticancer activities against various types of cancer cells. It can induce apoptosis and cell cycle arrest of tumor cells but have also the ability to induce cellular senescence **[4].**

This paper outlines a new approach to treat glioblastoma. Studies have been made on the effect of lomustine and curcumin both separately but not in synergy. Therefore in this study we combine curcumin with lomustine in order to reduce the lomustine concentration and thus to decrease the secondary side effects and to improve the cancer treatment. The aim of the study is to determine if curcumin combined with lomustine have a higher cytotoxic effect and to evaluate a potential synergistic effect. Although combination of molecules can be toxic if one of the agents used is chemotherapeutic, the toxicity is significantly less important because of the different pathways targeted. Combination with a natural anticancer product may be able to prevent the toxic effects on normal cells while simultaneously producing cytotoxic effects on cancer cells.

2. Material and Methods

2.1. Cell lines

U87-MG human glioblastoma cells and BJ Fibroblasts cells were obtained from the partnership laboratory Sup'Biotech/CEA-SEPIA and cultured in 500ml DMEM GlutaMax (ThermoFisher) 1X supplemented with 50 ml FBS, 1% penicillin, streptomycin (100U/ml penicillin, 100µg streptomycin) and 1% NEAA. Cells were incubated at 37°C with 5% of carbon dioxide.

2.2. Chemicals

Pure curcumin, pure lomustine and WST-1 were purchased from Sigma-Aldrich. The berberine chloride pure was obtained from Dynveo. The curcumin, lomustine and berberine were dissolved in DMSO to prepare highly concentrated stock solutions (100µM) for use in cell culture. The stock solutions were preserved at -20°C.

2.2 Treatments

Realization of stock solution of curcumin and berberine at 100mM, and lomustine at 50mM.

Range of dilutions of the stock solutions of curcumin, berberine and lomustine in DMEM GlutaMax were prepared, these ranges lies between 0 to 200 µM depending on the tests.

Moreover, combination of curcumin, berberine and lomustine were prepared with different given ratio.

To finish, solutions were added in the 96 wells plates and incubated for 24h or 48h at 37°C, 5% carbon dioxide.

2.4 Viability assay: WST-1

In order to evaluate the impact of curcumin, lomustine and berberine on cell viability, a WST-1 assay (Roche) was carried out using comparable doses of curcumin, lomustine

and berberine respectively, alone and combined, untreated cells were attended as control. and allowed to adhere for 24 hours.

After 24 hours, and 48 hours, WST-1 reagent (Roche) was added, 10 µL/well, was added. After 1 to 3 hours, the absorbance was measured at 450 nm and 600 nm using a multiskanTM spectrophotometer reading plate (Thermo Scientific™ 51119200).

2.5 Statistical analysis

Experiments were made in triplicate and data were reported as mean ± SD.

3. Results

First, the influence of curcumin and lomustine concentration on cell viability has been evaluated. Secondly the impact of the time exposure on cell viability is investigated. Lastly, the synergy of curcumin and berberine on UG87 is analyzed.

3.1 Evaluation of optimal curcumin and lomustine concentration

To evaluate the dose response of curcumin and lomustine, U87 cells have been exposed to different concentrations of treatments during 48h.

Cytotoxicity assays for lomustine compound, performed in the U87 cell line showed that it exhibits viability-inhibitory activity (Fig. 1). However, the results showed that after 48h of treatment, lomustine concentration higher than 15 µM do not seems to impact significantly the cell viability. Given that our objective is to reduce the concentration of lomustine while decrease cell viability. The optimal lomustine concentration that has been chosen for our experiments is 10 µM.

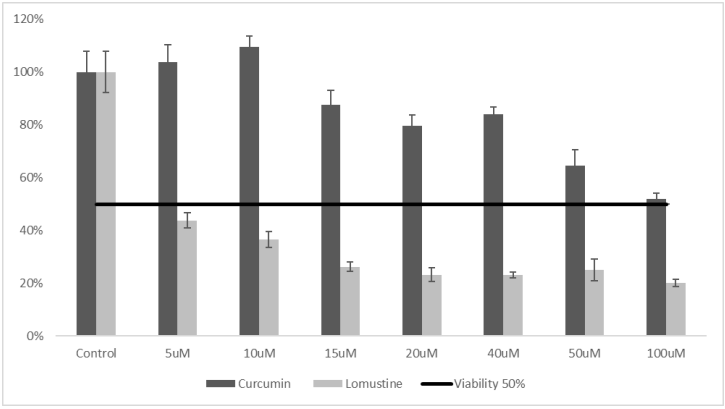

Figure 1 : Hystogram of U87-MG cell viability after 48h of treatment by curcumin and lomustine in wide range of concentration.

Cytotoxicity assays for curcumin compound, performed in the U87 cell line showed that it exhibits viability-inhibitory activity as lomustine. (Fig. 1). After 48h of treatment, lomustine inhibits constantly the viability of glioblastoma cells by time and concentrations (from 10 µM of to 100 µM). For example, at 20 µM curcumin the cell viability is up to 80%. However, 50 µM curcumin concentration reduces cell viability to 65%. Furthermore, the maximal cytotoxic effect occurs after treatment with 100 µM curcumin which induces the death of 48% of the cells. The results of the experiment found clear support for the cytotoxic activity of curcumin on U87 cells. Nevertheless, curcumin seems to be effective at high concentration.

The comparison between curcumin and lomustine reveals that lomustine gives clearly better cytotoxic effect than curcumin at low concentration (10 µM). Moreover the EC50 of lomustine and curcumin are respectively equal to 10 µM and 100 µM. This issue has been expected because lomustine is a chemotherapeutic treatment used to treat glioblastoma. Our goal is to evaluate a synergistic treatment based on low lomustine concentration and curcumin in order to obtain an equivalent or higher cytotoxic effect than lomustine alone.

3.2 Impact of exposure time on cell viability

In this part the impact on the exposure time of curcumin, berberine and lomustine alone has been investigated.

In this study curcumin has been used at low concentration because it has been shown that curcumin have a cytotoxic effect on normal cell at high concentration. As we can notice on Figure 2, for all treatments, the longer is the exposure time, the lower is the cell viability. At this point we obtained a value of cell viability higher than 100% which means that our control is not reliable and errors may have occurred during the experiment. For instance at 24h cell viability was equal to 97%, 130% and 136% for a concentration of 20 µM of curcumin, berberine and lomustine respectively. In comparison to a 48h exposure, we obtained a cell viability of 95%, 131% and 111%.

Furthermore, Figure 2 suggests that there is a proportional relationship between the exposure time and the cytotoxic activity of curcumin, berberine and lomustine treatment.

Then the toxicity on non-cancerous cells: fibroblast (BJ) treated with curcumin, lomustine and berberine has been evaluated. As it is shown on the Figure 2, berberine exhibits viability-inhibitory activity of 25% of the cells at a concentration of 25 µM, after 48h of exposure. Moreover lomustine and curcumin showed only negligible cytotoxic effect on BJ cells even at higher concentrations.

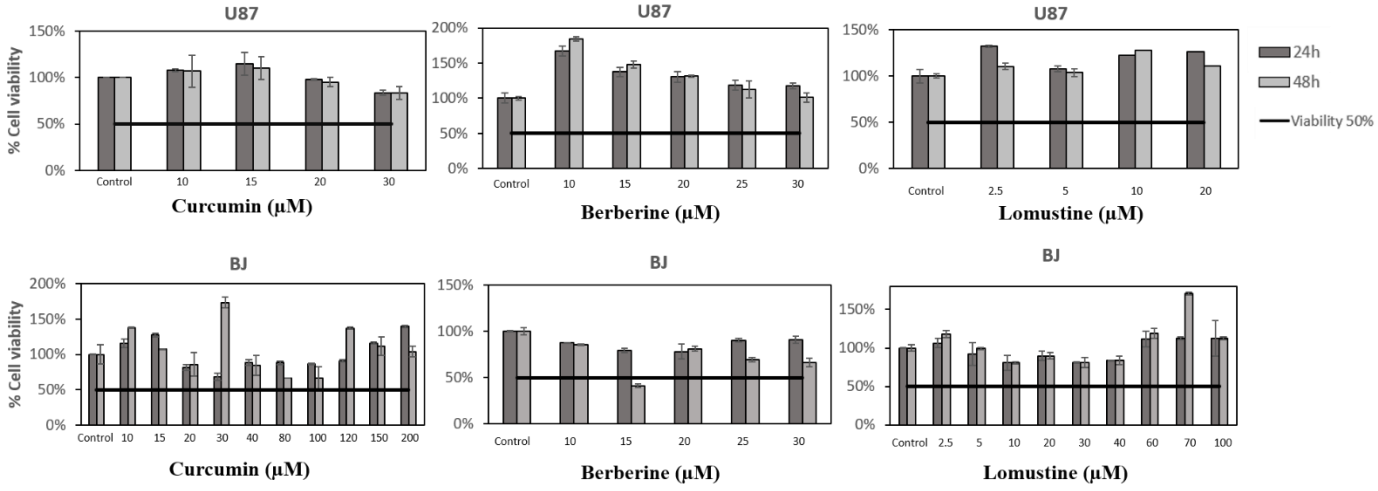

Figure 2: Cell viability (%) of U87-MG and BJ cells after treatment with curcumin, lomustine, berberine at 24 and 48h.

3.3 Evaluation of curcumin, lomustine and berberine synergy.

The cytotoxic effect of curcumin and berberine has been documented in several reviews, but in none of them the synergy effect of these two compounds were studied.
Therefore we investigated if the two combined compounds can have addition effect compared to the single treatments.

According to figure 3.A, the combination berberine and curcumin has better impact on the cell viability compared to the other combinations. With berberine 10 µM and curcumin 25 µM, we can observe around 65% of cell viability and when the concentration of curcumin was raised up to 30 µM, the viability dropped to 55%.

Combination of curcumin and lomustine resulted in a high reduction of cell viability when the concentration of lomustine was set to 10 µM. Below this concentration, the combination showed no eventual additive effect compared to curcumin alone.

In the figure 3B, we realized combinations of the three molecules all together and with different proportions between them. The highest effect was observed when treating cells with equal concentrations of the three molecules.

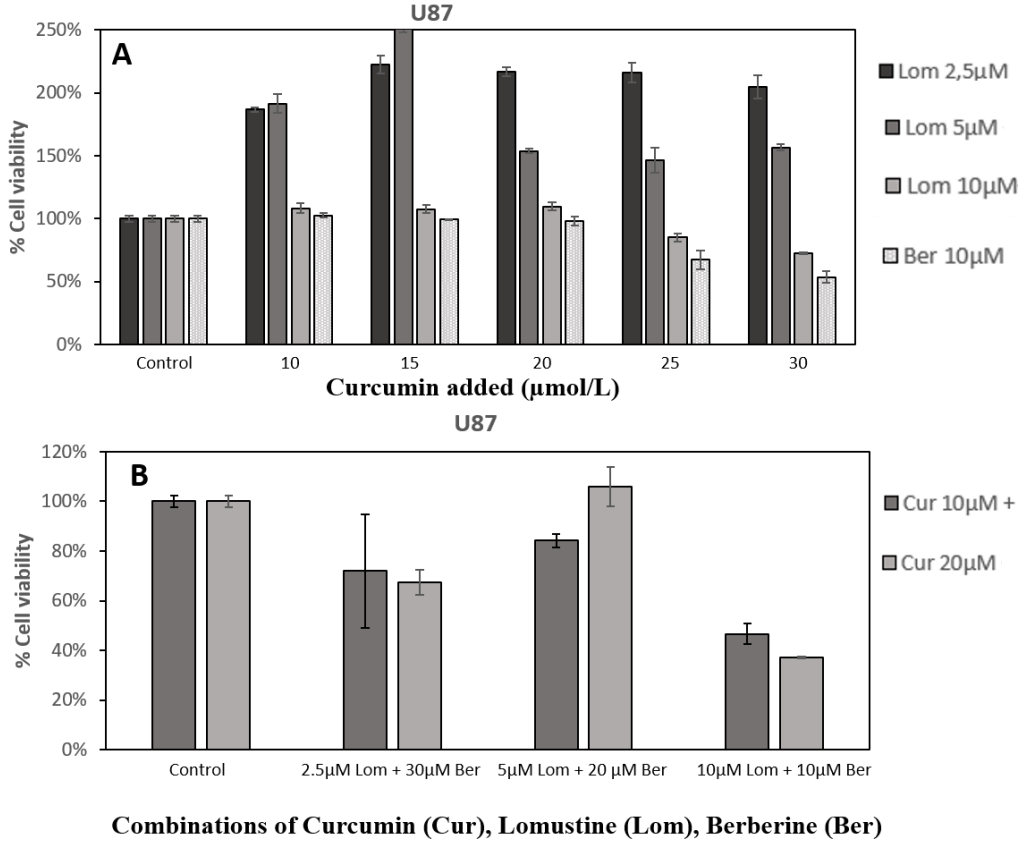

Figure 3: Cell viability (%) of U87-MG cells after treatment with combined curcumin, lomustine, berberine at 48h.

4. Discussion

Until today, glioblastomas are incurable malignant tumors. Implementation of multimodal therapies and advances in surgical techniques are not enough to increase significantly the survival of affected patients. One of the actual treatments include the chemotherapeutic reagent lomustine that have described anticancer activities in glioblastoma. However, there is some resistance problems and a lot of secondary side effects in patients. Fortunately, new therapeutic strategies are constantly under investigation. The objective is to find an efficiency drug to use in combination of chemotherapy specifically against tumors cells without inducing undesirable side effects.

Different studies were performed, and several reviews were published on variety of effects of curcumin such as antioxidant, anti-toxic, anti-inflammatory, cancer chemopreventive and potentially chemotherapeutic properties **[6].**

Curcumin and berberine are natural compounds. It has been proved to be a safe agent. In addition, therapeutic effect on various cancers have been noticed. As these drugs show a potential anti-cancer properties, it has been tested and the results are described on this scientific paper.

In this study, we show that curcumin and berberine potently inhibit proliferation of GBM cells. Our data further provide only an information about the cell viability but mechanisms of action have to be decipher in future experiments. Indeed, we know that side effects are mainly due to the treatment that kill both cancer and healthy cells. In order to assess the toxicity on non-cancerogenic cells, fibroblast cells BJ were treated with the three compounds. The data obtained, showed that higher the concentrations of the compounds were, the lower the cells viability was. Also, the cells were more affected after 48h of incubation than after 24h. There are not cytotoxic effects on normal cells, we can see that at 150 µM curcumin, there is more than 100% cell viability, which means that even with high concentration of curcumin the fibroblast survives, the same goes for berberine and lomustine. In scientific literature, it has been shown that curcumin potently hampers GBM cell proliferation, migration and invasion. Migration assay such as soft agar test will be performed in the future.

The effects are even more present with the combination of the compounds. Although, cell death was observed when incubated with curcumin, but not with the berberine and lomustine. First cell viability was reduced when the cells were incubated in curcumin with the concentration starting from 20 µM. The cytotoxic effect increases with the concentration and the time of incubation; indeed, the cells were more affected at 48h of incubation than 24h.

When cells were incubated in combinations of compounds, a significant reduction of the cell viability has been observed. Thus, the viability of U87 cells is about 60% when incubated in lomustine 5 µM with 30 µM curcumin, lomustine 10 µM with 25 µM curcumin. By combining curcumin and lomustine, it is possible to increase the concentration curcumin and reduce the concentration of lomustine to obtain cytotoxic effect. The reduction of lomustine is important because by doing so, we reduce its undesirable side effects.

When curcumin is combined with berberine, data shows a significant U87 cell viability reduction down to 58%, with the following concentrations: 10 µM berberine and 30 µM curcumin.

In the combination of the three compounds, we observed even more effects on the cell viability, which is at 45% with 10 µM curcumin with 10 µM berberine and 10 µM lomustine. When we increase the concentration of curcumin, the cell viability decreases whether 35% with 20 µM curcumin with 10 µM berberine and 10 µM lomustine.

As we notice a synergistic effect for some combination, it means that targets of both molecules are different and it will be important to decipher the mechanism of action of each drug.

5. Conclusion

Our investigation demonstrated a highly effective combination therapy in an in vitro glioblastoma cell model: U87MG. Curcumin and lomustine combination potently inhibited U87-MG cell growth at a defined concentration and mechanism have to be decipher yet. Future studies should address the mechanisms by which this combination imparts this possible synergistic/additive effect. As our results demonstrated for the first time, that it is possible to decrease the lomustine concentration and increase the curcumin concentration in the treatment of glioblastoma cells (U87). Promising cancer treatment could be done with a massive reduction of undesirable side effects of lomustine despite its efficacy to improve the patients' health.

To improve this study, other tests could be performed, for instance, the cell migration assay because the glioblastoma cells are derivates of endothelial cells that can migrate. In addition the TUNNEL assay in order to evaluate apoptosis. Lastly, Software such as Graphpad prism could be used to determinate the precise EC50 of the compounds.

Acknowledgements

This research paper was made possible because of the determination, help and support of the entire team.

We would like to express our gratitude to Dr. Rafika JARRAY, our tutor and supervisor along with all the "fil rouge" team of Sup'Biotech for their guidance and help through this wonderful journey.

REFERENCES

1. C. (2013). Glioblastoma and Other Malignant Gliomas A Clinical Review.
2. Fisusi, F. A., Siew, A., Chooi, K. W., Okubanjo, O., Garrett, N., Lalatsa, K.,Schätzlein, A. G. (2016). Lomustine Nanoparticles Enable Both Bone Marrow Sparing and High Brain Drug Levels – A Strategy for Brain Cancer Treatments.
3. Harvey, K. A., Xu, Z., Saaddatzadeh, M. R., Wang, H., Pollok, K., Cohen gadol, A. A., & Siddiqui, R. A. (2014). Enhanced anticancer properties of lomustine in conjunction with docosahexaenoic acid in glioblastoma cell lines, 1–10.
4. Liu, Q., Xu, X., Zhao, M., Wei, Z., Li, X., Zhang, X., & Liu, Z. (2015). Berberine Induces Senescence of Human Glioblastoma Cells by Downregulating the EGFR – MEK – ERK Signaling Pathway, 355–364.
5. Sa, Gaurisankar, and Tanya Das, 'Anti Cancer Effects of Curcumin: Cycle of Life and Death', Cell Division, 3 (2008).
6. Sordillo, L. A., Sordillo, P. P., & Helson, L. (2015). Curcumin for the treatment of glioblastoma. Anticancer Research, 35(12), 6373–6378.

SNP in CYP2C19 gene's impact for the metabolism of Clopidogrel

Entering the Era of Personalized Medicine with Pharmacogenetics

Chloé Lortal, Léa Lortal, Margaux Mäder*, Juliette Warnier
Sup'Biotech, Villejuif, France
*Corresponding author: margaux.mader@supbiotech.fr

Abstract - In the last few years, genetic testing has greatly progressed. Everyone can get tested, for medical purposes or personal reasons. Some direct-to-consumer companies like the famous one 23andMe can even now predict how effective medications will work on a person based on genes and mutations. Our team decided to work on the CYP2C19 gene which allows the metabolization of antiplatelets Clopidogrel and one of its Single Nucleotide Polymorphism (SNP): rs4244285. We aimed to determine whether this mutation was present or not in specific cells: our own DNA, fibroblasts and tumoral cells. In order to do so, we first extracted the DNA from these different sources, purified it and performed a Polymerase Chain Reaction (PCR). We then carried on with a Restriction Fragment Length Polymorphism (RFLP) and sequencing. Our data were not sufficient enough to conclude on our study, but it allowed us to improve the related processes, experiments and manipulations.

Index Terms – CYP2C19, DNA, Genetic testing, Personalized Medicine, SNP

INTRODUCTION

'Genetic testing is a type of medical test that identifies changes in chromosomes, genes, or proteins. The results of a genetic test can confirm or rule out a suspected genetic condition or help determine a person's chance of developing or passing on a genetic disorder.' (Genetic Home Reference, 2018 [7]).

A genetic test identifies changes in the DNA of a person, such as single nucleotide polymorphisms (SNPs).
Genetic testing has become very popular worldwide and new technologies make it accessible to the general public. Many direct-to-consumer companies such as 23andMe or health practitioner focusing companies like Lifecode Gx provide this kind of service today.

Moreover, genetic testing now plays a key role in the development of personalized medicine. Indeed, the genetic profile of a person can be a tool for health professionals to individualize prevention, diagnosis and treatment. Personalized medicine allows a doctor to directly prescribe the appropriate drug, effective and without side effects for the patient. This saves more time than if the patient takes a drug without being tested genetically to know if it metabolizes well, and has less binding effects and less costs too.

We chose to study Clopidogrel, an antiplatelets which is commonly used in the world. In addition, its associated gene, CYP2C19, metabolizes many drugs as well, and its mutation for Clopidogrel is well studied, very specific and already tested in the United States.

The SNP rs4244285 on the CYP2C19 gene decreases the effectiveness of antiplatelets such as Clopidogrel.

Indeed, this variant reduces CYP2C19 enzyme's ability to metabolize Clopidogrel into its active form, and therefore patients with this SNP are less responsive to Clopidogrel treatment than others.

The Clopidogrel needs to be converted into an active metabolite thanks to oxidation reactions. It binds irreversibly to the platelet P2RY12 receptor and therefore block adenosine diphosphate-mediated platelet activation and aggregation (Kim JY, Cheong HS et al., 2014 [4]).

It has been shown that when individuals have 2 non-functional alleles (*2 or *3) of the CYP2C19 gene, they have no enzyme activity (oxydase) and cannot activate Clopidogrel so the drug has no effect. These individuals are classified as poor metabolizers. It concerns approximately 2% of Caucasians, 4% of African Americans, and 14% of Chinese. The individuals carrying only one non-functional allele are considered as intermediate metabolizers. 45% of the global population is thought to be intermediate metabolizer and have difficulties to metabolize the drug. The normal genotype is *1/*1 and is represented by 35% of the population. Some people have a *17 allele which make them metabolize faster the drug. Approximately, 10% of the population are classified as rapid metabolizers (*1/*17) and less than 5% are classified as extensive metabolizers (*17/*17) (Dean, 2012 [5]).

Before starting this project, we went to a pharmacy and asked the pharmacist about this antiplatelets. He showed us the box where it is written that a genetic test is actually necessary before taking Clopidogrel. We asked him if people that take Clopidogrel actually did a genetic test and his answer was negative (Clinical Pharmacogenetics Implementation Consortium, 2018 [3]).

Our project was to discover if the members of the Genomics team of the Sup'Biotech laboratory could correctly metabolize Clopidogrel. The goal was therefore to find out if the DNAs of the team members contained this mutation and

we chose to also look at the results for fibroblasts and for cancer cells as controls. This paper describes how we proceeded and the results obtained. This study took place over one year and in two stages.

ETHICS AND REGULATION

With the increasing use of genetic tests, the debate on ethics has become more urgent and complex.

First, it is necessary to differentiate between sequencing and genotyping. DNA sequencing involves determining the order of nucleotide chaining for a given DNA fragment while genotyping aims at determining the identity of a genetic variation at a specific position on all or part of the genome, for a given individual or group of individuals (Séquençage Génome, 2011[8]).

Some insurance companies may apply what is called 'genetic discrimination', raising their prices for someone that has a genetic predisposition to Alzheimer's disease for example.

For this project, we met with Dr. Fabien Milanovic, Lecturer and Head of the Pole of Biotechnologies in Society (PBS) to discuss the regulations of DNA research. This preliminary work was important to ensure that what we were about to do was legal because we would actually be working on our own DNA to check if it had the mutation on the CYP2C19 gene. In France, sequencing is prohibited. However, nothing is mentioned about genotyping and working with our own DNA (A. Léchenet, 2014 [2]).

Despite our efforts and thorough research, this legal blur has not been resolved. Indeed, we called in France the Ministry of Health, the Ministry of Education, the Protection Committee and six law firms to ask them about the right to work on our own DNA. Unfortunately, none of these institutions has been able to answer this question. We also contacted 23andMe, the biggest genetic testing company in the world and Genoscreen, a sequencing company. Both of them did not have an answer either, or at least, that is what they told us.

In France, the different laws of bioethics have laid down great principles for carrying out examinations of the genetic characteristics of people:

'The genetic examination can only be performed for medical, judicial or scientific research purposes, and only in authorized laboratories.' This practice is notably governed by articles 16-10 of the civil code (Légifrance, 2018 [6]).

This remains unclear because one can ask the question if what we did in the laboratory falls into the category "genetic examination". So, since our project was only about one gene and not on the entire genome, it enters the category of genotyping but is it considered as "genetic examination"?

This question remained unanswered along our project but it allowed us to do a lot of research on this subject and we found this problematic very interesting. There is indeed a lot to say about sequencing, genotyping, aspects of laws and ethics in France and around the world. In France, ordering a non-prescribed genetic test is prohibited. Moreover, is it "dangerous" to work on your own DNA? This raises the question and the power of biohacking and the "Do-it-yourself biology", which is a growing biotechnological social movement in which individuals, communities, and small organizations study biology and life science using the same methods as traditional research institutions. However, we will see in this article that it is not so easy to obtain results and to sequence or genotype DNA even with a team of biology students and a fully equipped laboratory.

MATERIAL & METHODS

USED CELLS: We used fibroblast BJ cells (Ref CRL-2522, ATCC collection) and cancerous U87 cells (Ref HTB-14, ATCC collection) from another group: Curcumin (Villejuif, France).

24 000 000 U87 cells were available to work with and only 450 000 BJ cells. For the U87 cells: we put 500µl in culture, 1mL was used for the extraction and the remaining cells was frozen. For the BJ cells: 2 mL in culture and the remaining for the extraction. No cells were frozen. We also used cells from saliva of two students: student A and student B.

CELL CULTURE: U87 and BJ cells were obtained from Curcumin group (Villejuif, France). The cells from the saliva are coming from two students: student A and student B. The medium is purchased from Curcumin laboratory too. It has the following composition: 950mL of Dulbecco's Modified Eagle Medium (DMEM), 1% of antibiotic (Penicillin G and Streptomycin) and 10% of fetal calf serum.

During all the process of culture, cells were cultured at 37°C in a humidified atmosphere of 5% CO2 and used a 80-90% confluence. Cells were harvested by rinsing once with Phosphate Buffered Saline (PBS), incubating with 2mL of 0.25% trypsin-EDTA solution during 5 min at 37 °C in 5% CO2 and collected. After that, cells were counted manually with a Malassez cell.

DNA EXTRACTION: DNA from saliva was extracted using the DNeasy blood and tissue kit (Ref. 69504 Qiagen). The protocol was the user-developed protocol (Ref. DY-07 Qiagen) from the above kit. DNA from BJ cells and U87 cells was extracted with the same kit but with the protocol named purification of Total DNA from Animal Blood or Cells.

Cells were washed with PBS and we used proteinase K, provided by the kit, in order to digest proteins. A buffer AL has been used to lyse membranes. The buffer AW1 has the main goal to denature the proteins of the cells. The last buffer used was AW2 in order to wash the salts out. During all these steps it was asking to vortex in a homogenous way during 5-10 sec and centrifugation steps must be carried out at room temperature (15–25°C).

Confirmation of DNA extraction was performed on a 1% agarose gel. We verified the results on an agarose gel.

PRIMER DESIGN: The first human primer pair was designed using PrimerBlast software and APE software. The size of the amplicon is 424 bp. The second couple of primer comes from an article. [Alcoser et al., 2011] The amplicon measures 189bp and represents a fragment of the prostaglandin E receptor 2 gene. The primer has been purchased to Eurofins.

Forward 1: 5'-TGAGCCCCTCCCACTTCTAA-3'
Reverse 1: 3'-TCACAAATACGCAAGCAGTCAC-5'
Amplicon 693 bp

Forward 2: 5'-ATTACAACCAGAGCTTGGCAT-3'
Reverse 2: 3'-CACAAATACGCAAGCAGTCA-5'
Amplicon: 304 bp

Forward primer 3: 5'-TCCGGGTCTTTGCAGTCGTA-3'
Reverse primer 3: 3'-TTAGTCACCGGCAGGCTTTC-5'
Amplicon: 424 bp

Forward primer 4: 5'-GCTGCTTCTCATTGTCTCGG-3'
Reverse primer 4: 3'-CCAGGAGAATGAGGTGGTC-5'
Amplicon: 189 bp

PCR: We first studied an article from Alcoser.S & al (2011 [1]). But finally, we used the protocol from NEB *(Ref. M0273)*. The PCR was carried out on a thermocycler of Mycycler® using 120 ng of DNA, previously extracted in a 50 µl reaction volumes. The conditions (chosen during the PCR optimization) were as follow: denaturation at 94°C; 30sec, 30 cycles with a temperature of annealing of 54.8°C, and a final extension at 68°C during 5 minutes. The forward and reverse primer were added to each PCR tube to obtain the same final concentration (0,2 mM). Samples were usually run in duplicate on the same reaction plate. The negative control was the water sample and we used the U87 and BJ cells as positive control. We verified the results on a 1% agarose gel.

RFLP (RESTRICTION FRAGMENT LENGTH POLYMORPHISM): The DNA contained in the PCR products was mixed with the enzyme SmaI, the Cutsmart buffer and ultrapure water. Then the mix was incubated for 1h hour in a water bath at 37°C. Finally, the mix was centrifuged at 13000 rpm for 30 seconds and put on ice. To visualize the RFLP, the digested PCR products were separated on 1% agarose gel alongside the 100bp DNA ladder.
SmaI is a restriction enzyme that cleaves the sequence CCC GGG. Therefore, if the CYP2C19 gene from the cells or from the student does not have the mutation, SmaI will cleave the sequence and we will obtain 3 bands for the heterozygote (693bp, 507bp and 188bp) and 2 bands for the homozygote (507bp and 188bp). If there is a mutation, SmaI will not cleave the sequence and we will obtain a band at 693bp. The size of the fragments is given in the case of the first set of primers. We verified the results on a 1% agarose gel.

RESULTS

DNA EXTRACTION: The yields of the DNA extraction were on average 30 ng/µl for the U87 cells and on average of 9 ng/µl for cells of student B (Figure 2:).
The absorbance was measured thanks to a micro drop in order to calculate the ratios Abs_{260}/Abs_{230} (Normally between 1,8 and 2,2) and the ratio Abs_{260}/Abs_{280} (Normally between 1,8 and 2).

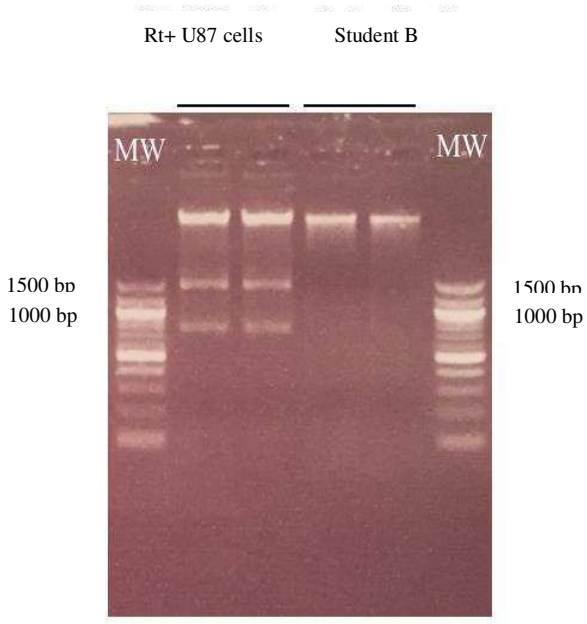

Figure 1:
1% agarose gel electrophoresis showing the DNA extraction of experiment 2 on U87 cells and cells of student B.

Our data show a first ratio at 1,54 for the U87 and 0,54 for the cells of the student B. The second ratio was 2,5 for the U87 cells and 3 for student B's cells. These data show a contamination of both samples that could be explained by a bad elution and a presence of solvent or a contamination during the sampling. As we want an optimal verification, we made a verification by a 1% agarose gel with duplicated U87 cells and cells of student B (Figure 1:). This verification shows us clear bands at the expected size, about 3000 base pairs, for all samples. The ladder chosen (100bp) was certainly not the most optimal because the highest band is 1500bp.

An observation was made only for the U87 cells: two distinct bands at 1500bp and 900bp. It could be ARN 18S and 28S but it does not appear at the good size which normally appear at respectively, 200bp and 500bp.

Sample	Quantity (ng)	Concentration (ng/µl)	Abs_{260}/Abs_{230}	Abs_{280}/Abs_{260}
EXPERIMENT 1:	16 300	81	1,58	2,06
U87	5 850	39	0,72	2,17
BJ	2 500	12,5	0,5	2,75
Patient A	4 000	20	0,53	2,22
Patient B				
EXPERIMENT 2:	9 000	30	1,54	2,5
U87	2 700	9	0,37	3
Patient B				

Figure 2:
Extraction of DNA in U87 cells and cells of student B, quantity, concentration, contamination

PCR: We performed a PCR optimization on U87 with two different couples of primers (the third and the fourth ones). Both sets have the same annealing temperature, therefore we did the optimization on both couples at the same time. We made a temperature gradient of four temperatures: 53.2°C; 54.4°C; 56.2°C; 57.0°C. We did not have results for the third couple of primers. For the fourth couple, we had a light band at 56.2°C and a brighter band at 57.0°C.

For the final PCR, we selected the fourth couple of primers and we decided to work at 57.0°C. We did the PCR on DNA from U87 and student B and used water as control. We have a band for the PCR product of student B but it does not correspond to any expected size (Figure *3*:).

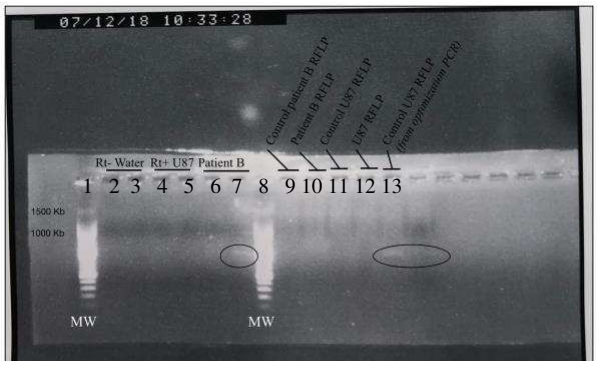

Figure 3:
1% agarose gel electrophoresis showing the PCR on the left and the RFLP on the right
1st well: 100bp DNA ladder
2nd and 3rd wells: PCR product water/4th couple of primers
4th and 5th wells: PCR product U87/4th couple of primers
6th and 7th wells: PCR product student B/4th couple of primers
8th well: 100bp DNA ladder
9th well: RFLP control for student B (Final PCR)
10th well: RFLP student B (Final PCR)
11th well: RFLP control for U87 (Final PCR)
12th well: RFLP U87 (Final PCR)
13th well: RFLP control for U87 (PCR optimization)

RFLP: We digested the PCR products from the PCR optimization (U87 where we had a band) and from the final PCR (U87 and student B) with the restriction enzyme SmaI and the CutSmart buffer. The control was the PCR product with the Cutsmart buffer but without the enzyme SmaI. As we use the fourth couple of primers, we should have obtained 1 fragment if there is a mutation, 2 fragments if there is no mutation and homologous alleles, and 3 fragments if there is no mutation and heterozygous alleles.

For the RFLP issued from final PCR of U87 and student B, we have no results. However, for the RFLP issued from the PCR optimization of U87 we have a band at an unexpected size again (the same as the PCR product). As the control does not contain the enzyme, the band might only correspond to the amplicon. For the true RFLP sample, we have a band at the same unexpected size again. It could mean that there is no mutation with homozygous alleles, but we cannot conclude (Figure *3*:).

DISCUSSION

This project conducted over a year has been a source of continuous improvement even if our data did not allow us to answer to the question yet. Initially, we wanted to know if the three types of DNA studied had the mutation on the CYP2C19 gene to be able to conclude on the efficiency of the metabolism of Clopidogrel. However, the team was able to understand and learn from its mistakes. Each result has been studied very carefully, each manipulation decorticated to allow criticism. Weeks after weeks, our experiments were improved and completed in order to tend to the expected results.

The successful DNA extraction is a good indicator to us: we know and we are certain that the problem is coming from further steps.

The principal interrogation was about the PCR that we realized several times. We first decided to do a PCR optimization for each set of primers to test and use the best annealing temperature. Once done, the real PCR was performed and we did not have results from that. We wonder what could have been wrong in order to reach a successful experiment. Realizing a PCR could be tricky and need an organization and a verification at each step. We were working in a new laboratory we were not used to and we did not test the thermocycler on the couple of primers which have been already used by our colleagues in the same environment and that worked. Furthermore, we did not choose a housekeeping gene, a gene coding for essential proteins in the cell's

survival, during the first week. We changed that during the second part of our project to compare and try to understand all the mechanism related to PCR process. We directly tested our couples of primers designed on PrimerBlast. During our further verifications, we realized that our first primers also attached to another part of the genome. Strangely enough, we did not get a band of this size at the PCR. This is where our hypothesis that the thermocycler may not work correctly comes from because if our primers could attach to another part of the genome, we should have seen it on the agarose gel. Even the couple of primers taken in an another scientific article did not induce a strong band on the gel.

The RFLPs were not performed in optimal conditions. Indeed, we took the PCR product and added the restriction enzyme SmaI and its associated buffer CutSmart without a purification step. As a result, the enzyme SmaI was in presence of PCR buffer and One Taq polymerase which may have interfered with its activity. We tried to create ratios for their dilution but it also diluted the DNA. However, as we did not extract a large amount of DNA, especially from saliva, performing DNA purification from the PCR product might have induced a loss of material.

The team was able to perform the experiments always in a more accurate way. It was also really interesting to learn about the sequencing and the genotyping, on genetic tests and personalized medicine but especially on the ethical and legal part of this theme.

We are now convinced that genetic tests will be part of personalized medicine in the future (and are already starting to be!), but in an environment supervised by health professionals and in a legal framework to avoid any overflows.

ACKNOWLEDGMENTS

This study was supported by Sup'Biotech Paris, Dr. Yates, Dr. Jarray, Dr. Mogensen, Dr. Milanovic, Ms. Léa Lortal, the Curcumin group and all the tutors that we met during these two years.

REFERENCES

[1] Alcoser, S., Kimmel, D., Borgel, S., Carter, J., Dougherty, K. and Hollingshead, M. (2011). Real-time PCR-based assay to quantify the relative amount of human and mouse tissue present in tumor xenografts. BMC Biotechnology, 11(1), p.124.

[2] Alexandre Léchenet (2014). Business, éthique, légalité... Le séquençage de l'ADN en question (http://www.lemonde.fr/les-decodeurs/article/2014/08/18/le-sequencage-du-genome-comment-ca-marche_4472313_4355770.html) [Accessed 5 May. 2018]

[3] Clinical Pharmacogenetics Implementation Consortium (CPIC®),US Department of Health & Human Services (https://cpicpgx.org) [Accessed 4 Apr. 2018]

[4] Kim JY, Cheong HS et al. (2014). Screening for 392 polymorphisms in 141 pharmacogenes, Biomed Rep; 2 (4): 463–476 (http://europepmc.org/articles/PMC4051470)

[5] Laura Dean (2012). Clopidogrel Therapy and CYP2C19 Genotype, Medical Genetics Summaries (https://www.ncbi.nlm.nih.gov/books/NBK84114/)

[6] Legifrance.gouv.fr. (2018). Arrêté du 27 mai 2013 définissant les règles de bonnes pratiques applicables à l'examen des caractéristiques génétiques d'une personne à des fins médicales | Legifrance. [online] Available at: https://www.legifrance.gouv.fr/affichTexte.do?cidTexte=JORFTEXT000027513617&categorieLien=id [Accessed 10 May 2018].

[7] Reference, G. (2018). *What is genetic testing?*. [online] Genetics Home Reference. Available at: https://ghr.nlm.nih.gov/primer/testing/genetictesting [Accessed 23 Apr. 2018].

[8] Séquençage Genome (2011). Déterminisme génétique et liberté individuelle (http://www.sequencage-genome.com/determinisme-genetique-et-liberte-individuelle) [Accessed 5 Apr. 2018]

AUTHOR INFORMATION

The authors are all engineer students in biotechnologies at Sup'Biotech Paris.

All authors read and approved the final manuscript.

Preliminary tests for the development of a device to detect endocrine disruptors in water by enzyme extracts from *Pleurotus ostreatus*

Article authors: **AOUSJI Oumayma*, EL KASSIS Cyrille*, YOUSSOUF Tasrine*.**
With the participation of: **BERGER-PICARD Nicolas*, JULLIEN Agathe*, MUNCK Célia*, N'DOUBA-AVI Roxane*.**
Sup'Biotech, Villejuif, France
*Students at Sup'Biotech (Engineer school in biotechnologies)

Abstract – **Many daily life products and materials contain endocrine disruptors (EDs) that are a threat to the human health and the environment, notably through water contamination. The diversity of structure of EDs makes difficult to easily detect them in water. Even if EDs are a broad group of chemicals compounds, the main one contains aromatic groups, such as Bisphenol A, phthalates, polycyclic aromatic hydrocarbons (PAHs), polychlorinated biphenyls (PCBs), dichlorodiphenyltrichloroethane (DDT) (Garcia-Morales et al., 2015). By contrast to EDs, the Remazol Blue, an aromatic dye widely used in textile industry, is easily detectable (Palmieri, Cennamo, & Sannia., 2005).**

The aim of this study is to evaluate the substrate competition of some phenolic EDs and the Remazol Blue dye for lignolytic enzymes by following the rate of discoloration of the dye with the ultimate objective of being able to detect phenolic EDs (or even aromatic compounds) in water. Indeed, aromatic compounds may be degraded by lignolytic enzymes secreted by white-rot fungi as *Pleurotus ostreatus* which is known to produce high level of such enzymes, especially laccase. (Novotnýeněk et al., 2001)

In the first set of experiments, three different methodological approaches allowing to follow the discoloring of Remazol Blue dye by the specific oxidative enzymes produced by *Pleurotus ostreatus* have been compared in order to select the most relevant one for the competitive inhibition assay. In the second set of experiments, the discoloring of Remazol Blue in presence of Bisphenol A or ethinyl oestradiol has been evaluated.

The first results obtained of the enzymatic assay of Remazol Blue with the laccase showed a discoloration rate from 60% to 100% (80 µM of dye: 98.3%, 200 µM: 67.3%, 400 µM: 66.4%). Then, the addition of EDs showed a loss of degradation efficiency by oxidative enzymes. In Bisphenol A samples, at a dye concentration of 400µM, 27% of discoloration is observed, for a 400 µM EDs, whereas we can observe 40% of discoloration for an ED's concentration at 40µM while the control is at 45%. The same tendency is seen with the ethinyl oestradiol.

Index Terms – Endocrine disruptors, Competitive inhibition, Oxidative enzymes Laccase, Bisphenol A, Remazol Blue, *Pleurotus ostreatus*

INTRODUCTION

Endocrine disruptors (EDs) are chemical compounds which may interfere with the endocrine system and are highly suspected to be involved in reproductive system alteration as well as in increased incidence of some cancers. They are found in various materials such as food, cosmetics, seeds or polluted air (Cajthaml., 2015) and finally in water. Their ubiquity and potential damaging effects on health have made aware of the need to develop analytical tests in order to detect such compounds.

Pleurotus ostreatus is a white rot basidiomycete mushroom that secretes oxidative and hydrolytic enzymes (Jayasinghe et al., 2008). Through its capacity to produce oxidative enzymes such as laccase, lignin peroxidase or manganese peroxidase that degrade lignin, this fungus represents a serious potential alternative in the treatment of phenolic dyes and EDs from industrial wastewater (Dai, Wang, Chi, Wang, & Zhao, 2016). The laccase is a multicopper enzyme able to catalyze the oxidation of phenolic compounds (Palmieri et al., 2005). Enzymes secreted by *Pleurotus ostreatus* are able to degrade chemical complexes containing aromatic compounds mainly found in dyes and EDs. Remazol Blue is an azo dye largely used in the textile industry (Palmieri et al., 2005) that is biodegradable by *P. ostreatus* enzymes (Murugesan & Kalaichelvan, 2003). Articles also refer to this capacity of decomposition for EDs such as bisphenol A (BPA) and ethinyl oestradiol (Cajthaml., 2015).

The present project aims to develop a new analytical approach which should allow to rapidly and easily detect EDs in water. This analytical approach is based on the structural characteristic of EDs which are mostly aromatic structures. These aromatic structures are shared by components such as dyes, molecules easily detectable by spectrophotometry. The principle of the test we have developed is to create a substrate competition between EDs and dyes for specialized enzymes responsible for the degradation of aromatic structures. Two well-known endocrine disruptors are tested, the bisphenol A and the ethinyl oestradiol, a molecule mainly contained in the contraception pill (Cajthaml.,2015). As expected, we observed a competition between the two aromatic molecules, illustrated through a decrease of the degradation of the dye in the presence of EDs.

MATERIAL AND METHODS

1- FUNGAL STRAINS

Based on the bibliography six strains were studied (*Panus tigrinus*, *Polyporus picipes*, *Irpex lacteus*, *Trametes versicolor*, *Phanerochaete chryosporium*, and *Pleurotus ostreatus*), and *P. ostreatus* was chosen for its high production of laccase, its fast growth and its ability to degrade aromatic cycle. The strain of *P. ostreatus* used has been provided by the LRPIA and it was cultured on Malt extract agar for seven days at 28°C until the mycelium had colonized the agar plate.

2- PLEUROTUS OSTREATUS CULTURE AND ENZYMATIC EXTRACTION

The solid media was prepared by adding 10g of oat bran or sawdust in the corresponding Erlenmeyer. The sawdust media was produced by following a sawdust SFF protocol from the LRPIA. To obtain the Tween 20 solution at 0.01%, the dissolution of 50 µL of Tween 20 (Sigma Aldrich-P7949-100ML) at 100% in 50mL of distilled water was done. Then, the inducer solution that increases the propagation power of the fungi was developed by mixing 4mL of Tween 20 at 0.01% with 7.98 mg of CuSO4 (Sigma Aldrich-1027841000) at 1,25mM in a final volume of 40ml. In the aim of getting 65% humidity for each substrate, 18,56mL of the inducer solution was added in sawdust and oat bran Erlenmeyer. After having autoclaved for 20 minutes at 121°C, agar plugs per Erlenmeyer were added, from a fungal colony previously cultured in rice, used as inoculum. Finally, the Erlenmeyer had undergone incubation at 28°C for 10 days without any agitation or light. Once the fungus has grown, the enzyme was extracted from a sample of 10g of *P. ostreatus* that was mixed into an acetate sodium buffer. After the consecutive steps of agitation for 30 minutes at 30°C and centrifugation for 10 minutes at 4°C, the supernatant containing the enzymatic extract was kept at 4°C or -20°C according to the need for use.

3- REMAZOL BLUE PREPARATION

The Remazol Blue (Sigma Aldrich-R8001-25g) was prepared by dissolving Remazol Blue in pure water which gives a molar concentration of 0,0016M. The dissolution has been performed in CMR conditions. Once the Remazol was dissolved, a filtration using 2 kinds of filter (0.45 and 0.2 filter) has been done to sterilize the solution. The following scale of concentration was done:
80µM, 200µM, 400µM, 600µM, 800µM

4- BUFFER PREPARATION

Stock solutions of acetic acid and sodium acetate were prepared. Both were diluted in water in order to obtain a concentration of 50 mM. Then, the acetic acid solution

was added to the sodium acetate solution until a pH of 5,1 was reached. The pH was followed by a pH-meter.

5- THE 3 APPROACHES TO FOLLOW THE DISCOLORATION OF REMAZOL BLUE: SOLID MEDIA, LIQUID MEDIA, ENZYMATIC TESTING

5.1. Solid Media

In a 2L bottle, the solid media was prepared by adding 5g of Glucose (180 g/mol), 5g of Potassium nitrate (101,1 g/mol), and 0,0954g of Copper Sulfate (159,609 g/mol), weighted by a precision scale. Then, 0,75mL of Tween 20 have been added. The bottle is completed with distilled water until 1,5L. Finally, 22,5g of agar 1,5% was added and the bottle was autoclaved. Then, aliquots of dyes were prepared in order to obtain 3 different concentration: 25mg/L, 75mg/L, and 125mg/L, for the 3 different dyes. Once the dyes were added to the tubes 20 mL the medium were added, homogenized and poured into the Petri dishes. When the colored media was hardened, the fungi was added using a sterile inversed tip of 1000µL, an agar plug of the fungi was dived into the middle of the Petri dishes. The measurement of the halo formed by the digestion of the colorant by the fungi was then obtained by measuring the halo diameter in centimeter.

5.2. Liquid Media

In a sterile 50 mL falcon, the liquid agar media was added to the dye to obtain the concentration of interest for a total volume of 20mL. Then, 2 mL of the mix was loaded into a 6 well plate under the hood. Using a sterile inversed tip of 1000µL, an agar plug of the fungi was dived into the well using a sterile toothpick. The 6 well-plate was incubated at 30°C. Sample was obtained by pipetting 200µL of the media (in a way to avoid taking fungi with the media). The 200µL was transferred into a 96 well-plate to perform a measurement of wavelength to determine the discoloration.

5.3. Discoloration of Remazol Blue using crude enzyme extract

The supernatant containing the enzymatic crude extract can be stored at -4°C or at -20°C if not used immediately. By following the plate plan, the dye solution and citrate sodium buffers were added at the adequate concentration and the calculated volume. Finally, the enzyme was added to each well. After that, the absorbance of samples was taken every 15 minutes at 592 nm.

6- ENDOCRINE DISRUPTORS PREPARATION

Firstly, some tests of dissolution in water were required. The bisphenol A is a molecule that is poorly soluble in water. So, to obtain a solution of Bisphenol A, different ethanol's percentages were tested in the solution. Four concentrations (400µM, 200µM, 80µM and 40µM) were established for the endocrine disruptor. For a concentration of 400µM of bisphenol A, 10% of ethanol in the mother solution was used.

The solution of oestradiol of 400µM is prepared by dissolving 4,5mg of oestradiol in a 20% ethanol solution.

7- COMPETITIVE INHIBITION ASSAY USING ENDOCRINE DISRUPTORS

In a 96-well plate, the effect of the endocrine disruptors on the dye degradation was tested. As a dye, the degradation of the dye with the enzyme alone, was used, also the effect of the enzyme on endocrine disrupters alone, and finally each component by itself. To test the effect of the endocrine disrupters on the reaction, they were added to obtain a competitive degradation with the ligand of the laccase. The Bisphenol A was dissolved and diluted at 10% of ethanol in water and the ethinyl oestradiol at 20%. These percentages were identified as a percentage under the limit (20%) for which the Bisphenol A and the ethinyl oestradiol are still dissolved and the ethanol has no significant effect on the dye degradation by the laccase.

RESULTS AND DISCUSSION

1- DISCOLORATION OF REMAZOL BLUE IN LIQUID MEDIA

The liquid media test was performed by adding the *P. ostreatus* in the media containing Remazol Blue. As it can be observed on the pictures above (Figure 1), the control test shows that the Remazol Blue in the media do not degrade naturally but can form some precipitation. In the case of the sample it can be observed a high degradation of the Remazol Blue of the media in 4 days. After 25 days the dye has almost been completely

degraded. The results obtained by the absorbance were distorted (so they have not been presented in this article) by the presence of the precipitation that impacts the absorbance lecture. This technique could be used but the formation of the precipitation is an obstacle to the quantification and determination of the efficiency of the technique. The liquid media could be an interesting way if the quantification was done properly.

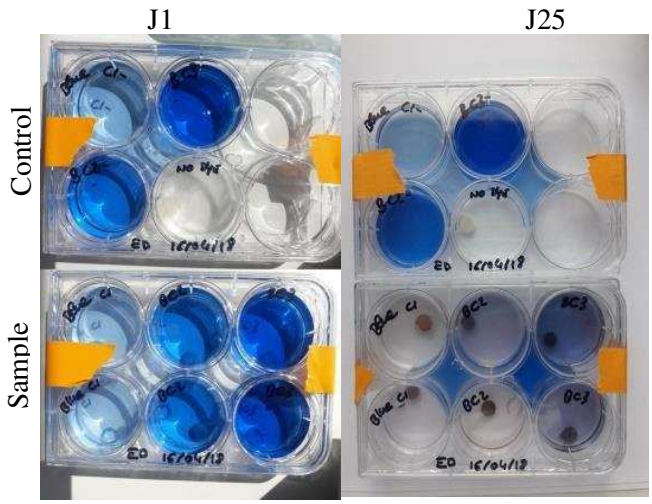

Figure 1: Plates at day 1 (J1) and day 25 (J25) with different concentrations of Remazol Blue (80µM, 200µM, and 400µM) showing discoloration of the dye due to the effect of the laccase, the enzyme released by *P. ostreatus*.

2- DISCOLORATION OF REMAZOL BLUE IN SOLID MEDIA

The pictures (Figure 2) and the histogram (Figure 3) showed the action of fungi on the degradation of Remazol Blue in a solid medium. A discolored halo had been appearing since the first day of culture and increased considerably by the time. The fungus also developed through days. A filamentous structure arose and grew from the plug at the center of the agar plates.

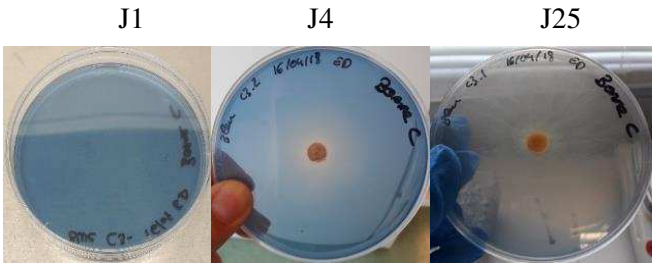

Figure 2: Plates at J1, J4, and J25 with Remazol Blue showing discoloration of the dye due to the effect of the enzyme released by P. ostreatus in a solid medium.

The results suggested that the degradation of the dye is correlated to the growth of fungi. Furthermore, the picture shows 100% of degradation of the dye in 25 days of culture which is an impressive and promising result for this pathway. However, it can be limited by the quantification factor (the halo diameter).

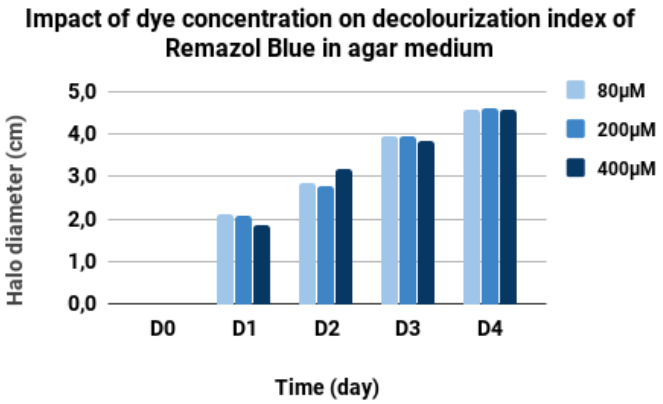

Figure 3: Impact of dye concentration (80µM, 200 µM, and 400 µM) on discoloration index of Remazol Blue in agar medium.

3- DISCOLORATION OF REMAZOL BLUE USING CRUDE ENZYME EXTRACT RESULTS

A significant degradation of the Remazol Blue dye was observed for each concentration in presence of enzyme extract (Figure 4). After 15 hours of incubation, between 60% to almost 100% of dye was decolorated. A positive correlation was observed between the rate of discoloration of each dye and the amount of enzymatic extract. Hence, the enzymes of fungi are responsible for the dye discoloration.

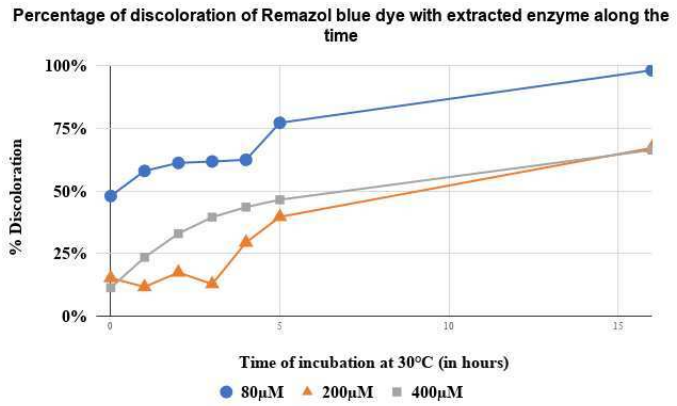

Figure 4: Percentage of discoloration of Remazol Blue dye with extracted enzyme according to the time.

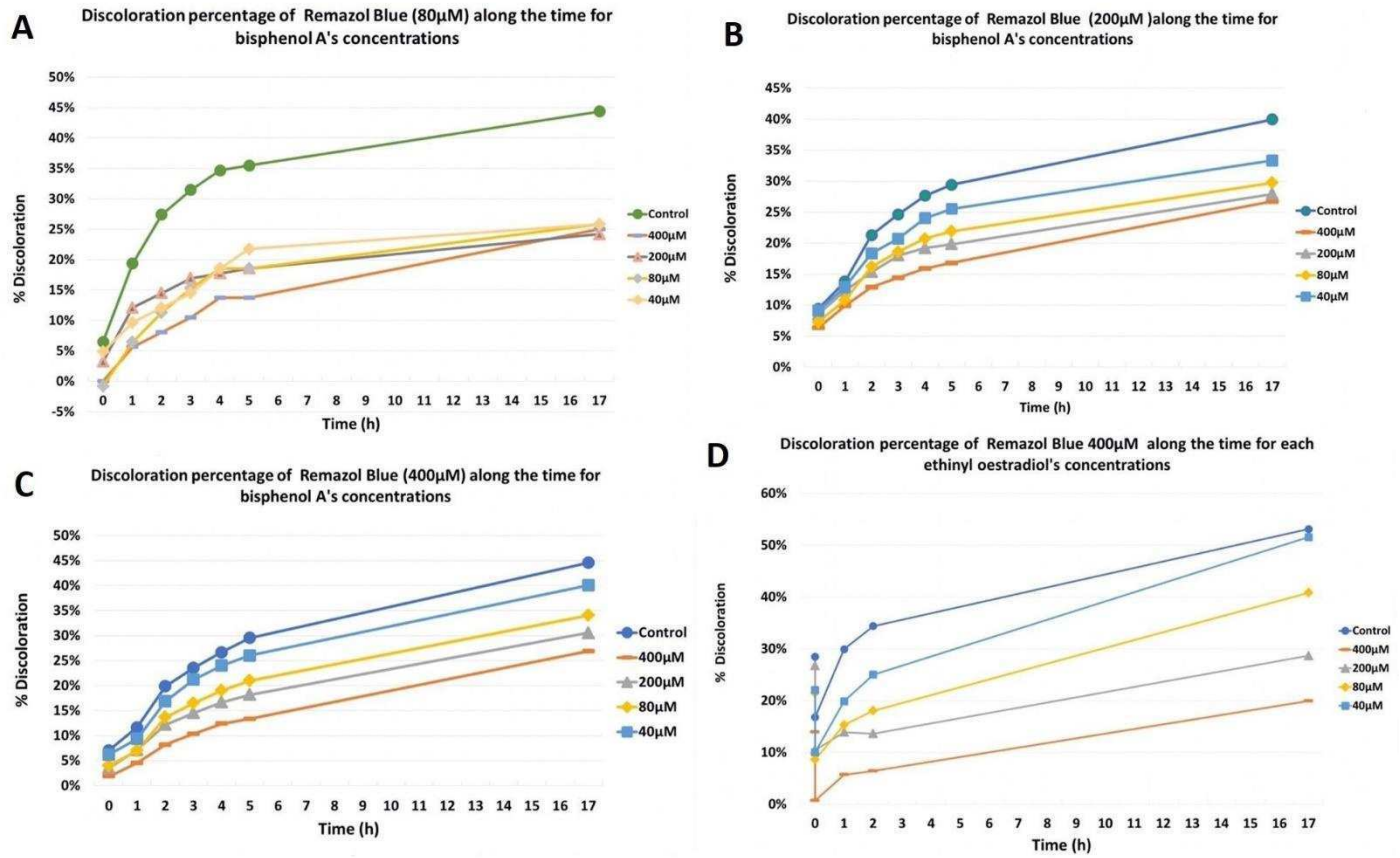

Figure 5: A) Percentage of discoloration of Remazol Blue 80µM in function of time for each Bisphenol A concentration 400µM, 200µM, 80µM and 40µM. B) Percentage of discoloration of Remazol Blue (200µM) in function of time for each Bisphenol A concentration 400µM, 200µM, 80µM and 40µM. C) Percentage of discoloration of Remazol Blue (400µM) in function of time for each Bisphenol A concentration 400µM, 200µM, 80µM and 40µM. D) Percentage of discoloration of Remazol Blue (400µM) along the time for each ethinyl estradiol concentration 400µM, 200µM, 80µM and 40µM.

4- RESULTS OF THE ENDOCRINE DISRUPTORS IMPACT ON THE ENZYMATIC DEGRADATION OF THE DYE

4.1. Impact of Bisphenol A

80µM of dye: In the case of the weakest concentration of dye, the percentage of discoloration is highly impacted in the presence of endocrine disruptors (for all the concentrations tested) (Figure 5A). In fact, after 15 hours of reaction, the tested EDs concentrations converge to 25% of discoloration, which correspond to only the half of the control (which reach 44% of discoloration).

200µM of dye: In the case of the second concentration of colorant tested, the same phenomenon as for a concentration of 80µM (Figure 5A) was observed. It was observed that in the presence of ED, the discoloration of the sample is still impacted (Figure 5B). But in that case, we can observe a concentration dependent phenomenon. The more ED we have, the more the discoloration is inefficient. For a concentration of 400µM, 27% of discoloration is reached and for a concentration of 40µM, 33% of discoloration is reached when the control reaches 47%. The difference of impact between 400µM, 200µM, and 80µM is not relevant.

400µM of dye: For the most concentrated sample, the same phenomenon can be observed, and the concentration impact is also shown (Figure 5C). The more ED is present, the more the laccase seems inefficient to degrade the Remazol Blue. A gradient of discoloration is clearly observed proportionally to the ED concentration. It has been highlighted for 400µM: 27% of discoloration, for 200µM: 31%, for 80µM: 33% and finally for 40µM the lowest concentration of ED, 40% of discoloration is observed while the control

is at 45%. The results obtained and described just before are promising. Indeed, it seems that the laccase is sensitive to the presence of endocrine disputer either by inactivate or disrupt the laccase activity or either by being a ligand and so been a competitive ligand leading to a slowdown of the reaction of the degradation. More studies are needed to understand the phenomenon but for now these results are promising in the objective of creating a small test for detection of EDs into water. Furthermore, even the smallest concentration of EDs has a quantitative impact which can be interesting by taking sample in usual used water which could contain very small quantities of ED and still be capable to detect this infinitesimal quantity.

4.2. Impact of Ethinyl oestradiol

To verify and to confirm the tendency of endocrine disruptor impact on the discoloration of Remazol Blue, the ethinyl oestradiol was tested such as the BPA. The enzymatic test was made with four different concentrations of EDs. Results proved that both kind of EDs have the same trend of discoloration (Figure 5D). The sample containing the highest concentration of ethinyl oestradiol (400µM), has the lowest percentage of discoloration with 20% at 17h and the sample with a concentration of 40µM has a final percentage close from the control with 52% at the same time. The samples having concentration of 200µM and 80µM have respectively 29% and 41% at 17h. It is noticed that during the first minutes of reaction, as opposed to the BPA's test, there is for each concentration a sharp decrease of discoloration's percentage. This phenomenon has been associated to the time of homogenization required before that the reaction occurs.

CONCLUSION

The results showed efficient degradation of the Remazol Blue for the 3 methods of discoloration. The enzymatic assay seems to be the most adequate experiment as it displayed the faster action of degradation with non-diluted enzyme extract. We demonstrated that the development of fungi and especially their enzymes are responsible for the degradation of cyclic molecules such as dyes. Outcomes of Remazol Blue may be negatively impacted by the precipitation of the dye in liquid media. This phenomenon can be the result of the addition of surfactants in commercial azo dyes. A too high concentration of dye induces the formation of aggregate at the bottom (Ribeiro & Umbuzeiro., 2014). Furthermore, the results obtained by the competitive degradation between EDs and the Remazol Blue have shown a decrease of the capacity of the Lignolytic enzymes to degrade the Remazol Blue, mostly on a long-term evaluation (15h). The results are positive for an approach of EDs detection by a simple colorimetric technic. These results help to define new perspectives as the combination of the EDs, and the study of the role of the EDs in the degradation of Remazol Blue and their impact on the laccase. Some perspectives can also be expected with these results as for example a device that can be used to detect, in daily used water, dangerous endocrine disrupter easily.

ACKNOWLEDGMENT

We want to thank Agnès Saint-Pol, Valentina Glicorijevic and Jacqueline Bert, for their advices and for guiding us in this fascinating project. It was a real pleasure to work on it.

REFERENCES

Cajthaml, T. (2015). Biodegradation of endocrine-disrupting compounds by ligninolytic fungi: Mechanisms involved in the degradation. *Environmental Microbiology*, *17*(12), 4822–4834. https://doi.org/10.1111/1462-2920.12460

Dai, J., Wang, H., Chi, H., Wang, Y., & Zhao, J. (2016). Immobilization of laccase from Pleurotus ostreatus on magnetic separable SiO2support and excellent activity towards azo dye decolorization. *Journal of Environmental Chemical Engineering*, *4*(2), 2585–2591. https://doi.org/10.1016/j.jece.2016.04.037

Garcia-Morales, R., Rodríguez-Delgado, M., Gomez-Mariscal, K., Orona-Navar, C., Hernandez-Luna, C., Torres, E., … Ornelas-Soto, N. (2015). Biotransformation of Endocrine-Disrupting Compounds in Groundwater: Bisphenol A, Nonylphenol, Ethynylestradiol and Triclosan by a Laccase Cocktail from Pycnoporus sanguineus CS43. *Water, Air, and Soil Pollution*, *226*(8), 1–14. https://doi.org/10.1007/s11270-015-2514-3

Jayasinghe, C., Imtiaj, A., Lee, G. W., Im, K. H., Hur, H., Lee, M. W., … Lee, T. (2008). s e m y z n E c i t y l o n i n g i L f o n o i t c u d o r P e h t d n a i g n u F t o R e t i h W y b s e y D c i t a m o r A e e r h T f o n o i t a d a r g e D, *36*(2), 114–120.

Murugesan, K., & Kalaichelvan, P. T. (2003). Synthetic dye decolourization by white rot fungi. *Indian*

Journal of Experimental Biology, *41*(9), 1076–1087. https://doi.org/10.1137/1.9781611974331.ch50

Novotnýeněk, Rawal, B., Bhatt, M., Patel, M., Šašek, V., & Molitoris, H. P. (2001). Capacity of Irpex lacteus and Pleurotus ostreatus for decolorization of chemically different dyes. *Journal of Biotechnology*, *89*(2–3), 113–122. https://doi.org/10.1016/S0168-1656(01)00321-2

Palmieri, G., Cennamo, G., & Sannia, G. (2005). Remazol Brilliant Blue R decolourisation by the fungus Pleurotus ostreatus and its oxidative enzymatic system. *Enzyme and Microbial Technology*, *36*(1), 17–24. https://doi.org/10.1016/j.enzmictec.2004.03.026

Role of epigenetic processes in the cellular regeneration of *Platynereis dumerilii*

Tom Agnero-Rigot*, Camille Kergaravat*, Edouard Riey*, Erwan Martin*
Corresponding author: camillekergaravat@gmail.com
*Sup'Biotech, Villejuif

ABTRACT- Regeneration of body part is a phenomenon that has interest scientist for centuries. Epigenetic processes have a significant impact on gene expression and therefore potentially on regeneration. In this study we aim at investigating if epigenetic mechanisms are involved in regeneration process of the worm *Platynereis dumerilii***. Using drugs, three epigenetic mechanisms were inhibited during this study: DNA methylation, acetylation and methylation of H3K27. Worms were amputated and then, incubated in drugs during 5 days. Morphology of the posterior part was observed every day and scored according to the regeneration stage that has been reached. We showed though these experiments that DNA methylation and acetylation of H3K27 could be implicated in the regeneration of Platynereis** *dumerilii***.**

Key words: Regeneration, *Platynereis dumerilii*, Epigenetics

INTRODUCTION

Every animal species can regenerate from wounds and from trauma in some extend by replacing damaged cells in the tissues (Carlson, 2007). Nevertheless, some animals have developed more efficient regeneration processes to restore entire body parts.Cold blooded animals can regenerate lost locomotor limbs. Many reptiles and amphibians present important regeneration ability. They can use it as a defense mechanism doing autotomy to avoid predators (Carlson, 2007). This evolutive advantage has been conserved throughout generations. Two forms of regeneration have been described.
The first one called epimorphosis refers to a regeneration by a blastema formation made of undifferentiated cells. Following a wound, blastema will be formed and the stem cells composing it will proliferate, differentiate, and restore the lost parts. Morphallaxis by contrast is a rearrangement of existing cells in order to regenerate the injured area (Agata et al., 2007)

Platynereis dumerilii is an interesting model organism used in biology and genetics. It is a small worm with a life cycle that can be reproduced in laboratory (Planques et al., 2018). They are stored in seawater and the breeding is done in rooms that reproduce the moon light phases. (Fischer and Dorresteijn, 2004).

Furthermore, this worm possesses a fast-growing period coupled with tiny needs and the possibility to reach a large number of individuals within a simple plastic box.

Platynereis dumerilii presents other advantages. It is an invertebrate, so there is no restrictive regulation for its use in scientific experiments. On the other hand, the regeneration pattern of the worm has been already experimented and documented (Planques et al., 2018).
In addition, treatments can be easily administered to the worm by adding drugs in its medium (sea water).
Although it is a recent model organism, its ease of manipulation and its homogenous phenotype has lead to the development of many experiments for evolutionary developmental comparisons and cellular analyzes (Planques et al., 2018).
Genetics can be studied with this species by performing targeted mutagenesis, stable transgenesis, and conditional cell ablation in both swimming larvae and adult worms (Raible and Tessmar-Raible, 2014).

Epigenetics is the changes in the genes expression without any changes in the genome sequence. These changes are notably produced by DNA methylation and various modifications of histones proteins. Histones are involved in DNA folding and compacting. The modifications of the histone protein include acetylation, methylation, ubiquitylation, phosphorylation, sumoylation, ribosylation and citrullination The modification of histones proteins results in repression or overexpression of genes by changing the conformation of histones during the transcription process. (Sadakierska-Chudy and Filip, 2015).

DNA methylation, catalyzed by the DNA methyltransferases (DNMTs) is a key player in epigenetics because of its ability to regulate gene expression by recruiting proteins involved in gene repression or by inhibiting the binding of transcription factor(s) to DNA (Jin et al., 2011). Histone methylation is the addition of one to three methyl groups to a Lysine or an Arginine. Depending on the site and the number of methyl added, histone methylation can increase or decrease gene expression. Methylation of H3K4, for instance, correlates with gene activation in most systems, whereas H3K9 and H3K27 methylations are described as gene repressors (Okamura et al., 2010). Demethylation is the opposite process and can also induce the same effects. Histone acetylation is the addition of an acetyl group on a Lysine group. It can increase gene expression by activation of gene transcription (Okamura et al., 2010). Deacetylation is the opposite process and can also induce the same consequences.

To investigate the possible implication of epigenetic processes in the regeneration of *Platynereis dumerilii,* we exposed amputated worms to drugs treatment inhibiting epigenetic mechanism.

Experiments have been conducted to study the link between epigenetics and animal regeneration. In 2015, Hayashi et al. has shown a relationship between trimethylation of H3K27 and limb bud regeneration in *Xenopus laevis* tadpoles by inhibiting the trimethylation of H3K27 with DZNep treatment.

Three drugs were tested in this study. An inhibitor of DNA methylation, the 5-aza-2'-deoxycytidine(Kwon et al., 2017), C646 an inhibitor of the acethylation of H3K27. More precisely this drug blocks the activity of the histone acetyltransferase (HAT), which is responsible for the actetylation of H3K27(Wu et al., 2017). Finally, we suspended the methylation of the H3K27 by treating worms with DZnep.

MATERIALS AND METHODS

Culture of *Platynereis dumerilii*

P. dumerilii worms were obtained from a breeding culture established in the Institut Jacques Monod, according to the protocol of Dorresteijn et al. (1993).

Selection and amputation of the worms

Worms from 3 to 4 months old with 30 to 40 segments were used. They were anaesthetized in a MgCl2 7.5% with sea water solution (ratio 1 :1). Sharp amputation of their posterior part by 1/6 of their body length were performed using a micro-knife (SharpointTM). The amputation was done perpendicularly to the body axis between two segments. After amputation worms were treated with drugs or controls (DMSO 1% or sea water).

Drug treatments

Different epigenetic process were blocked using inhibitors: DZNep (Sigma ML0305), C646 (Sigma ML0002) and 5-Aza-2'-deoxycytidine (Sigma A3656). Drugs were dissolved in sea water from DMSO stock solutions at 1 mM for DZNep, 10 mM for C646 and 5-Aza-2'-deoxycytidine. Each drug and control were renewed daily to ensure activity. DZNep solutions were tested on worms at 1, 5 and 15 µM; C646 at 1, 5 and 15 µM; 5-Aza-2'-deoxycytidine at 10, 50 and 100 µM. Worms were incubated in 2 mL of drug treatment or control in 12-wells plate for 5 days.

Scoring and statistical analysis

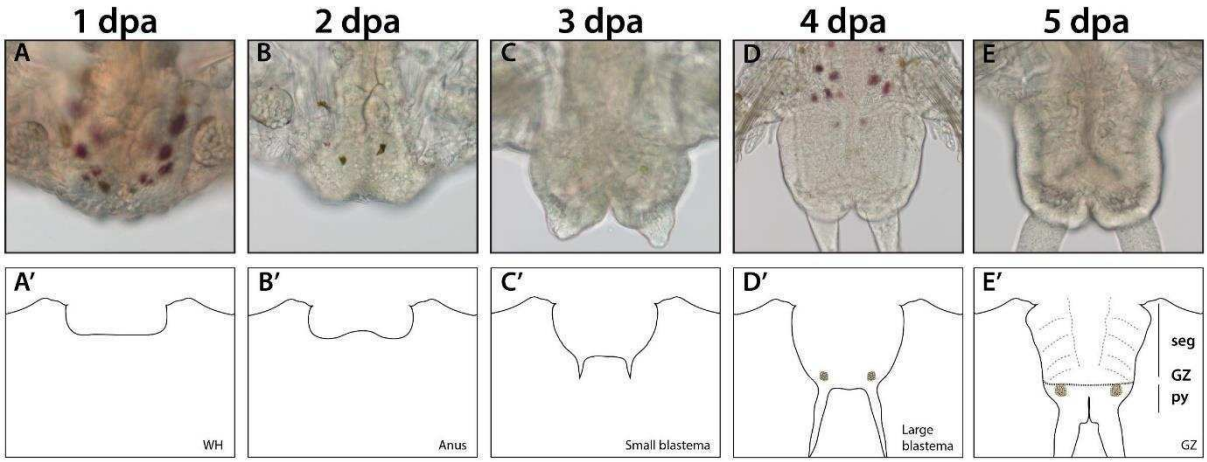

Figure 1: Bright-field microscopy images and schematic representations of the five stages of regeneration. In normal conditions those stages should be reached at 1,2,3,4 and 5 days post-amputation, respectively (DPA). Adapted from Planques and al (2018)

The worm posterior parts were observed under the dissecting microscope every day and scored according to the regeneration stage that has been reached (Figure 1). There were four different dissecting microscopes and observers. To avoid variability in scoring, some worms were observed and score by several persons. Some worms showed a morphology that was intermediate, between two successive stages and were therefore scored as 1.5, 2.5, 3.5, and 4.5 (Planques et al.).
Graphic representations of morphological experiments and statistical analysis were performed using the Prism 7 software (GraphPad).

2- way ANOVA on 2 factors repeated measures using Dunnett correction was performed. Worms which died during experiment were removed from statistical analysis as well as the worms which showed aberrant morphology, probably due to toxicity of the drugs.

Toxicity test

Non-amputated worms were incubated in 2mL of drug treatment (same drugs and concentration as the amputated ones) in 12 wells-plate for 5 days. Drugs were renewed, and worms observed every day to determine if they showed abnormal morphological changes such as self-amputation of their posterior part, loss or deterioration of their head and anal tentacles.

RESULTS:

Drug	Self-amputation (%)	Death (%)	Anal tentacles deteriorated (%)
DZNep 1 µM	100	100	100
DZNep 5 µM	83	50	83
DZNep 15 µM	83	83	100
5-aza 10 µM	50	0	100
5-aza 50 µM	33	0	100
5-aza 100 µM	17	0	50
C646 1 µM	17	0	67
C646 5 µM	17	0	67
C646 15 µM	17	0	83

Table 1: Table showing the morphological incidence of each drug on non-amputated worms (n=6 for each drug). Self-amputation refers to the abnormal loss of segments at the posterior part of the worms. Anal tentacle deterioration expresses a loss or a shortening of one or several tentacles.

Drug toxicity

To determine the toxicity of the drugs, non-amputated worms were incubated in drugs. DZNep, C646 and 5'aza solutions were tested on worms. Worms were incubated in 2 mL of drug treatment or control in 12-wells plates for 5 days. DZNep showed a high toxicity profile with a death rate between 53% and 100% for the three concentrations. The worm death usually happened after the animal self-amputation. 5-aza seems less toxic than DZNep with no death, however we can observe that this drug causes self-amputation and the deterioration of the anal tentacles for all the concentration. We observed the same profile for C646. The C646 drug remains toxic but less than the two other drugs with a low ratio of self-amputation and anal tentacles deterioration.

Nevertheless, the deterioration of the anal tentacles and the self-amputation of worms prove that these drugs are toxic for *Platynereis dumerilii*. Table 1 shows that every drug has a morphological impact on posterior part of non-amputated worms, and it must be considered in the interpretations of the results of our experiments.

To test the hypothesis, that epigenetic processes are involved in the regeneration of *Platynereis dumerilii,* worms where treated with drugs inhibiting epigenetic process and analyzed their effects on regeneration. They were put immediately after amputation in three different drugs for five days and scored the worms every day for the stage that has been reached. For statistical analysis dead or auto-amputated worms where removed.

DNA methylation

To test the involvement of DNA methylation, worms were incubated with different concentration of a DNA methylation inhibitor: 5-aza. For the three used concentrations, the worms' regeneration was delayed compared to the control, especially for the 100 µM concentration (Fig.2 (A)). At 5dpa the controls were at stage 3 to 4 whereas the treated worms were at stage 2 maximum. We can note that the delay starts at 2dpa, indeed at 1dpa controls like treated worms reached stage 1. This finding suggest that methylation of DNA is a mechanism involved in the regeneration of *Platynereis dumerilii* from 2 days after amputation.

Acetylation of histone

We incubated worms with C646, an inhibitor of H3K27 acetylation. Most of the worms treated at 15 µM reached the stage 1 or 2 (Fig.2B). The worms treated at 5 µM were slightly delayed compared to the controls, at 5 dpa they reached on average the stage 3. The 1 µM treated worms had similar score to control worms. We can highlight that the delay for the two higher concentrations occurs since 3 dpa. Indeed, the three used concentrations and the controls have the same profile until 2 dpa. On the other hand, a high mortality was observed in the 15 µM group representing 43% of the population. Therefore, we can assume that the H3K27 acetylation is involved in the regeneration process of *Platynereis dumerilii*.

Methylation of histone

To assess the implication of methylation of histone in the regeneration process of *Platynereis dumerilii,* worms were treated with DZnep an inhibitor of H3K27 methylation. The drug was highly toxic for the animals with the death of 77%, 47%, 43% of worms for respectively 1 µM, 5 µM and 15 µM concentrations. In the remaining population we observe for the three conditions that the regeneration is blocked compared to the controls (Fig.2C). At 5 dpa treated worms reached the stage 2 maximum whereas the controls were at stage 4 on average. It shows that worms are blocked between the regeneration stage 2 and 3. Despite those results further study are required to conclude about the implication of H3K27 methylation in regeneration of *Platynereis dumerilii* due to the loss of the majority of our individuals.

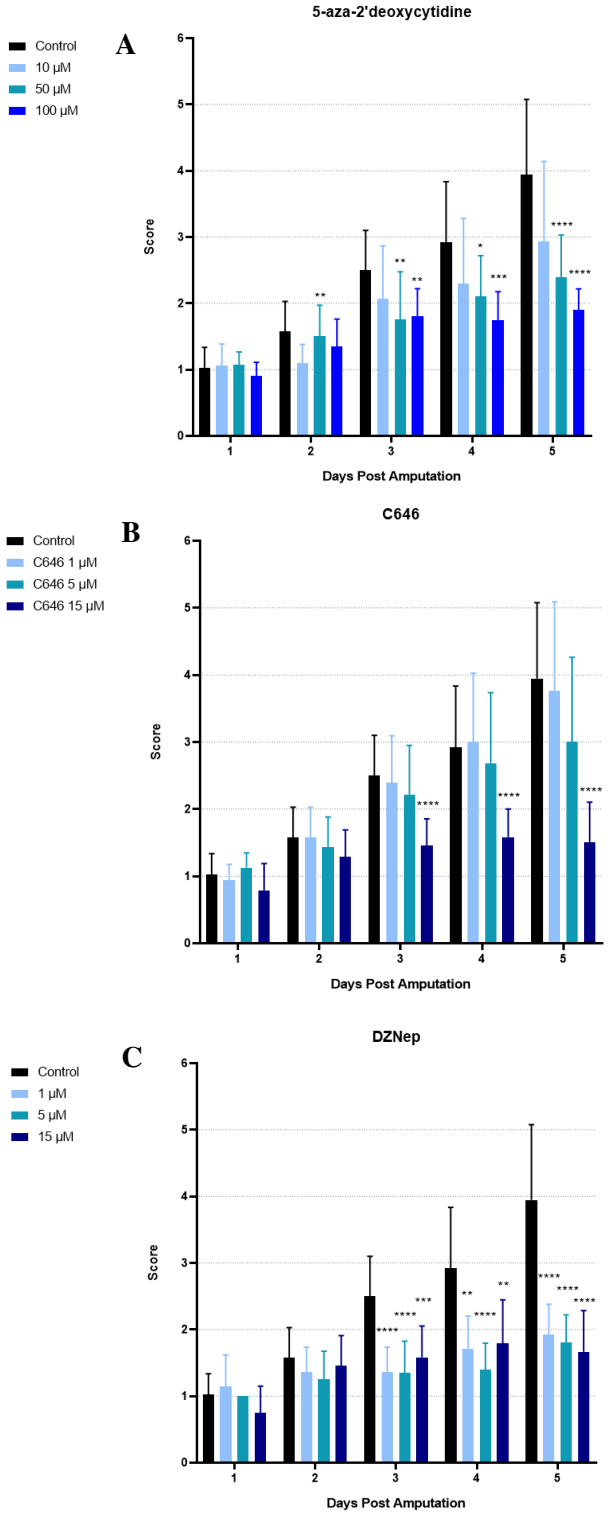

Figure. (2): Bar charts, which shows the developmental stage reach 1, 2, 3, 4 and 5 days post amputation. Morphological observations were performed every 24h under microscope. n represent the number of worms showed in the graphs. (A) Worms were treated with 5-aza-2'deoxycytidine at 10 (n=15), 50 (n=19) and 100 (n=10) µM concentrations (B) Worms were treated with C646 at 1 (n=19), 5 (n=16) and 15 (n=12) µM concentrations (C) Worms were treated with DZNep at 1 (n=7), 5 (n=10) and 15 (n=12) µM concentrations.

DISCUSSION

In order to investigate the different epigenetic mechanisms involved in the *Platynereis dumerilii* regeneration we treated a worm population with different drugs. We inhibited DNA methylation with 5-aza-2' deoxycytidine. Our results suggest that this mechanism is implicated in the regeneration of the worms specially two days after amputation. They could not reach the regeneration stage 3, even 5 days after amputation.
We repressed the acetylation of H3K27 with C646. We showed in this experiment that the acetylation of H3K27 seems to be important for the regeneration at 3dpa, moreover for the highest concentration no stage 3 was reached.
We blocked the methylation of H3K27 with DZnep. In this case the regeneration seemed to be blocked before the stage 3. Unfortunately, we had a mortality rate between 43% and 77% for each different concentration, which does not permit a conclusion about the role of methylation of H3K27 in the regeneration of *Platynereis dumerilii.* Although another study on the zebrafish tad pod using DZnep suggests that methylation of H3K27 is involved in the regeneration of amputated limb(Hayashi et al., 2015).

Establishing definitive conclusions was complicated by the toxicity of the drugs for our models. Indeed, the three drugs caused the death or the self-amputation of some non-amputated and amputated worms.

DZnep was the most toxic one with a minimal of 43% death rate by experiment. C646 and 5-aza-2' deoxycytidine also showed some toxicity by the alteration of anal tentacles of non-amputated worms. There were dead worms in the amputated population too. Regarding those toxicity issues, we must be careful in the interpretation of our results.

Furthermore, the used treatments are not 100% specific and can have off targets side effects (Miranda et al., 2009). Thus, it is difficult to figure out if the blockages are due to the toxicity of the drug or due to the inhibition of epigenetic processes. However, working with living models implies a natural variability and some unexpected results.

To confirm our results about the implication the different epigenetic mechanisms implicated in the regeneration of *Platynereis dumerilii* we should use different drug treatments inhibiting the same mechanism but targeting different molecular pathways. We performed a first test with RG-108 on worms to support the hypothesis that methylation of DNA is implicated in regeneration. More experiments and samples are needed to obtain significant statistical power in order to exploit the results and then conclude. Similarly, we should find other treatment of each studied mechanism.

Another option could be to use siRNAs to shut down the genes, which were inactivated by our epigenetic modifications. This technic could permit to minimize off target side effects and worms death.

ACKNOWLEDGMENT

We would like to thank the "Stem cells, development and evolution" team at the Jacques Monod Institute for receiving us at their laboratory for this project.
We are grateful to Anabelle Planques for her help and advices during our experiments and for the time she dedicated to help us in the redaction of this article.

REFERENCES

Agata, K., Saito, Y., Nakajima, E., 2007. Unifying principles of regeneration I: Epimorphosis versus morphallaxis: Unifying principles of regeneration. Dev. Growth Differ. 49, 73–78. https://doi.org/10.1111/j.1440-169X.2007.00919.x

Carlson, B.M. (Ed.), 2007. Principles of regenerative biology. Elsevier/Academic Press, Amsterdam ; Burlington, Mass.

Fischer, A., Dorresteijn, A., 2004. The polychaetePlatynereis dumerilii (Annelida): a laboratory animal with spiralian cleavage, lifelong segment proliferation and a mixed benthic/pelagic life cycle. BioEssays 26, 314–325. https://doi.org/10.1002/bies.10409

Hayashi, S., Kawaguchi, A., Uchiyama, I., Kawasumi-Kita, A., Kobayashi, T., Nishide, H., Tsutsumi, R., Tsuru, K., Inoue, T., Ogino, H., Agata, K., Tamura, K., Yokoyama, H., 2015. Epigenetic modification maintains intrinsic limb-cell identity in Xenopus limb bud regeneration. Dev. Biol. 406, 271–282. https://doi.org/10.1016/j.ydbio.2015.08.013

Heerboth, S., Lapinska, K., Snyder, N., Leary, M., Rollinson, S., Sarkar, S., 2014. Use of Epigenetic Drugs in Disease: An Overview. Genet. Epigenetics 6, GEG.S12270. https://doi.org/10.4137/GEG.S12270

Jin, B., Li, Y., Robertson, K.D., 2011. DNA Methylation: Superior or Subordinate in the Epigenetic Hierarchy? Genes Cancer 2, 607–617. https://doi.org/10.1177/1947601910393957

Kwon, H.-M., Kang, E.-J., Kang, K., Kim, S.-D., Yang, K., Yi, J.M., 2017. Combinatorial effects of an epigenetic inhibitor and ionizing radiation contribute to targeted elimination of pancreatic cancer stem cell. Oncotarget 8. https://doi.org/10.18632/oncotarget.21642

Michael F. W. Festing; Design and Statistical Methods in Studies Using Animal Models of Development, ILAR Journal, Volume 47, Issue 1, 1 January 2006, Pages 5–14, https://doi.org/10.1093/ilar.47.1.5

Miranda, T.B., Cortez, C.C., Yoo, C.B., Liang, G., Abe, M., Kelly, T.K., Marquez, V.E., Jones, P.A., 2009. DZNep is a global histone methylation inhibitor that reactivates developmental genes not silenced by DNA methylation. Mol. Cancer Ther. 8, 1579–1588. https://doi.org/10.1158/1535-7163.MCT-09-0013

Okamura, M., Inagaki, T., Tanaka, T., Sakai, J., 2010. Role of histone methylation and demethylation in adipogenesis and obesity. Organogenesis 6, 24–32.

Planques, A., Malem, J., Parapar, J., Vervoort, M., Gazave, E., 2018. Morphological, cellular and molecular characterization of posterior regeneration in the marine annelid Platynereis dumerilii. Dev. Biol. https://doi.org/10.1016/j.ydbio.2018.11.004

Raible, F., Tessmar-Raible, K., 2014. Platynereis dumerilii. Curr. Biol. 24, R676–R677. https://doi.org/10.1016/j.cub.2014.06.032

Sadakierska-Chudy, A., Filip, M., 2015. A Comprehensive View of the Epigenetic Landscape. Part II: Histone Post-translational Modification, Nucleosome Level, and Chromatin Regulation by ncRNAs. Neurotox. Res. 27, 172–197. https://doi.org/10.1007/s12640-014-9508-6

Wu, Y., Ma, S., Xia, Y., Lu, Y., Xiao, S., Cao, Y., Zhuang, S., Tan, X., Fu, Q., Xie, L., Li, Z., Yuan, Z., 2017. Loss of GCN5 leads to increased neuronal apoptosis by upregulating E2F1- and Egr-1-dependent BH3-only protein Bim. Cell Death Dis. 8, e2570. https://doi.org/10.1038/cddis.2016.465

The use of biosourced inputs for hydroponic culture of aromatic herbs

Jean-Rémi Loup, Nicolas Merieux, Julia Naudin, Claire Persyn*
Sup'Biotech, Villejuif, France

*Corresponding author : claire.persyn@supbiotech.fr

Abstract - **Hydroponic is a new trendy technique for plant growth in limited and uncultivable areas. It uses a nutritive solution sputtered onto plants' roots, giving them necessary nutrients to grow. The company Aeromate is using this technique for aromatic plant culture on Paris' roofs. Aeromate also wish to share this practice with particulars. Currently, the nutritive solution used for this kind of culture is made from petrochemical inputs. In collaboration with Aeromate, the presented project aims to find a biosourced nutritive solution to be more environmentally-friendly and locally available. The nutritive solutions were then thought to come from organic and green wastes. Four mixes were prepared and tested in a hydroponic prototype. Compared to traditional mineral imputs, a solution composed of compost and lemon juice showed promising results. A new prototype was built, and an easier solution composed of vermicompost juice was tested, still compared to the chemical solution. Observations are optimistic and show plant growth in both cases. The present study shows that using biosourced nutritive solutions in the hydroponic technique is a promising way to develop a new urban agriculture accessible to everyone.**

Index Terms - Biosourced, Hydropony, Biopony, Nutritive solutions, Agriculture

INTRODUCTION

Hydroponic is an off-ground technique where plants are not cultivated in soil but in an inert substrate[1]. The nutrients are provided by the regular irrigation of this substrate. The nutritive solutions transport the nutrients in the form of dissolved salts that will be taken up by plants. This technique works for flowers, herbs, and veggies, and has a lot of benefits compared to traditional techniques. Plants grown in hydroponic system receive a more balanced diet and are less in contact with soil borne pests, fungi and diseases. It also reduces the number of troublesome weeds, so herbicides are less needed. In addition, there is a better yield, a lower turnaround time between planting and a decrease for the crop maturation cycle[2]. The current trend is to develop this kind of techniques to improve the agricultural industry. The company Aeromate, for example, wants to improve the cities environment for all, thanks to urban agriculture. However, nutritive solutions currently used in hydroponics systems are made of petrochemical, mineral inputs, which are harmful for the environment. There is a need for a more eco-friendly solution. In collaboration with Aeromate, the aim of this study is to propose a way to replace these petrochemical products by developing a biosourced nutrient solution. This solution should be available to all and composed of necessary nutrients for plant growth.

First an identification of these nutrients was done thanks to literature review and website consultation[2,3,4,5,6,7,8,9,10]. Then we tried to adjust quantities of intrants to obtain finally four reproductible mixes[11,12,13,14,15] (Annex 1). These nutritive solutions, made of biosourced inputs like organic wastes, were tested. First, a hydroponic prototype was built, basil seeds were germinated and transplanted into the prototype. After that, nutritive solutions and plant growth were assessed thanks to several parameters to determine which solution would best replace petrochemical inputs. Thanks to this first experimental step, the liquid compost was selected as the most reliable and efficient input.

Second, the hydroponic prototype was improved to resolve difficulties encountered with the first one. Focus was put on the comparison of currently used chemical fertilizer and the liquid compost that was previously selected. To compare these two inputs, the growth of various plant species (mustard, spinach, rocket) was studied. So far, the liquid compost solution seems to fulfil one of the objectives: it can be made at home by anyone. Compost can be obtained just by putting the organic wastes from the kitchen and the green wastes from the garden into a composter. It can also be made from vermicompost, that are easy to implement in urban area and require only a small amount of space. From those composts, a compost juice can be easily made and locally-used as the nutritive solution for plant growth[16,17].

MATERIALS AND METHODS

This part is divided in 2 parts with a chronological logic. The first describe the first prototype that was developed from January to July, and then the second part is about the second prototype developed from September to December.

1. Prototype 1

1.1. Nutritive solutions

The nutritive solutions were selected in order to provide a possible use of domestic waste for plant growth. The mix 1 is currently used by Aeromate and serves as the control in this experiment. It allows to compare biosourced solutions with a chemical one. The other mixes were prepared with recovery

wastes or compounds purchased online. The protocols for each solution are detailed on the Annex 2. The mixes were diluted and incubated at ambient conditions (25°C, dark room, no agitation) for 2 weeks with 10L containers filled with 3L of water, and then transferred to the plastic seal container[11]. Annex 3 details the different parameters (inputs, incorporation methods and conditions) for the preparation and resume interest for the hydroponic device.

1.2. Building of the prototype 1

The idea was to compare the growth of a basil species using different biosourced mixes. 5L plastic buckets with their lid were used as mixes containers. In those lids, three holes of 5cm were done with a bell saw in order to insert the 5cm diameter and 5cm deep basket pots. Ultrasonic foggers were used to spread the mixes on plant roots, each bucket having its own fogger.

A structure was built in order to adapt the light's height at 20cm above the plants. The dimensions of the prototype are 120 x 80 x 55 cm. A polychromatic 1m strip LED was used as light source, with a light/night periods of 16/8h respectively, controlled by a 24h timer. Millard soft walls were disposed to concentrate the light (Figure 1, Figure 2)

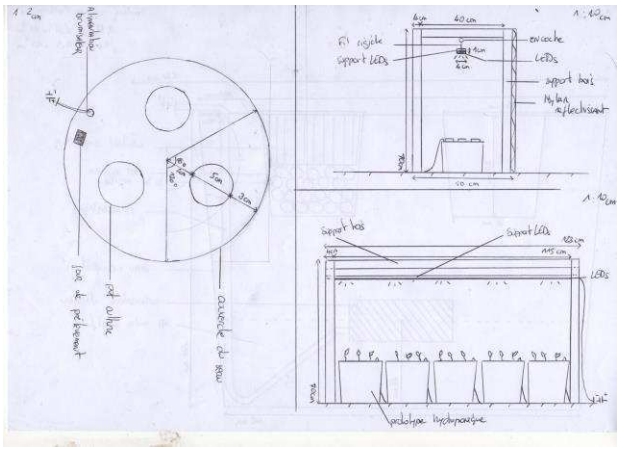

Figure 1- Scheme of the Biopony prototype 1

1.3. Germination

The basil species *Ocinium pollini-coccineo*[18] was chosen because it is an usual basil adapted to temperate countries and used by Aeromate. The germination was realized in coconut fiber at room temperature and humidified regularly (every 2 days). Then plants were transplanted in the hydroponic system, in triplicate for each mix, after the emergence of the first cotyledon.

1.4. Measures

Measures allowing to follow both mixes quality (nutritive media) and plant growth were done : pH, electrical conductivity (Portable pH and EC test, Platinium, accuracy/resolution: 0.1, calibrated before use), nitrite/nitrate and phosphate contents were performed (Table 1).

The pH defines the availability of nutrient for the plant[19]. It is noteworthy that the optimal pH for hydroponic device is around 6 [20,19], in order to control pH in solution, adding of sulfuric acid (1M) were performed when the potential was to high (around 8). Electrical conductivity (EC) is a measure of the total dissolved solids in a solution, permitting an evaluation of the quantity of nutrient in solution. It must be close to 1 mS/cm so that plants can easily pick up the nutrients[2]. The pH and EC of water have been measured as a control: the pH was at 7,6 and the EC at 0,5 mS/cm.

The Nitrite/Nitrate test and Phosphate test (WKS strip nitrite/nitrate REF : 0220649; WKS strip phosphate REF : 0220635) consist into colour bands.

Measurements were planned once a week. Final measurements were initially intended for the study of the nutritive quality and flavour of the basil plants (Table 1).

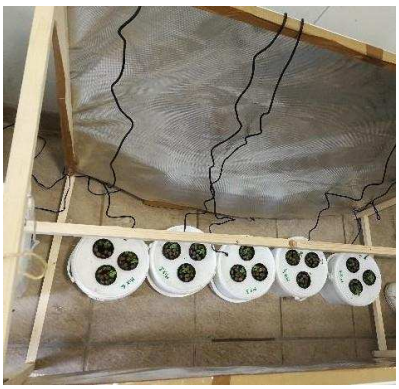

Figure 2 - Photography of the Biopony prototype 1

Table 1- Measures for the growth study of basil plants on each medium

Weekly tests		**Final plant's growth evaluation**
Nutritive media	**Plants**	**Leaves**
pH measurement	Leaves measurement and counting	Flavour test
Conductivity measurement	Pictures	Novacrop tests (nutritive quality)
	Stem measurement and counting	Dry and wet weights

2. Prototype 2

2.1. Nutritive solutions

Two different growing media were tested, one per line of culture. The first one is the control medium, composed of 8L of tap water with 1.8mL of each of the two growing petrochemical inputs used by Aeromate (FloraMicro and FloraGro, GHE flora serie).

"FloraMicro" composition: Total nitrogen (N) : 5%; Soluble potassium (K2O) : 1.3%; Boron (B) : 0.01%; Calcium (CaO) : 1.4%; Copper (Cu); chelated EDTA : 0.01%; Iron (Fe) chelated 6% EDDHA - 11% DPTA : 0.12%; Manganese (Mn) chelated EDTA : 0.05%; Molybdenum (Mo) : 0.02%; Zinc (Zn) chelated EDTA : 0.015%.

"FloraGro" composition: Total nitrogen (N): 3%. Available phosphate (P2O5): 1%. Soluble potassium (K2O): 6%; Soluble magnesium (MgO): 0.8%.
The second medium is made of a vermicompost juice, given by DM Compost, an urban compost society situated in the Val-de-Marne. A solution composed of 500mL of vermicompost juice in 10L of tap water was initially prepared. Then the tank was filled with 1 L of solution 1 in 7L of water, in order to have an electrical conductivity of 0.6 (close to the control medium) and to avoid a too strong concentration of inputs in the medium.

2.2. Building of the prototype 2

The dimensions of the new hydroponic prototype are detailed in Figure 4. Pumps (Platinum, submersive pump, ref: 030-006-0021; 1000L/h, 220/240V, 30W) were bought in a specialised growth shop, whereas the material for the support and water circuit were given by Aeromate. The starting medium is a commercial one bought in a traditional growshop in France (RootIT, rooting sponges, composed of black sphagnum peat moss, certificate by NF U44-551; organic material 99.8% (% raw material), with retention capacity of 20mL by moss.

2.3. Germination

For this experiment, regarding the difficulty encountered with basils for the first prototype, 3 different types of plants were selected: Winter spinach (*Spinacia oleracea)*; Mustard (*Sinapsis Alba*); Rocket (*Eruca Sativa*). These species are currently grown by Aeromate and were selected based on their gustatory quality during a meeting on Aeromate premise. For the germination, 6 plants of each species were planted in order to have at least 4 of each to perform the experimentation. The germination was realized by putting seeds in coconut fibres and regularly humidified (every 2 days) (Figure 3). Plants were then transposed in the hydroponic system after the emergence of the first cotyledon, and around 2 to 4 cm of growing (Figure 5). For a better significance, a duplicate of each type was cultured per nutritive solution. In overall there is 6 plants by growing line and 12 plants in total.

2.4. Measures

As for the first prototype, the pH and the electrical conductivity were measured. The length and width of stems, cotyledons (primitive leaves) and leaves, were also measured, as well as their number. This monitoring was made every 3 days to follow the plants' growth.

Figure 4 - Scheme of the prototype 2. P is the immersed pumps on the 10L nutritive solution tank. A 1 to 2 % slope is not shown on the scheme from left part to right one

Figure 5 - Photography of the prototype 2, after transplantation.

RESULTS

Prototype 1

The first prototype was built to test several nutritive solutions and determine which one is the fittest to replace petrochemical inputs. These mixes were developed to meet the standard needs of a plant, using components that are easily found in everyday life, if possible as waste. To test these bio-sourced solutions, three *Ocimum pollini-coccineo* basil plants per solution were transplanted after germination, starting the experiment on Day 0. The germination did not encounter any problem with a good development of basil cotyledons after one week. Seeds were inserted in a growing moss. This basil specie grows in temperate climate and has a quick growth rate, then giving quick results.

From day 1, four basil plants already died (respectively, two in mix 3, one in mix 4, and one in mix 5). After one week, all basil plants were dead for mixes 3 and 5. Plants from mix 2 seemed to have a similar growth as with the mix 1, which is the petrochemical input used by Aeromate.

During the experiment, measures of pH, electrical conductivity, nitrite/nitrate and phosphate contents were performed. Results are shown in Table 2 and Table 3. The temperature was not controllable during that experiment and rose significantly. As it influences the pH, those results cannot be properly interpreted.

The nutritive mixes were not transparent and colorless. They dyed the bands of the Nitrite/Nitrate test and Phosphate and made it difficult to observe the true color of the tests. Therefore, it is also hard to interpret those results.

As for the Electrical conductivity, the value was kept around 1^2. When the N°2 sample was taken for mix 4, the Electrical conductivity reached 3,5. a dilution by half was performed between samples N°1 and N°2 to reach a value closer to 1 (Table 2)

Table 2- pH and electrical conductivity for each mix. Samples n°1 have been collected on 2018/06/14, n°2 on 2018/06/19 and n°3 on 2018/06/21. Empty cases represent mixes where every plant died.

	pH			Electrical conductivity (mS/cm)		
Measure	1	2	3	1	2	3
Mix 1	7	7,4	8,1	1	1,2	1,4
Mix 2	7,2	7,4	9,2	0,7	0,8	0,8
Mix 3	7			0,3		
Mix 4	5,6	6,5	9	2,2	1,3	1,7
Mix 5	6,8			1,9		

Table 3 - Nitrate/nitrite and phosphate tests realized for each mix. Samples n°1 have been collected on 2018/06/14, n°2 on 2018/06/19 and n°3 on 2018/06/21. Empty cases represent mixes where every plant died.

	Nitrite/Nitrate test			Phosphate test		
Measure	1	2	3	1	2	3
Mix 1	0,5/ 500	0/ 500	0,5/ 500	50	25	25
Mix 2	0,5/0	0,5/1 0	0/0	25	50	25
Mix 3			50			
Mix 4	0,5/ 100	0,5/1 0	0/0	25	10	25
Mix 5			50			

In the end, plants grown in mixes 1, 2 and 4 survived the longest. However, detailed data of their growth are not available because they did not survive long enough to realize the measures. As the mixes 2 and 4 allowed the plant to survive as long as the control mix 1, they seemed like the perfect candidates for a new session of growth. But only mix 2 was kept, because of its simpler composition.

Prototype 2

For this second prototype, the support and water circuit were built with material generously given by Aeromate. This allows to have a more suitable structure than the first prototype. The best mix of the previous experiment was selected for this second part. It is mainly composed of infused compost. In order to simplify and normalize the composition of this mix, a liquid concentrate of vermicompost was used. A vermicompost is a compost obtained from the degradation of early compost by different vermicompost species[21]. The dilution rate of the vermicompost is 10%, based on what is actually performed and recommended by several industrials who provide and sell vermicompost. This allows to prevent burning the roots of young shoots with a pure vermicompost juice. It was not possible to quantify the amount of nutrients inside, as the vermicompost juice came from a local producer which did not perform any characterization.

The evaluation of nutritive solution quality was processed just by measuring the electrical conductivity and the pH for the bioavailability of nutrients in solution (Figure 6). During the experiment, the pH was adjusted on day 10 from 8,2 (Aeromate mix) and 8,5 (Compost mix) to 6,9. It went up again, so on day 16, another adjustment was made. As a strong acid is used for the adjustment (sulfuric acid 1M), the pH decreased too much and reach a value around 3 for both solutions. To protect the plants, each mix was remade, with a pH adjusted to 6,8 in both cases.

Concerning the plants, the germination operated well, even though spinach took a little bit longer than others. The evaluation of plants' growth has been determined by counting the number of stems, leaves and thanks to stems and leaves measurement (Figure 8). The foliage surface was estimated by multiplying the leaf length and width (Figure 7).

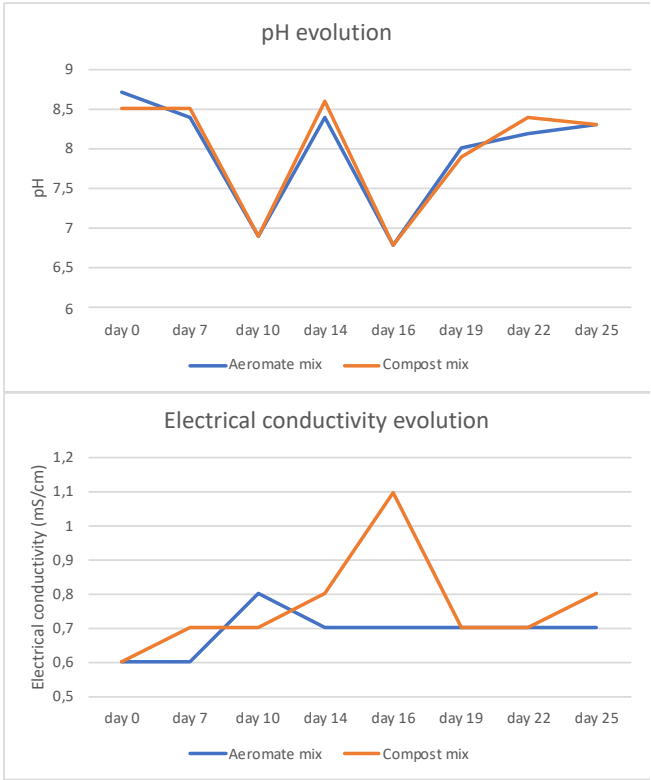

Figure 6 - pH and electrical conductivity evolution of Aeromate and compost mixes through time. On day 10, pH was adjusted, on day 16, the solutions were renewed.

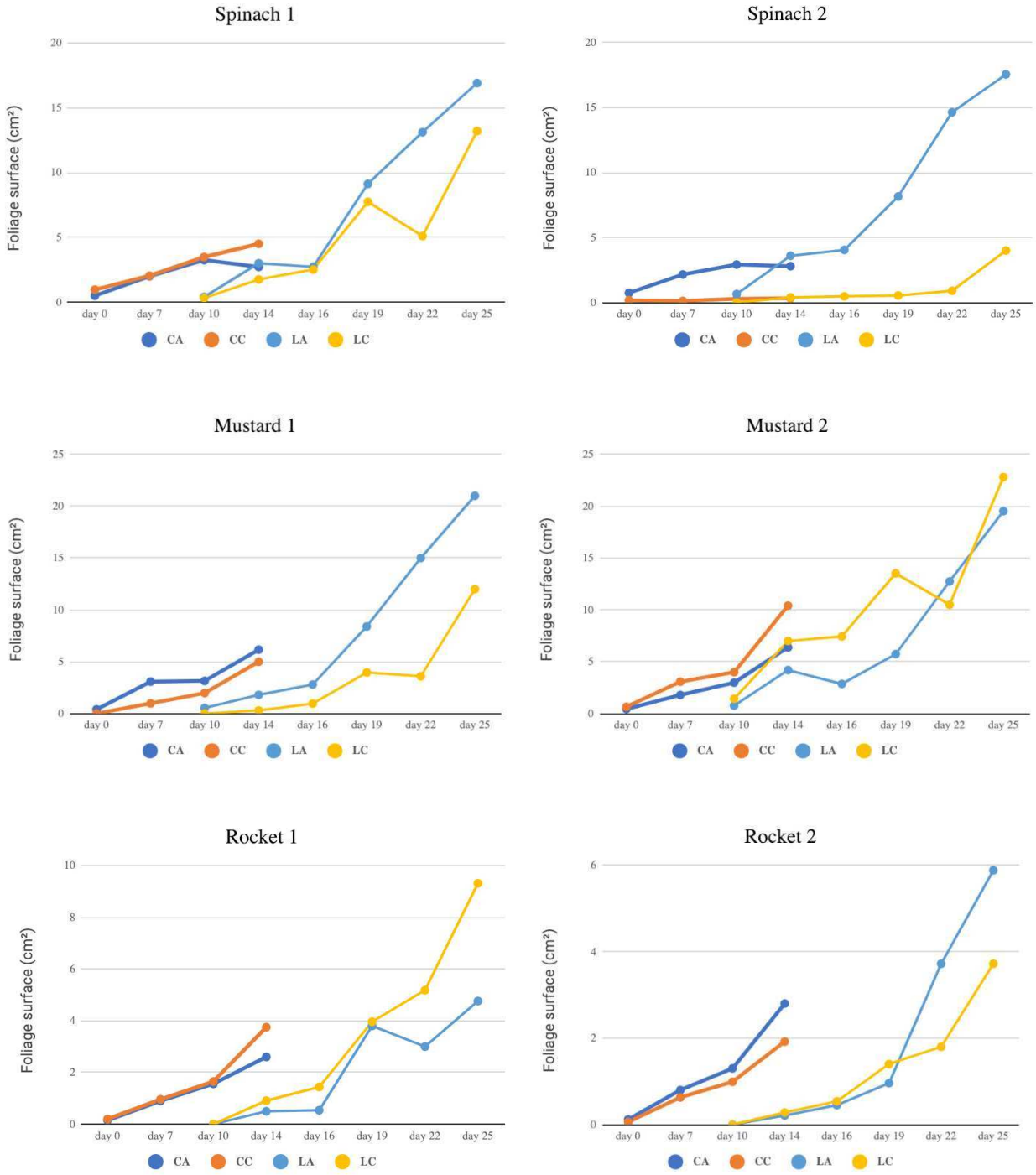

Figure 7- Foliage surface evolution over time for each plant. CA: cotyledon of Aeromate mix, CC: cotyledon of compost mix; LA: leaves of Aeromate mix, LC: leaves of compost mix. Cotyledons are primitive leaves and were measured until the appearance of the first real leaves.

Figure 8 - Stem length evolution over time for each plant. SA: stem of Aeromate mix; SC: stem of compost mix.

DISCUSSION

In this study, 4 nutrients mixes were initially made to replace petrochemical inputs used for plant growth. The first step was to identify the need of plants. Various information have been found about nutrients (NPK and other minor minerals) and growth conditions (pH, light exposition, temperature) requirements to perform an efficient hydroponic culture[2]. This survey allowed the development of mixes preparation protocol, using mostly domestic waste in order to be feasible at home and transform hydroponic inputs into biosourced ones. The hydraulic device was developed to compare the efficiency of the different mixes. It became quickly evident that the prototype was not optimized for the hydroponic culture and observed results were not easily interpretable. The hypothesis was that the first problem came from the nutritive mixes. Their complexity might have had an impact on the bioavailability of the nutrients. In addition, they contained many non-soluble components, inducing important sedimentation. It was difficult

to filtrate the different mixes before putting them into the prototype. It might also have interfered with the proper misting of the solutions by the pumps incorporated in the prototype. Indeed, instead of producing the expected mist, the pumps produced water jets. It was observed that the dead basils cited above were right on top of the water jets. Those jets might have been too hard on the crops. Another problem encountered was that the pumps produced a lot of heat and the room did not provide enough ventilation to cool down. Temperatures above 30°C were reached inside the room and probably even reached higher values in the mixes. This might have had a negative impact on the plants' survival.

That explained why results were not easily interpretable. But plants of two mixes survived and to fit the project goal that everyone can realised it himself, it was decided to focus on the mix 2: the one composed of compost. This mix was simplified to only use diluted vermicompost juice as a nutrient solution, without lemon. However, this juice was not characterized to know the nutrients it contained, so that will be a requirement if other experiments are done with this medium.

For the second experiment, the hydroponic system was optimized using basic hydroponic pump like Aeromate's installations. In the same extend, a better temperature control was realized, even if stable conditions are hard to maintain in a non-optimal room, usually not dedicated to hydroponic culture. However, difficulties were encountered to stabilize the pH at 6. It always seems to go up to 8 even after adjustment with sulfuric acid. Some strategies must be thought about because it would be dangerous and not optimal to ask to everyone at home to use a strong acid to reduce the pH of their biosourced solution.

These results are nevertheless optimistic. The foliage surface and stem length of plants grown in the compost solution are usually slightly below those of the plants grown in the petrochemical input. Indeed, they seem to follow a similar growth rate and no disparity in mortality or seeds development was observed. As the measures should always go up, the decreasing values are due to a problem of manipulation. Since it is the first time that the test was done with the juice of compost only the general tendency is observed in this study. It would be interesting to test another measurement method such as a video tracking with an image processing (imagJ for example). Otherwise, further analysis on vermicompost juice's composition and growth experimentations are, of course, needed. Yet, the use of vermicompost as an input have great application in urban area, with the growing crave for urban vegetable gardens and the valorization of green spaces, a large amount of raw resources will be more and more available for citizens. That gives to biosourced inputs an interesting opportunity to replace petrochemical ones.

ACKNOWLEDGMENT

We thank our tutors, Louise Douillet and Louis De Saint- Cyr for their help during this year of work; Mrs Mogensen for her kindness and support during the development of our project; Mrs Souad for lending us a room to store our prototype. We also want to thank DM compost, especially Mrs. Victoria Laurent and Mr. Jérôme Sandier, for giving us the vermicompost juice and allow us to visit an interesting place where local recycling is performed.

REFERENCES

1. NC. Le petit hydroculteur. *culture hydroponique* (2002). Available at: http://www.culture-hydroponique.com/culture-hydroponique.htm.
2. Baxter, R., Hastings, N., Law, A. & Glass, E. J. . *How to Hydroponics*. *Animal Genetics* **39**, (2008).
3. NC. Guide des vitamines. *Source alimentaire en zinc* Available at: http://www.guide-vitamines.org/oligoelements/zinc/sources-alimentaires-zinc.html.
4. NC. VEG et CRU. *Ortie* (2015). Available at: http://vegecru.com/ortie.
5. NC. Le lot en action. *La consoude, trésor des jardins, ennemie des labos* Available at: https://www.lelotenaction.org/pages/content/archives/la-consoude-tresor-du-jardin-ennemi-des-labos.html.
6. NC. Société Chimique de France. *Gypse* Available at: http://www.societechimiquedefrance.fr/extras/Donnees/mine/caso/texcaso.htm.
7. Troy Buechel. Promix. *Chaux calcitique et chaux dolomitique* (2018). Available at: https://www.pthorticulture.com/fr/zone-du-savoir/chaux-calcitique-et-chaux-dolomitique/.
8. NC. Au Jardin.info. *Composition du marc de café* (2008). Available at: https://www.aujardin.org/viewtopic.php?t=92988&start=.
9. NC. Faire Son Jardin.fr. *La fertilisation* Available at: http://www.fairesonjardin.fr/fertilisation.html.
10. NC. Informations Nutritionelles.fr. *Jus de fruits* Available at: https://informationsnutritionnelles.fr/jus-de-fruits.
11. NC. Manufacturer of Humboldts SEcret Supplies. *How To Make Your Own Organic Hydroponic Fertilizer* (2013). Available at: https://humboldtssecret.com/how-to-make-organic-hydroponic-fertilizer-ezp-39.html.
12. Anhwange, B. A., Ugye, T. J. & Nyiaatagher, T. D. Chemical Composition of Musa Sepientum (Banana) Peels. (2009).
13. Ehowgarden. Youtube. *How to Make Liquid Fertilizer for a Hydroponics System : Hooked on 'Ponics* (2014). Available at: https://www.youtube.com/watch?v=D8c6kU1F7q4.
14. Cyrill.e. ConsoGlobe. *Comment composter et réaliser un compost avec ou sans composteur ?* (2010). Available at: https://www.consommerdurable.com/2010/05/comment-composter-et-realiser-un-compost-avec-ou-sans-composteur/.
15. Eddy Mercier. Composter, c'est facile ! *Les paramètres physico-chimiques* (2018). Available at: http://compostage.info/index.php?option=com_content&view=article&id=42%3Ales-parametres-physico-chimiques&catid=5%3Acontenu&Itemid=6.
16. NC. Transition Verte. *Nutriments: le thé de vers* (2012). Available at: http://www.transition-verte.com/nutriments-le-the-de-vers/.
17. NC. Permaculture Design. *Le vermicomposteur : une boîte à vers pour faire un compost de qualité* (2017). Available at: https://www.permaculturedesign.fr/vermicomposteur-valoriser-dechets-fertilisant-naturel-compost-vers/.
18. NC. Association Kokopelli. *Tulsi Kali* Available at: https://kokopelli-semences.fr/fr/p/A0203-tulsi-kali.
19. NC. Culture Indoor. *L'EAU* Available at: https://www.cultureindoor.com/content/26-les-conseils-engrais-et-eau.
20. NC. City Plantes. *Gestion du pH* Available at: http://www.cityplantes.com/content/21-gestion-du-ph-pour-la-culture-en-interieur-et-la-culture-en-hydroponie.
21. NC. Vers attitude. *Le lombricompost* Available at: http://versattitude.blogspot.com/p/blog-page_14.html.

AUTHOR INFORMATION

Jean-Rémi Loup, Nicolas Merieux, Julia Naudin, Claire Persyn, Students in biotechnology, SupBiotech.

Engineering *E. coli* BL21(DE3) for the production of rat pro-Nerve Growth Factor (proNGF), RNA III Inhibiting Peptide (RIP) and the toxin/anti-toxin couple CcdB/CcdA

Jonathan Naccache, Eléa Paillares, Gabriela Sachet-Fernandez
Institut Pasteur, Paris, France

***Abstract* - This article presents NeuronArch, a synthetic biology project developed during the 2018 edition of the International Genetically Engineered Machine competition (iGEM) with the iGEM Pasteur Team. NeuronArch is an interface made of an engineered biofilm that was imagined for amputees wearing prostheses. The aim of this device is to allow them to regain natural perceptions while preventing the formation of pathogenic biofilms. The engineered *Escherichia coli* used in the interface has three main functions: the production of rat pro-Nerve Growth Factor (proNGF), which allows nerves to grow back; the production of RNAIII Inhibiting Peptide (RIP), which inhibits the quorum sensing of *Staphylococcus aureus,* reducing its production of virulence and adhesion factors; the integration of a thermosensitive kill-switch that kills the bacteria when released in the environment. In this study, we explain how we designed, cloned and characterized the three main biobricks of our project. The results show that all of them were successfully cloned. The characterizations of RIP, proNGF, and of the kill-switch are also fully detailed. However, analyzing more replicates of the proNGF biobrick would allow a stronger characterization. Furthermore, finding a more suitable protocol for the observation of biofilm formation would allow having more consistent results.**

Keywords: proNGF; RIP; biofilms; prosthetic-joint infections; *S. aureus*; amputees; osseointegration; temperature sensitive kill-switch.

"BioBricks™ is a standard for interchangable parts, developed with a view to building biological systems in living cells. BioBrick™ parts can be assembled to form useful devices, through a process often referred to as 'Standard Assembly'. BioBrick™ parts are composable; allowing endless numbers of Biobrick™ parts to be pieced together to form complex systems." - iGEM

Part Reference	***Components***
BBa_K261600	T7 promoter_ RBS_prongf-hlya_Ter_T7 promoter_RBS_TEVp-hlya_Ter
BBa_K261601	T7 promoter_RBS_dsbA-RIP_RBS_malE-RIP_Ter
BBa_K261602	PLac promoter _ RBS_ccdA_PcspA promoter_RBS_ccdB
BBa_K261603	J23107promoter_RBS_agrC_DoubleTer_J23107_RBS_agrA_DoubleTer_ P2promoter_RBS_ dsbA_RIP_RBS_malE_RIP_ DoubleTer

Table 1. iGEM registry ID and description of designed Biobricks. *Inducible promoters: T7, PcspA, P2. Constitutive promoters: PLac,J23107. RBS stands for Ribosome binding site and Ter for Terminator. See Appendix 1, 2 and 3.*

INTRODUCTION

Prostheses aim to enhance the quality of life, independence, mobility, and safety of amputees. The worldwide frequency of amputations has created an increased demand for improved prosthetic technologies. Within developing countries, the population with physical disabilities in need of a prosthesis is estimated at about 0.5%. There are currently almost 2 million people living with limb loss in the United States. In 2050, this amount could exceed 3 million people **[1]**.

Reconnect Nerves

Over the past decade, many new types of prostheses have emerged. One of them is the myoelectric prosthesis, which captures the electromyographic (EMG) signal of residual limb muscle through surface electrodes on the skin. This kind of robotic prostheses allow amputees to recover some autonomy and to accomplish simple everyday gestures. However, they are still limited by a small number of controllable movements and by the lack of sensory feedback **[1]**.

Osseointegration of prostheses describes the direct attachment of the implant to the skeleton. This kind of prosthesis provides the patient with precise and reliable control of the new limb, regardless of the environmental conditions or the patient's position. The opportunity to record and stimulate the neuromuscular system allows intuitive control and a better understanding of sensory perception **[2]**. After limb amputation, the main issue with the human-machine communication is due to the nervous damages. In fact, the electrical signal cannot be transmitted because peripheral nerve cells are no longer able to activate target muscles or relay sensory information from the limbs back to the brain.

To overcome this issue, we thought of a way to help the motor nerves of amputees grow back and connect to our interface by using pro-Nerve Growth Factor (proNGF), a protein specialized in the regulation of nerve development, survival, plasticity, and nervous system function **[3]**. The first biobrick we created, BBa_K2616000 (**Appendix 1**), expresses two proteins. Firstly, an N-ter His-tagged proNGF, linked in C-ter to the type I export signal HlyA. Between the two, we added a TEV protease cleavage site. Secondly, TEV protease, a protein from Tobacco Etch Virus that recognizes a specific sequence and cleaves it. We also linked the TEV protease to the same export signal. Once exported from the cell, the TEV protease can cleave the proNGF from HlyA and free the pro-neurotrophin in the external medium (**Fig. 1**). A part of the proNGF might be cleaved inside the cell, but this shouldn't be a problem as long as a sufficient number of proteins are cleaved outside of the bacteria.

Fight infections

Biomedical implants, such as prostheses, catheters, and several other implanted devices, are meant to improve the patients' quality of life. Nevertheless, because they are artificial, handled from outside the body, and rarely have antimicrobial properties, they increase the risk of infections. In fact, device-associated infections account for 25.6% of all health-care-associated infections in the USA **[4]**. Orthopedic implants infections are caused by the development of pathogenic microorganisms on an inert material, allowing bacterial adhesion and biofilm formation on the implant. Biofilm-related infections frequently lead to chronic infections and require implant replacement. They are therefore responsible for a significant medical and economic burden **[5], [6]**. For example, A study led in France **[8]** estimates that the revision of infected prostheses multiplies the cost of the total procedure by a 3.6 factor. Bacterial biofilms aggregate strongly adhere to the biomaterial surfaces. In this bio-mechanical configuration, the implant-infecting biofilms can elude innate and adaptive host defenses as well as antibiotic therapies **[7]**.

It has been shown that *Staphylococcus aureus* (*S. aureus*), a Gram-positive coccus, is the most commonly isolated microorganism from orthopedic-associated infections, accounting for more than 40% of hip and knee prosthetic-joint infections **[8]**. In most cases, the treatment after a prosthetic-joint infection involves the removal of the implant followed by several weeks of antibiotic treatment.

To overcome the problem, we chose to disrupt the quorum sensing of *S. aureus* as an anti-biofilm strategy. It has been shown that pathogens use quorum sensing to regulate and coordinate the biofilm's architecture and the production of toxins and virulence factors **[9]**.

We engineered the bacteria composing our biofilm by introducing the genes encoding for AgrC and AgrA, the two proteins responsible for the detection of Auto Induced Peptides (AIPs), the relays of quorum sensing. We encoded them under the constitutive promoter

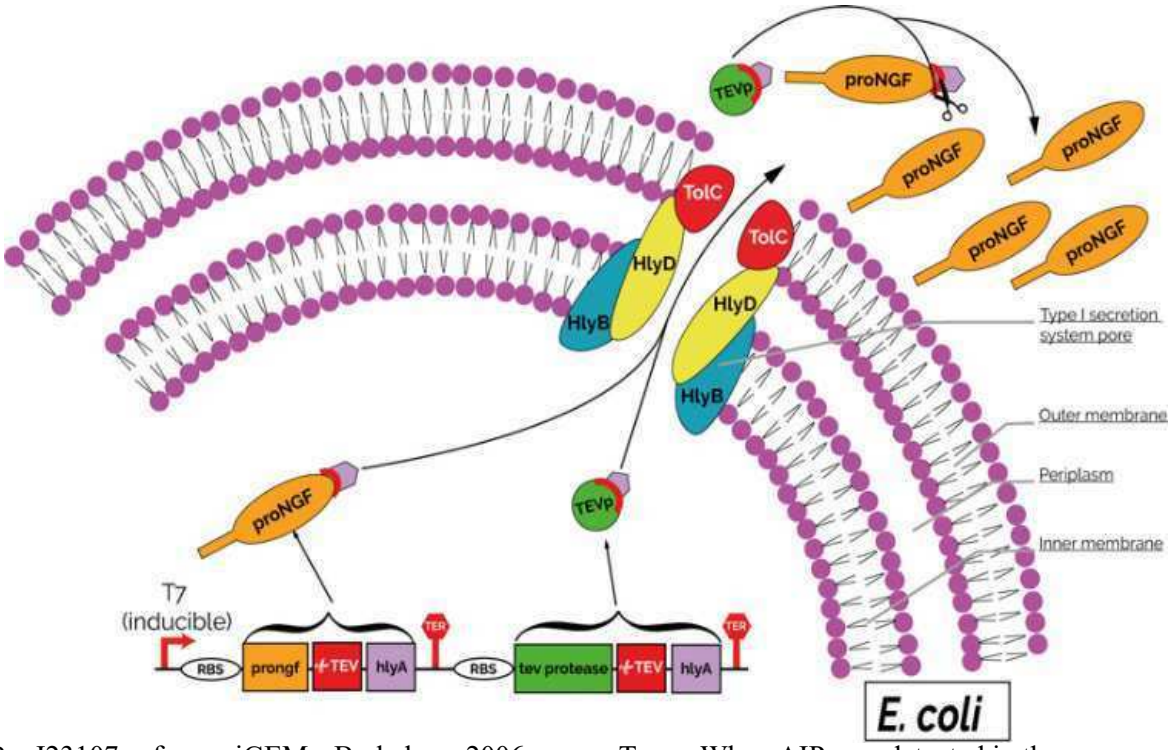

BBa_J23107, from iGEM Berkeley 2006 Team. When AIPs are detected in the

Figure 1. *proNGF cassette production and secretion from E. coli*

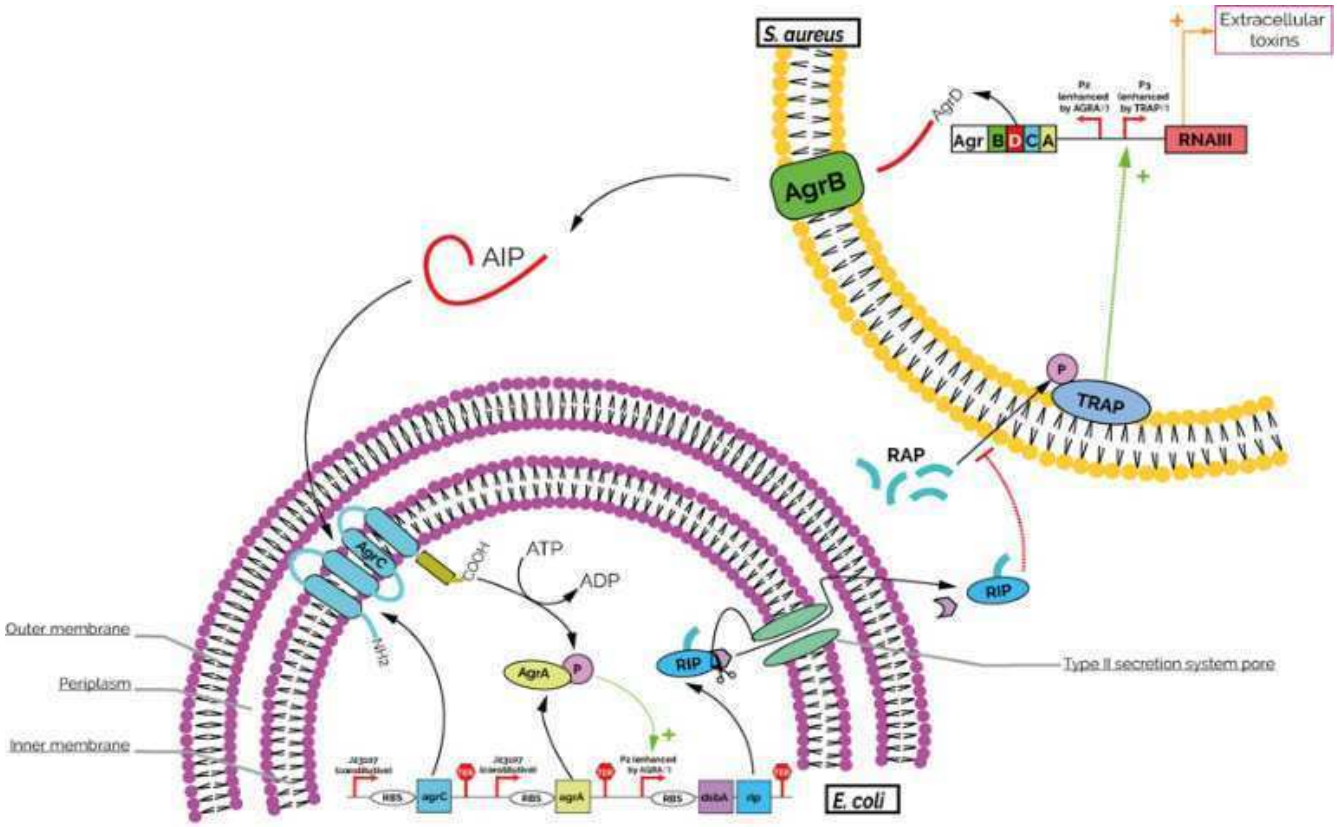

Figure 2. *AIP Detection and RIP secretion cassette.*

environment by the transmembrane protein AgrC, AgrA is phosphorylated, and then activates the gene promoter P2 (**Fig. 2**).
The biobrick BBa_K2616001 (**Appendix 2**) encodes for a protein called RIP, a small peptide of seven amino-acids that has been proven to inhibit the biofilm formation of *S. aureus*. RIP competes with RNAIII Activating Protein (RAP). This leads to an inhibition of the Target of RNAIII Activating Protein (TRAP) phosphorylation. Indeed, RIP and RAP compete for the same receptor, but RIP, unlike RAP, inhibits TRAP phosphorylation. This inhibits RNAIII transcription and thus attenuates virulence factor production, inhibits cell to cell communication and decreases adhesion capacities **[10], [11] (Fig. 2).**

To allow RIP secretion in our biofilm, the Sec-dependent Type II secretion system targets RIP to the periplasm of *E. coli*. The peptide is fused to an amino-terminal signal sequence, that is recognized by the chaperone SecB, and then addressed to SecA and translocated across the inner membrane through the SecYEG complex. The advantage of this system is that the signal sequence is cleaved during translocation through SecYEG. Several different signal sequences have been characterized (all formed of 18 to 30 amino acids) **[12]**. Two of them, MalE and DsbA, were used for peptide export into the periplasm. Once there, due to the small size of RIP, a leaky release through the outer membrane of the bacteria should allow us to obtain RIP in the medium.
The detection proteins AgrC and AgrA are present in the engineered bacteria composing our biofilm, and thus, can detect the AIPs in the environment when *S. aureus* is present. AIPs will bind to AgrC, that will phosphorylate AgrA. This will induce the production and secretion of RIP, placed under a P2 promoter, and inhibit *S. aureus* Q.S and thus, biofilm formation. The function of this biobrick was analyzed through biofilm assays, in particular crystal violet staining, a known colorant of biofilms.

Cryodeath kill-switch

The kill-switch was implemented to make sure that our engineered bacteria won't be able to grow if it escapes the human body. The cryodeath kill-switch, invented by Finn Stirling in 2017, is triggered by temperatures under 37°C **[13]**. We modified the original sequence and created our third biobrick, BBa_K2616002 (**Appendix 3**), that functions by the means of the toxin/antitoxin couple CcdB/CcdA. The toxin targets and inhibits the GyrA subunit of DNA gyrase, an essential bacterial enzyme that catalyzes the super-coiling of double-stranded closed circular DNA **[14]**.
In the kill-switch, the transcriptions of CcdB and CcdA are regulated by two different promoters (**Fig. 3**). CcdA is expressed by the constitutive promoter Plac, which ensures a constant low production of antitoxin **[15]**. On the contrary, the toxin CcdB is expressed by the promoter PcspA. This promoter was originally discovered upstream of the Cold Shock Protein A (CspA) in many bacteria, as a way to cope with environmental stress. Indeed, when the temperature drops below 37°C, the promoter PcspA increases the level of expression of CspA gradually **[16]**. This promoter ensures a very low transcription rate at 37°C, but it increases drastically below 22°C.
Overall, at 37°C, the quantity of antitoxin CcdA is high enough to cope with the leaky low level of toxin produced. However, if the bacteria happen to be in an environment under 22°C, the toxin promoter is not repressed anymore, the quantity of toxin becomes too important, and the bacteria is not able to grow (**Fig. 3**). This allows us to make sure that our genetically modified organisms will not spread out in an open environment.

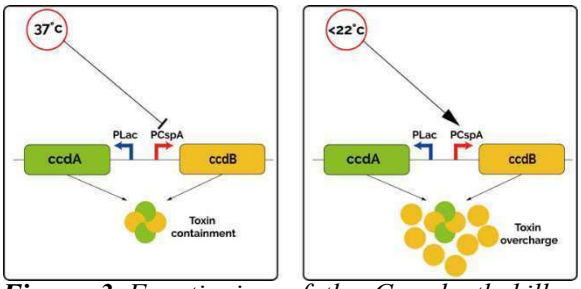

Figure 3. *Functioning of the Cryodeath kill-switch at 37°C and at 22°C.*

MATERIAL AND METHODS

Biobrick construction

The sequences of the genes and plasmids used (pSB1C3 and pET43.1a(+)) were found on addgene. The design and construction of the biobricks were done with the software Geneious, all constructs were codon optimized for *E. coli*.
Sequences have been synthesized in one, two or three fragments by Eurofins and delivered in pEX-A258. Plasmids were amplified in DH5-α Competent *E. coli* (High efficiency)

(NEB, C2987 I) (**Appendix 4**) and extracted with QIAprep™ Spin Miniprep Kit (Qiagen, 27106) (**Appendix 5**). The DNA fragments were cut from the commercial plasmid using the appropriate restriction enzymes and were selected by-electrophoresis (**Appendix 6**). The fragments of interest were excised from the gel with the QIAquick Gel Extraction Kit (Qiagen, 28706) (**Appendix 7**). The ligation of the different fragments in our two plasmids was performed thanks to the In-Fusion® HD Cloning Kit (Takara Bio) (**Appendix 8**). The constructs were then transformed in Stellar™ Competent Cells and selected on agar plates containing the appropriate antibiotic. The final plasmids were extracted from the bacteria thanks to the QIAprep™ Spin Miniprep Kit (Qiagen, 27106).

Bacteria

DH5-α Competent *E. coli* (High efficiency) was provided by NEB (New England Biolabs) through sponsoring. The DH5α strain was used for plasmid amplification and cloning. BL21(DE3)pLysS Singles™ Competent Cells (Merck, 70236) was used for protein expression because it contains the T7 RNA polymerase and has a high level of protein expression. GFP fluorescent *S. aureus* strain was kindly provided by Pr. J-M Ghigo, Institut Pasteur.

Competent cells transformation

Competent cells were transformed with our plasmids using conventional transformation techniques. The protocols varied depending on the type of competent cells we wanted to transform. See protocol for transformation of *E. coli* DH5-α (**Appendix 4**) and for *E. coli* BL21 (DE3) pLys (**Appendix 9**).

IPTG induction Protein expression

The genes coding for proNGF and RIP were under promoter T7, inducible to IPTG. Engineered bacteria were grown in Luria Bertani (LB) medium with the appropriate antibiotics in an inFORS minitron at 37°C and 180 rpm until the OD600 reached 0.4 to 0.8. IPTG was added to the culture at a final concentration of 0.1 to 0.5 mM depending on the characteristics of the expressed protein. The culture was then incubated at 37°C and 180 rpm for 3 to 5 hours (**Appendix 10**).

SDS-PAGE for proNGF detection

An SDS-PAGE was performed on a NuPAGE™ 4-12% Bis-Tris Gel (Invitrogen, NP0322BOX) using the Power Pac 300 from BIO-RAD (**Appendix 11**).

Western Blot for proNGF detection

Proteins on SDS-PAGE gel were transferred to the nitrocellulose membrane iBlot® 2 NC regular stacks (Thermofisher-Invitrogen, IB23001). The iBlot® 2 gel transfer device (Thermofisher-Invitrogen) was used for the transfer (**Appendix 12**).

Immunodetection of proNGF

The nitrocellulose membrane from the Western Blot was marked with a 6x-His tag antibody, Alexa Fluor® 647 conjugate (HIS.H8) (Invitrogen, MA1-21315-A647) (**Appendix 13**).

Mass spectrometry

Samples analyzed were cut directly on the Western Blot acrylamide gel. Gels were run in duplicate and one only was used for immunostaining as the other one was used for LC/MS/MS. Samples were then prepared and analyzed by Dr. Bastien Lefeuvre from the Mass Spectrometry platform of the Institut Pasteur.

Biofilm assay and Crystal Violet staining

S. aureus biofilm formation was performed on pre-sterilized 96-well plates. *S. aureus* overnight culture was diluted 100-fold in LB medium and secreted RIP peptide was added in increasing concentrations. The plates were incubated for 24h to 72h at 37°C. After removal of planktonic cells, plates were washed three times with water and air dried. Finally, fluorescence was read under a plate reader. (excitation 485nm, emission 510 nm).
A second assay was performed by adding 125 µL Crystal violet (0.1%) after wash steps in order to observe the variation in biofilm formation (**Appendix 14**).

Cortex culture

Cells from an E18 rat cortex (2 pieces of tissue) stored in Hibernate EB from BrainBits were dissociated in a solution containing 2 mg/mL Sterile papain (BrainBits PAP 6 mg) and Hibernate E-Ca (BrainBits HE-Ca 5mL). The cortex was incubated for 10 min at 30°C and the cells were then grown in the appropriate cell culture medium (**Appendix 15**).
Neurons were then seeded in a microfluidic chip and incubated at 37°C, 5% CO2, for 6-7 days (**Appendix 16**). After a few days, the neurons were fixed with 4% PFA and stained with DAPI (for the nucleus of the cells) and Anti-MAP2, clone AP20, Alexa Fluor (Merck, ref: MAB3418A5) and Anti-β-tubulin antibody coupled with Alexa Fluor 448nm (for the cells axons) (**Appendix 17**).

Temperature-dependent kill-switch

The efficiency of our kill-switch was tested at 4 different temperatures: 15°C, 20°C, 25°C and 37°C). We used BL21(DE3)pLysS *E. coli* transformed with the empty pSB1C3 plasmid as the negative control, and the same strain transformed with our biobrick for characterization. The bacteria growth was followed by measuring the optical density at 600 nm every 30 minutes for 6 hours, followed by two additional points at 18 hours and at 72 hours. Each experiment was done in triplicate and the standard deviation was calculated for every point.

RESULTS

Expression of recombinant proNGF

To examine recombinant proNGF expression in BL21, Nickel chelate affinity chromatography coupled with Mass-spectrometry and Immunodetection were performed. After Ni-NTA purification column and SDS-PAGE analysis, five gel slices around 20 to 35 kDa of the FPLC flow-through were analyzed by LC/MS/MS mass spectrometry.

As shown in Figure 4 (a), 14 unique peptides corresponding to proNGF were found in all fractions, covering 63% of the complete sequence. These results demonstrate the expression of proNGF. Analysis of Fraction 5 of the gel shows that proNGF protein is present in a mix of the cleaved and uncleaved polypeptide. Among identified peptides, some correspond to proNGF sequence (IDTACVCVLSR), to the fusion of proNGF and HlyA export signal (RGENLYFQGGSGLAYGSQGDNLPLINEISK) and to HlyA export signal (IISAAGSFDVKEER). The presence of mass spectrometry identified peptides corresponding to the fusion of proNGF and HlyA indicate some proNGF uncleaved from the export signal.

To further examine the cause for the low retention of His-tagged proNGF, batch purification analysis of proNGF under native and partial denaturation were conducted. As revealed in Figure 4 (b), after immunodetection with Anti-His Antibodies (Alexa Fluor 647) His-tagged proNGF was expressed in induced BL21, and in the non-retained fraction under partially denaturing conditions.

This shows that the purification was unsuccessful as the recombinant proNGF was not retained on the column, either in its folded or denatured state.

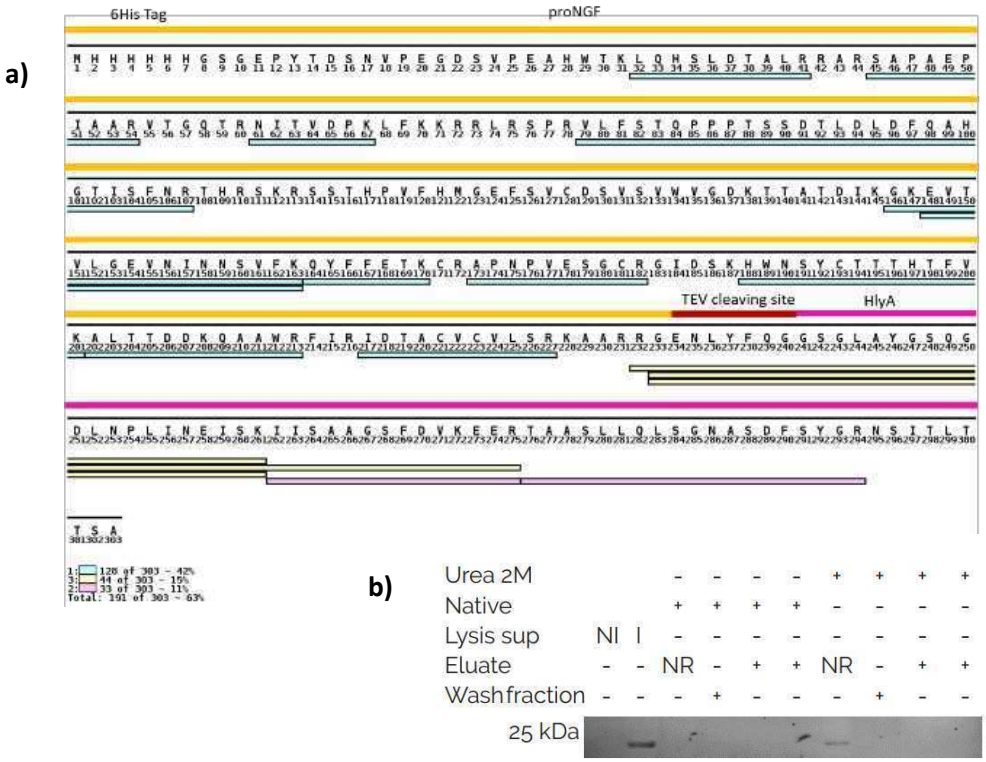

Figure 4. Recombinant proNGF expression validation. (a) Alignment sequences of proNGF fused to HlyA export signal and peptides identified by mass spectrometry. *Peptides that match proNGF amino acids sequence (light blue). Peptides that match HlyA export signal (light yellow). The sequence has been annotated to match corresponding protein amino acid sequences: His tagged proNGF (orange), TEV protease cleaving site (red), HlyA export signal (pink).* ***(b) Western Blot analysis of batch purified proNGF by Ni-NTA.*** *Batch purification of pellet supernatant of BL21(DE3)pLysS under native and partial denaturation (2 M urea). NI = Non-induced BL21, I = BL21 induced 1 mM IPTG, NR = Non-retained fraction.*

Rat cortex E18 primary culture with recombinant proNGF or commercial NGF.

As the purification of proNGF failed on the Ni-NTA affinity column, neurons were grown with several bacterial lysates of an induced colony of *E. coli* expressing the recombinant proNGF. Bacterial pellets were sonicated to allow a performant physical lysis without using detergent. Lysates were then heat-treated at 60 °C for 5 min to denature unwanted bacterial proteins. After fixation of the neurons and immunostaining of the axons by Anti-β-tubulin and nuclei by DAPI, cell survival and cell differentiation was measured. Figure 5 (a,b,c) shows the fluorescence microscopy of neuronal cells grown either with no commercial NGF or with 750 ng/mL. It appears clearly that the adjunction of commercial NGF increases the growth of axons and cell survival **(Fig. 5-b, c)**.

The effect of the recombinant proNGF was then compared to commercial NGF on survival and differentiation of the neurons. Growing concentrations of bacterial lysate were added to the neuronal cultures. Figure 5 (d,e) shows that our proNGF had a comparable effect on survival and differentiation than commercial NGF used at concentrations above 500 ng/mL.

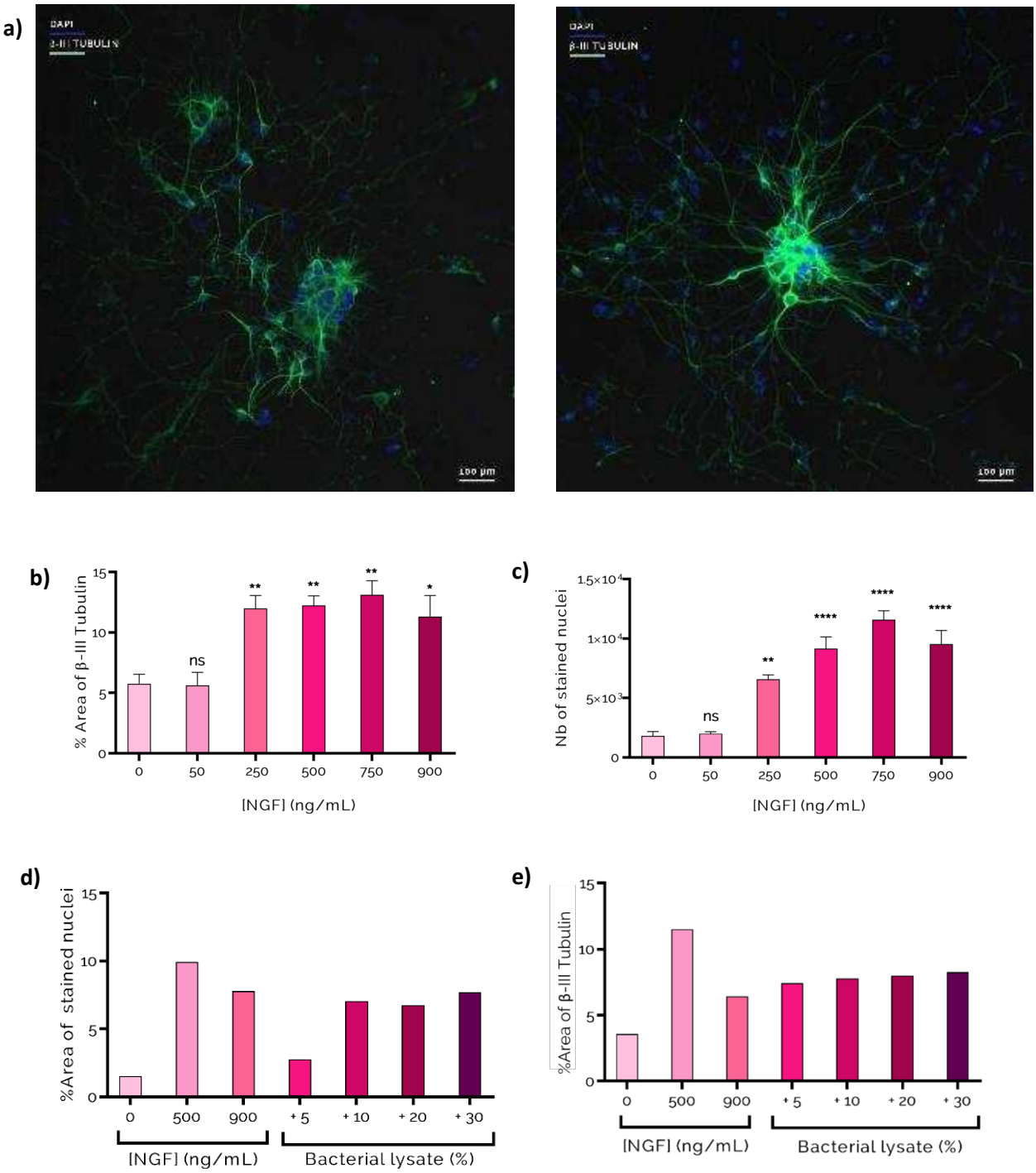

Figure 5. proNGF induces cell differentiation and survival. ***(a)*** *Fluorescence microscopy of E18 Sprague Dawley neuronal cells. Cells were grown with no NGF (left) or 750ng/mL NGF (right).* ***(b,c)*** *Quantification of the effect of commercial NGF on E18 Sprague Dawley neuronal differentiation (b) and survival (c). Data are presented as MEAN ± SEM. Significance between 2 different groups was determined using an Ordinary one-way ANOVA test on the software Prism6 (GraphPad).*
*(ns: non-significant, *: p<0.05, **: p<0.01, ***:p<0.001, ****: p<0.0001).* ***(d,e)*** *Recombinant proNGF induce cell differentiation and survival. Quantification of the effect of commercial NGF and recombinant proNGF on E18 Sprague Dawley neuronal differentiation (d) and survival (e).*

Measurement of the impact of RIP on S. aureus biofilm formation.

RIP is a seven-amino acid peptide, so identifying its expression using SDS-PAGE analysis was not possible. To investigate the expression of RIP and its effect on *S. aureus* Biofilm formation, RIP was added to biofilm and fluorescence was read following 48h **(Fig. 6)**. It was identified that RIP has a negative impact on biofilm formation as shown in Figure 6. There is an average 3- fold reduction of fluorescence from *S. aureus* biofilms when they were cultivated in presence of the bacterial lysate of an induced culture of BL-21 *E. coli* transformed with BBa_K2616001.

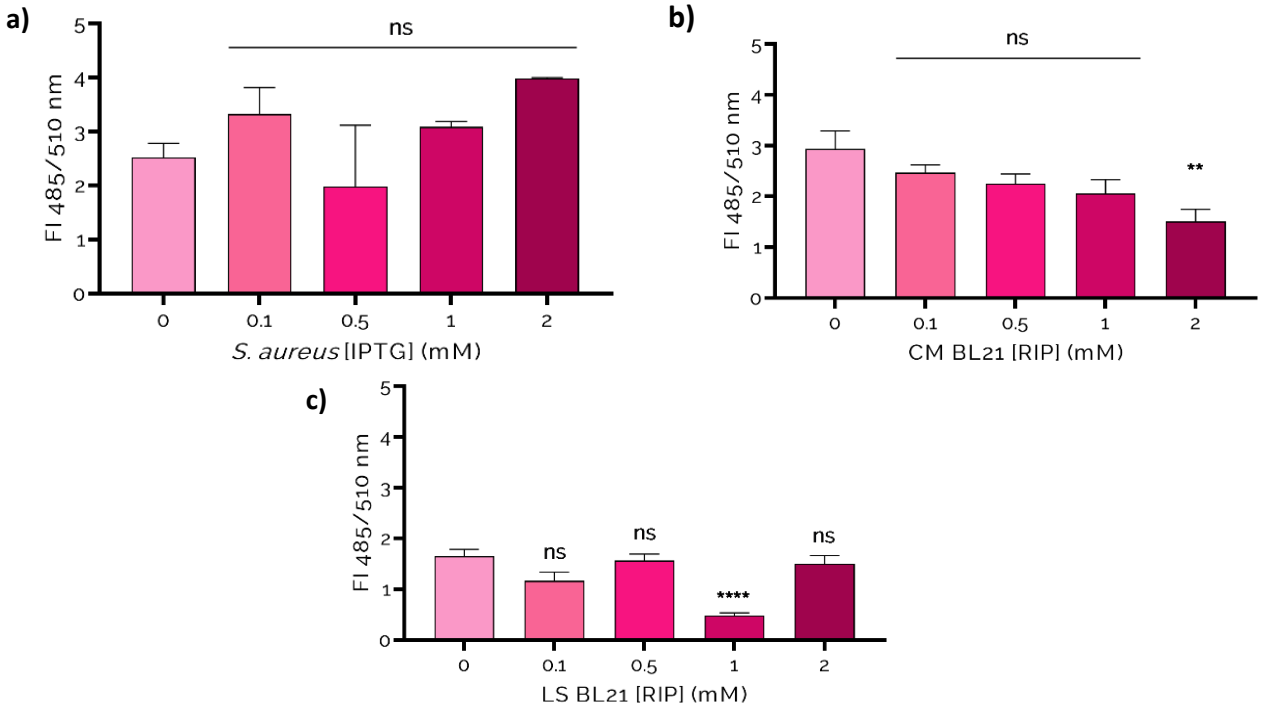

Figure 6. Fluorescence reading assay on biofilm formation. (a) *S. aureus alone with different [IPTG mM]* ***(b)*** *S. aureus with culture medium (CM) from BL21(DE3)pLysS expressing RIP* ***(c)*** *S. aureus with cell lysate (LS) from BL21(DE3)pLysS expressing RIP. (n=8) Data are presented as MEAN ± SEM. Significance between 2 different groups was determined using an Ordinary one-way ANOVA test on the software Prism6 (GraphPad).*
*(ns:b non-significant, *: p<0.05, **: p<0.01, ***: p<0.001, ****: p<0.0001*

Temperature effect on bacteria transformed with Cryodeath kill-switch growth.

To investigate whether temperature impacted kill-switch transformed BL21(DE3)pLysS growth, a growth curve was performed. As demonstrated in Figure 7, bacteria transformed with the kill-switch presented no measurable growth at 15°C (blue dotted line) and at 20°C (green dotted line) comparing the control population (blue and green lines) following 72h.

At 25°C, the kill-switch population didn't grow at all for the first 18 hours, but the growth eventually started to reach normal values at 72 hours. Finally, at 37°C there was no difference until 18 hours in the growth of the kill-switch population compared to the control bacteria.

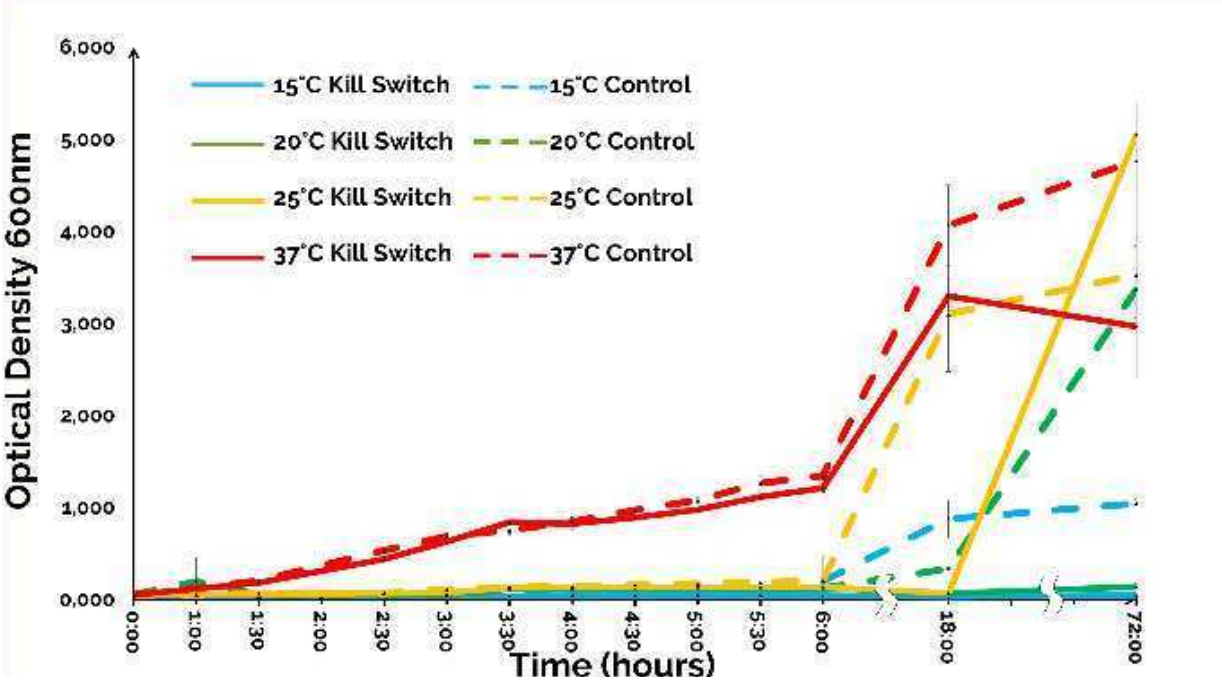

Figure 7. Effect of different temperature on the growth of Cryodeath BL21(DE3)pLysS E. coli. *Bacteria growth was followed by optical density measurement at 600 nm every 30 minutes for 6 hours, followed by two additional points at 18 hours and at 72 hours.*

DISCUSSION

Reconnect Nerves

Our first objective was to create a functional biobrick coding for rat proNGF in *E. coli,* with a secretion system to export it to the culture medium. From this ambitious starting point, we have achieved many advances. First, we sequenced our biobrick, achieving a 100% pairwise identity and confirming the correct cloning of our construct. Secondly, we proved the expression of recombinant rat proNGF using two different methods (immunodetection and mass spectrometry). Finally, we characterized our protein's functionality by measuring its effect on the growth of rat cortical neurons and comparing them to the ones exposed to commercial NGF. These results are particularly encouraging, although preliminary. Indeed, we successfully cloned and expressed a functional neurotrophin in *E. coli*, paving the way towards designing a biological interface to reconnect the nerves of amputees with bionic prostheses.

However, several issues must still be addressed. First of all, even though an export signal was integrated to our proNGF sequence, we were not able to prove its correct exportation. That could be a limiting factor, as the mean of export is central in the question of proper folding. Furthermore, in our device, the produced neurotrophins would have to be secreted in order to bind neurons and promote their growth **[17]**. Yet, because of their double membrane, protein secretion in Gram negative bacteria is more complex than in Gram positive ones, in which secreted proteins are directly released into the culture medium. Thus, engineering a Gram-positive bacterium could be a better secretion model in our case **[18]**.

We also were not able to purify the proNGF we produced either with Ni-NTA affinity column or with Ni-NTA beads. We believe that the N-terminal His-tag may be hidden in the protein fold. Consequently, we denatured the protein with 2 M urea before purification. This did not improve the binding. We also tried with an 8M urea concentration, without better results.

Additionally, the assays realized on neuronal differentiation and survival with proNGF were not duplicated, so the results we show are not statistical, even if they are still very encouraging. Therefore, we are left with a lot

of perspectives on this matter. First, we want to deepen the possibilities of exporting proNGF, maximizing yields and protein activity. Secondly, we want to realize more tests on neuronal growth, with accurate controls and statistical results. Finally, we would like to try to clone other neurotrophins (BDNF and VEGFA) to maximize the effects on neuronal growth.

Fight infections

Finding a way to fight against *S. aureus* prosthetic-joint biofilm infections was a central objective of this project. With this in mind, we initially designed a biobrick to detect the presence of the pathogen and secrete a small peptide in response, RIP, to inhibit its quorum sensing. However, this proved to be more difficult than we thought. Indeed, we struggled to assemble the biobrick, which was synthesized in three parts because of its important size. Due to a shortage of time and resources, we revised our objective and decided to begin by cloning the inhibiting peptide alone in order to measure its efficiency.

Once again, we proved the correct assembly of our biobrick through DNA sequencing.

To assess the efficiency of RIP, we performed several *S. aureus* biofilm formation assays to measure the impact of RIP in the medium. However, we faced an important variability challenge, which is customary in this kind of assays. Indeed, biofilms are known to be challenging to study. They are sensitive to a lot of parameters, like aeration or CO_2 content. Furthermore, they are particularly fragile and washing steps, intended to remove planktonic cells, can tear down the biofilms. Overall, this variability problem has caused an important loss of significance in our results. We tried many different protocols, without any luck and variability prevented us to state any definitive conclusions.

However, some results were encouraging, showing a diminution of biofilm formation correlated with the concentration of RIP in the medium. This placed us in a contradictory position on the assessment of RIP interest in the fight against *S. aureus* biofilms. One the one hand, we are not sure of the confidence we can have in our results due to their variability. One the other hand, some experiences with RIP showed promising results. From these findings, it appears that the best way to go on would be to try reducing the variability of biofilm assays by testing more protocols. On another note, it would be interesting to synthesize the whole initial biobrick in order to assess its efficiency.

Cryodeath kill-switch

The cryodeath kill-switch is an important safety implementation of our system. The results we obtained are more than satisfactory. Indeed, they confirm both the theoretical expectations and the data obtained by Finn Stirling with his version of the kill-switch. It appears that we can trust this system as a mean to ensure that our genetically modified bacteria won't spread in the environment under 22°C. Still, we don't have any way to ensure this containment at higher temperatures. Thus, the logical perspective in this matter is to develop another kill-switch for that case. Furthermore, additional tests could be done on the cryodeath kill-switch to assess if it is bactericidal or bacteriostatic. Our system could be modified to include an alternative mode of death induced by oxygen level or nutriment dependency. Combining different kill-switches would allow to maintain a high level of evolutionary stability (in the case of unwanted mutations) and provide a tighter control.

ACKNOWLEDGMENTS

We would like to express our deepest appreciations to all the people who contributed to our iGEM experience and to this report. First, we want to thank the Institut Pasteur and Dr. Deshmukh Gopaul, for his teachings and for giving us the opportunity to join the iGEM Pasteur Paris 2018 team. We would also like to thank our incredible coaches within the team, Anna Segu Christina, Guillian Graves, and Serena Petraccini. We also want to thank all the professionals who advised us and those who contributed to the project, our sponsors, the people who contributed to our crowdfunding, and the other iGEM teams we collaborated with. We also want to thank Sup'Biotech, the Sup'Biotech Innovation Projects office for their financial support, as well as Mr. Ougen, for his precious advice and the Fil Rouges bureau, for their kind supervision.

REFERENCES

[1] Pasquina, P. F., Perry, B. N., Miller, M. E., Ling, G. S. F. & Tsao, J. W. *Recent advances in bioelectric prostheses*. Neurol. Clin. Pract. 5, 164–170 (2015).

[2] Li, Y. & Br.nemark, R. *Osseointegrated prostheses for rehabilitation following amputation: The pioneering Swedish model*. Unfallchirurg 120, 285–292 (2017).

[3] Ivanisevic, L. & Saragovi, H. U. *Neurotrophins. in Handbook of Biologically Active Peptides*, 1639–1646 (Elsevier, 2013). doi:10.1016/B978-0-12-385095-9.00224-4

[4] Magill, S. S. et al. *Multistate Point-Prevalence Survey of Health Care–Associated Infections.*N. Engl. J. Med. 370, 1198–1208 (2014).

[5] Lamagni, T., Elgohari, S. & Harrington, P. *Trends in surgical site infections following orthopaedic surgery:* Curr. Opin. Infect. Dis. 28, 125–132 (2015).

[6] Shakibaie, M. R. *Bacterial Biofilm and its Clinical Implications.* 2, (2018).

[7] Arciola, C. R., Campoccia, D. & Montanaro, L. *Implant infections: adhesion, biofilmformation and immune evasion*. Nat. Rev. Microbiol. 16, 397–409 (2018).

[8] Lamagni, T. *Epidemiology and burden of prosthetic joint infections*. J. Antimicrob. Chemother. 69, i5–i10 (2014).

[9] Wolska, K. I., Grudniak, A. M., Rudnicka, Z. & Markowska, K. *Genetic control of bacterial biofilms.* J. Appl. Genet. 57, 225–238 (2016).

[10] Gov, Y., Bitler, A., Dell'Acqua, G., Torres, J. V. & Balaban, N. *RNAIII inhibiting peptide (RIP), a global inhibitor of Staphylococcus aureus pathogenesis: structure and function analysis.* Peptides 22, 1609–1620 (2001).

[11] Giacometti, A. et al. *RNA III Inhibiting Peptide Inhibits In Vivo Biofilm Formation by Drug-Resistant Staphylococcus aureus.* Antimicrob. Agents Chemother. 47, 1979–1983 (2003).

[12] Freudl, R. *Signal peptides for recombinant protein secretion in bacterial expression systems.* Microb. Cell Factories 17, (2018).

[13] Stirling, F. et al. *Rational Design of Evolutionarily Stable Microbial Kill Switches*. Mol. Cell 68, 686-697.e3 (2017).

[14] Reece, R. J. & Maxwell, *A. DNA Gyrase: Structure and Function.* Crit. Rev. Biochem. Mol.Biol. 26, 335–375 (1991).

[15] Malan, T. P. & McClure, W. R. *Dual promoter control of the Escherichia coli lactose operon*. Cell 39, 173–180 (2016).

[16] Keto-Timonen, R. et al. *Cold Shock Proteins: A Minireview with Special Emphasis on Csp family of Enteropathogenic Yersinia.* Front. Microbiol. 7, (2016).

[17] Clewes, O., Fahey, M. S., Tyler, S. J., Watson, J. J., Seok, H., Catania, C. Allen, S. J. (2008). Human proNGF: biological effects and binding profiles at TRKA, p75 NTR and sortilin. Journal of Neurochemistry, 29(9), 745–760.

[18] Schneewind O, Missiakas DM. Protein secretion and surface display in Gram-positive bacteria. Philos Trans R Soc Lond B Biol Sci. 2012;367(1592):1123-39.

Setting up an *in vitro* assay for drug testing based on 3D tumor spheroid imaging by Light Sheet Fluorescence Microscopy

Camille Leconte, Camille Sous*, Léonard Raimbault, Estelle Zhang
Sup'Biotech, Villejuif, France
*Corresponding author: camillesous94@gmail.com

Abstract **- Spheroids are 3D structures formed by cells under certain *in vitro* conditions. This structure is a more representative model of an *in vivo* tumor than 2D cell culture and has the advantage to avoid complexity, heterogeneity and low transparency of whole tissue while representing cell communication, cell proliferation and the action of drug on *in vivo* tumor. Our transversal project at Sup'biotech aims to elaborate an antineoplastic drug assay using spheroids observed by Light Sheet Fluorescence Microscopy. This project has been realized in two parts. First optimization of experimental parameters and protocol were done from HeLa-YFP spheroid generation to post-acquisition processing of the images (spheroids generation, agarose embedding, clarification step and post-acquisition treatment). These optimizations allowed to find a new way to embed spheroids in agarose by using a syringe as mold to give an appropriate agarose form for microscope observation. They also confirmed the need to clarify using ethyl cinnamate and the relevance of the volume calculator software (ReViMS). The second part of the project was related to the treatment of spheroid with a reference drug: paclitaxel. Paclitaxel effect is already known for 2D cell culture of this type of cells. Treatment with paclitaxel allows to verify if the implemented protocol on 3D model of spheroids can be relevant for a drug screening by comparing spheroids volume treated or non-treated.**

Index Terms - 3D modeling, Drug screening assay, HeLa cells Light sheet microscopy, Paclitaxel, Spheroids, Volume comparison

INTRODUCTION

The 2D cell culture is a very widespread model for drug testing. This type of culture provides a good control over the cellular environment and an easy observation and manipulation. [1] 2D culture thus makes it possible to control the quantity of nutrients and growth factors delivered to the cells and especially ensure that the quantity is similar for each cell. This allows to obtain a homogeneous growth and proliferation of cells in 2D culture. [2] 2D culture is widely used because it is simple and effective. However, 2D culture systems disadvantage is related to their incapacity to reflect the *in vivo* situation, where cells grow in a complex 3D micro-environment. [3] To counter this difficulty, researchers focused on 3D cells culture offering a higher degree of structural complexity and homeostasis, which is analogous to tissues and organs. On a cellular interaction point of view, 3D model is more representative of cell communication, cell proliferation and the action of drug of *in vivo* tumor. [4] These types of culture can also be used as effective simulators of tumor characteristics such as latency, hypoxia, anti-apoptotic behavior and receive stimuli of the local environment. [5] 3D model is also more representative concerning the cellular topology, the cellular signaling and metabolism of *in vivo* tumor. [6-7] The method in soft agar solution was the first developed 3D cultures carried out by Hamburg and Salmon in 1970. [8] Since then, closely related characteristics between the morphology and behavior of cells spreading in a tumor and in 3D cells cultures have been well characterized. [4] The comparison between the 2D and 3D models allowed us to choose the 3D model, which is better suited for our drug screening assay.

We decided to use YFP-HeLa cells spheroids as the 3D model of tumor. Spheroids are 3D cell structures created in a confined environment in which biological cells grow or interact with their surroundings in all three dimensions. There are different spheroid generation protocols to test drugs well explained. However, the acquisition and the post-acquisition treatments are not yet efficient for a drug screening like ours. [9] Knowing that, we wanted to achieve and optimize a protocol to carry out a drug screening assay.

Different types of microscopes for images acquisition are used in the literature such as widefield microscopy, confocal microscopy and light sheet fluorescence microscopy. [10]

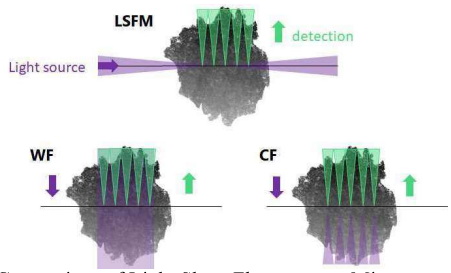

Figure 1: Comparison of Light Sheet Fluorescence Microscopy (LSFM), Wide Field (WF) Microscopy and Confocal Fluorescence (CF) Microscopy illumination of spheroids.

The widefield microscopy is the most commonly used technique for spheroid visualization but it does not allow 3D visualization of the spheroid whereas both confocal and light sheet microscopy do. However, the confocal microscopy has a longer acquisition time and photobleaching is more important compared to light sheet fluorescence microscopy (Figure 1). [11]

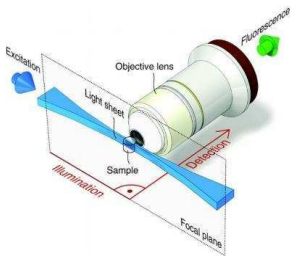

Figure 2: Principle of light sheet fluorescence microscopy (LSFM). [10]

The light sheet microscope (LSFM) allows a selective illumination of a single plane of interest of the sample which decreases the photobleaching. Moreover, LSFM available at the laboratory has a bidirectional source of light, allowing to illuminate the sample from the right or from the left or both sides which can be useful to go through the sample (Figure 2). [12]

In this study, we decided to optimize a protocol allowing a drug screening assay based on spheroid using LSFM. Protocol optimization has been made on different parts: spheroid generation, agarose embedding, clarification and post-acquisition image treatment.

MATERIALS AND METHODS

Cell culture and Reagent

HeLa cells lines were stably transfected with the episomal vector 2347 to express YFP (Yellow Fluorescent Protein) under the CAG promoter and puromycin resistance gene under the SV40 promoter (cell line from the SEPIA laboratory, CEA, Fontenay-aux-Roses). HeLa cells (J114 after transfection) were cultured in Dulbecco's modified Eagle's medium (DMEM) high glucose (Sigma D6546) supplemented with 10% Fetal bovine serum (FBS) (Dutscher, P 30-8500), 2mM L-Glutamine (Sigma, G7513), 10 mM HEPES (Sigma, H0887), 0.1X MEM-non essential amino acids (Sigma, M7145), 40 U/ml penicillin/streptomycin (Sigma, 11074440001) and 0.4 µg/mL Puromycin (Thermofisher A113803).

Generation of spheroid

HeLa cells were cultivated according to the 3D petri dishes® technique. [13] Petri dish was filled with 2% ultrapure agarose to create agarose micro-molds. Once the agarose has polymerized, micro-molds were removed from the dishes and placed in a 12-wells plate. Several micro-molds were made. All of them were equilibrated twice with 2.5 mL complete DMEM for 15 minutes to provide nutrients to the cells when seeded.

At 60-70% confluence, HeLa cell culture was trypsinized and counted with Malassez Chamber to know the concentration of cells. According to the 3D petri dish® protocol, size of spheroids depends on the number of cells seeded in agarose micro-molds. By following the protocol table, 3 different concentrations were seeded in the first experiments: 81,000 cells/190µL for 200 µm diameter, 273,000 cells/190µL for 300 µm diameter and 648,000 cells/190µL for 400 µm diameter. For the second experiment, 132,500 cells/190µL were seeded. Then, cells in agarose micro-mold were incubated for 24h at 37°C and 5% of CO_2.

Paclitaxel treatment

The protocol for paclitaxel treatment is adapted from Mathews Griner. [14]

This part has been performed on spheroids generated with 132,500 cells/190µL. Paclitaxel (Sigma, T 7402) was solubilized in DMSO (Merck, 317275) at 500 µM and diluted in complete DMEM 0.4 µg/mL puromycin at 500 nM. The final concentration of paclitaxel was 250 nM. Consequently, all treatments were done by replacing the half volume of wells. Three conditions were carried out (with three replicates per condition): first with 250 nM paclitaxel, the second with DMSO as negative control (same concentration of DMSO than the paclitaxel treatment), and the last condition with complete DMEM 0.4 µg/mL puromycin culture. Spheroids were then incubated in physiological conditions protected from light for 24h at 37°C and 5% of CO_2.

Fixation and agarose embedding

The culture medium was removed, and spheroids were fixed at 48 hours (24h of treatment) with 4% formaldehyde for 15 min at room temperature and rinsed twice with PBS. To obtain larger and circular samples for the microscope holder, PBS was removed and 700 µL of 1% agarose was rapidly dropped on spheroids. Agarose containing spheroids was dropped off into a cut syringe. Once agarose is polymerized, small slices of agarose gel were cut (figure 3), and the dehydration step was initiated.

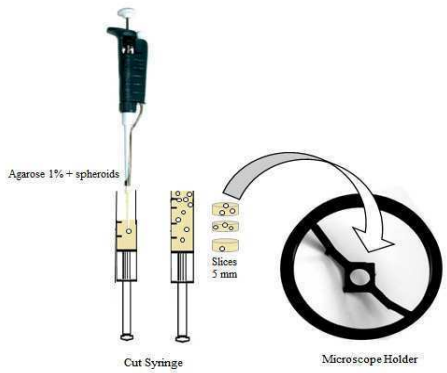

Figure 3: Agarose embedding technique of spheroids for sample holding on LSFM.

Dehydration and clarification

The clarification protocol was adapted from a previous study which used ethyl cinnamate as a clearing agent and proved its efficiency under LSFM to clear all tested organs including calcified bones. This clearing agent was previously used for fluorescence of immuno-histological labels and was maintained over weeks. [15]

Different conditions were tested beforehand to optimize the initial protocol for imaging improvement. For this purpose, we performed imaging of different size of spheroids, with or without clarification.

Without clarification, the different cellular components have different refractive indexes. This divergence deviates the laser beam and decreases the image sharpness which was not suitable for visualization under LSFM. Ethyl cinnamate (ECI) allowed both homogenization of the refractive indexes and preservation of the YFP fluorescence through time. [16] Spheroids without clarification are directly observed.

In order to properly clarify spheroids, we needed to keep the YFP in its protonated form to preserve fluorescence of cells under LSFM. For this, spheroids trapped in agarose gel were placed in successive ethanol baths at 30%, 50%, 70%, and 100% at pH 9 during 2h or 3h at 4°C under agitation. The 100% ethanol bath was carried out twice. Once dehydrated, samples were placed into ECI.

Sample observation and image treatment

Clarified spheroids were observed in the immersion medium (ECI or PBS for non-clarified spheroids) under the LSFM (LaVision BioTec microscope II) with the 488 nm illumination source. The intensity of the light, numerical aperture, orientation of the laser, and width of the sheet were adjusted prior spheroid acquisition. Z-stacks of 2 µm were acquired. Images were treated with different software. Reconstructions were made using ImageJ or ICY, and the spheroids volume were estimated by volume formula calculation ($4/3\pi R^3$) from observed diameter and using 3D modeling through the ReViMS algorithm (Reconstitution and Visualization from Multi Sections) after statistical triangle segmentation on ImageJ. [17]

RESULTS

Spheroid formation

HeLa cells were used to generate spheroids. HeLa cells were derived from cervical cancer cells. In our case, HeLa cells expressing YFP line was used to have the fluorescence. [18] This cell line has the advantage to grow easily and rapidly and were available in the host laboratory (CEA).

Generation of spheroids was performed using the 3D petri dishes® technique.

Different sizes of spheroids have been tested using 3D Petri dishes of theoretical diameters of 200 µm, 300 µm and 400 µm. The technique of Micro Tissue is fast and easy to implement the generation of a high number of spheroids per well in a Petri Dish using agarose gel. The main advantage is that the size of spheroids can be controlled by the number of cells seeded inside the agarose micro-mold. Micro-well in agarose allows the cells not to attach to the matrix and thus form a sphere during growth. The culture technique described here allows easy testing of the capacity of cells to form spheroids.

The fixation of spheroids with formaldehyde at 48 hours immobilize the cells while preserving their cellular structure and avoiding as much as possible a morphological deformation. [21]

The need of clarification

A comparison between clarified and non-clarified spheroids was carried out in order to optimize the protocol. There are two main categories of clarification: aqueous or solvent. The aqueous clarification has the disadvantage to produce soft sample which is harder for manipulation and loading into the LSFM. Solvent-based clearing techniques include two steps: (1) dehydration and (2) lipid solvation and homogenization of the refractive indexes of sample components. [16] Moreover, this technique was the best compromise due to its efficiency, rapidity and inexpensiveness. A lot of dehydration techniques and solvent clearing have been previously used and tested. [23] But ethyl cinnamate (ECI) reagent seems to be the best solution for our study. Indeed, most of solvents can cause the shrinkage of the sample such as iDISCO and can altered the fluorochromes properties or are toxic such as BABB [16-24] whereas ECI has the particularity to be non-toxic and to preserve the fluorescence. Concerning the dehydration step, ECI-clearing requires a dehydration by ethanol. Ethanol is able to conserve the morphological structure when performed with successive bath in increasing concentration with a specific duration for each bath. To preserve the YFP fluorescence, ethanol baths are calibrated at pH 9.

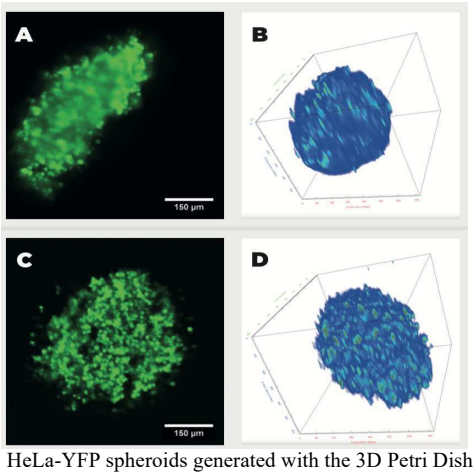

Figure 4: HeLa-YFP spheroids generated with the 3D Petri Dish protocol ® with a theoretical diameter of 400 µm. Comparison of clarified and non-clarified spheroid and reconstruction by ICY.
A and B: non-clarified spheroid. C and D: clarified spheroid using ECI.
Scale A and C: 150 µm

Spheroids without clarification were first analyzed. Results shown a blurry center and bottom of the spheroid (figure 4 A and B). Moreover, its outlines were not well-detected for the segmentation performed before volume modeling. To counter this problem, the same experiment was performed with a clarified spheroid (figure 4 C and D). the resulting image was clearer than without clarification and the clarification allows a better segmentation for modelling.

The clarification is therefore needed to have the most accurate volume estimate.

The need of a volume calculator software (ReViMS)

The results observed for the three sizes of spheroids under LSFM showed a gradual increase in the size of spheroids (Figure 5).

The microscope observation revealed that spheroids had a more falciform-like shape than a spherical shape. Due to this formation, the use of manual calculation with the diameter lead to false and biased estimation (figure 4A and C).

A comparison between the volume estimation using reconstruction of z-stacks images with ImageJ and ReViMS software and using diameter with the manual calculation was performed (Figure 5).

The manual calculation of volume was determined by taking the larger diameter of the spheroids used with the volume sphere formula.

The volume of theoretical 200 µm diameter spheroids have a substantial variation within the same calculation method. Due to these results, we conclude that this size of spheroids is not the best for our study.

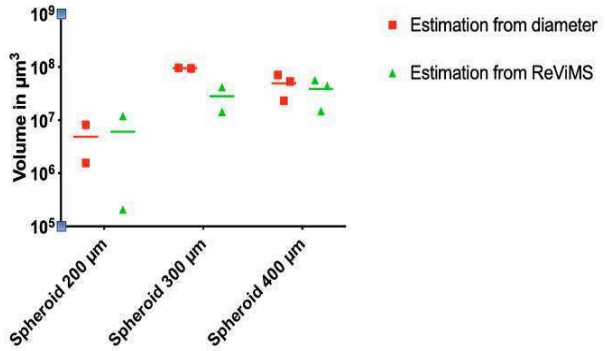

Figure 5: Graph showing the comparison of volume estimation between different theoretical diameter of spheroids (controls with DMEM) using ReViMS and the manual calculation with the formula. Two replicates have been considered for spheroids of 200 and 300 µm and three replicates for 400 µm. Y axis in log scale.

In comparison, theoretical diameter of 300 µm and 400 µm spheroids did not have this problem. But, as 400 µm spheroids are bigger than 300 µm, they could be more representative of *in vivo* tumor and easier to manipulate. According to these results, we decided to continue our study with theoretical 400 µm spheroids.

Cytotoxic effect of paclitaxel

In the second part, we used paclitaxel as a drug reference to treat the HeLa spheroids. Paclitaxel is a widely used drug against solid tumor such as ovarian, breast, prostate and lung cancer. [19] It is used as first-line single-agent therapy in cancer at dose of 250 mg/m2 by IV over 3 hours for human cervical cancer every 3 weeks with 100% of bioavailability. [25] This drug acts at the microtubule level by inducing the polymerization of tubulin which in turn induces the inhibition of microtubules depolymerization and blocks the cell division in the late G2/M phase of the cell cycle. [20]

To determine the concentration of paclitaxel needed for our experiment, we have based our test on literature. However, paclitaxel treatment on 3D cell culture was not well characterized as most information found was for 2D HeLa cell culture. [26]

Previous studies using paclitaxel and HeLa cells, tested within a range of 50 to 500 nM, resulted in a loss of viability dependent on the concentration and time of exposure to the drug. [27] The phenomenon observed was associated with a typical nuclear morphology of apoptosis and DNA breakage into fragments, suggesting apoptotic blebs. [28]

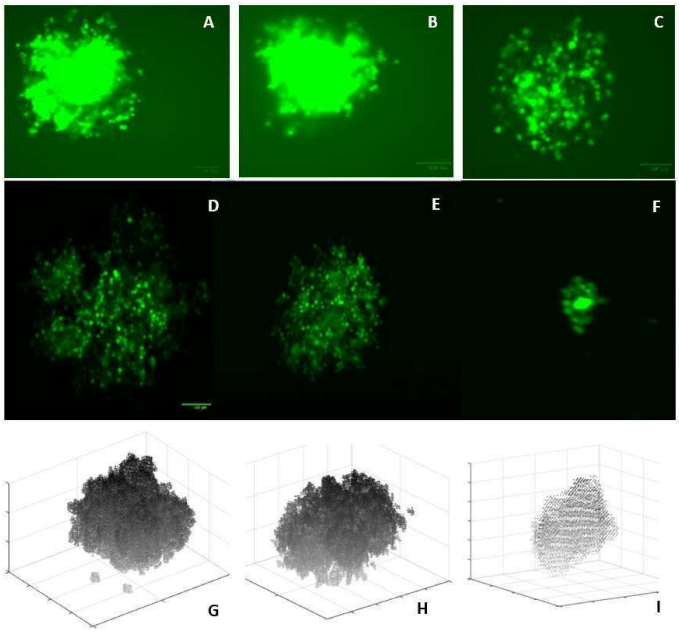

Figure 6: Visualization of DMEM (A, D, G), DMSO (positive control) (B, E, H) and paclitaxel 250 (C, F, I) of spheroids HeLa cells tagged YFP at J114 after transfection. Visualized under Wide Field Microscope (A, B, C). Z projection of all obtained from ICY (D, E, F). Spheroids volume estimation from ReViMS (G, H, I).

Yang, C. P., and Horwitz, S. [29] described different concentrations of paclitaxel used on 2D cell culture. Low concentrations of paclitaxel (5-10 nM) caused mitotic delay and checkpoint defects and high concentrations (20-50 nM) resulting in a mitotic block. As paclitaxel was not used on 3D HeLa cell models, paclitaxel concentration was based on human colon carcinoma cells (HCT116). Indeed, Shi, W. *et al* [30] found that a concentration of 500 nM of paclitaxel on 500 µm HCT116 spheroids for 72h disintegrate the

spheroids. Knowing that, 250 nM of paclitaxel was chosen to treat HeLa spheroids of 400 µm in order to have a high concentration with visible effect without disintegrating the spheroids.

The images of spheroids using DMEM and DMSO as controls showed approximative same shape and volume size with a dense structure (Figure 6 A, B, D, E). However, spheroids treated with paclitaxel showed a significant decrease in the density of cells and shape compared to the control groups (Figure 6 D, E, F). Spheroids seem to have been partially disintegrated by paclitaxel treatment, this observation might be due to an experimental mistake during the spheroid generation causing an initial size smaller than expected. (Figure 6 C, F, I)

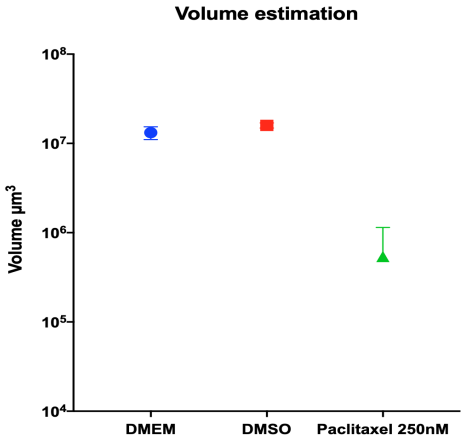

Figure 7: Volume estimation with ReViMS of spheroids after 48h of incubation and 24h of treatment with DMEM (blue), DMSO (red) or paclitaxel 250 nM (green). Results show the average volume of triplicates. Y axis in a log scale.

Volume estimations made by ReViMS are compared on the Figure 7. As previously explained, spheroids were smaller than expected (actual theoretical diameter estimated between 200 and 300 µm).

Because of this, several spheroids treated with paclitaxel were disintegrated. Our hypothesis is that the concentration of paclitaxel used was not optimal for this size of spheroid. The graph compares the volume of spheroids in triplicate after 48h of treatment (DMEM, DMSO and paclitaxel 250 nM). Volume of DMSO and DMEM treated spheroids are quite similar meaning that the DMSO has no effect on the spheroid growth. There is a significant difference for the volume of spheroids treated with paclitaxel and non-treated. Indeed, the volume of spheroids treated with paclitaxel decreases by a factor 10 compared to DMEM and DMSO. The effect of paclitaxel is well observed with this experiment. This experiment should be repeated with the good size of spheroids and several times to obtain statistical results.

DISCUSSION

Different parts of the protocol have been optimized. The agarose embedding technique that was set up is simple, fast and easy to handle for microscope observation. The comparison between clarified and non-clarified spheroids demonstrated the need for clarification which has been made with ECI due to its low cost and efficiency, the ability to preserve fluorescence and its simple handling.

The use of 3D petri dish for spheroid generation is simple, reproducible, inexpensive and fast technique but can be discussed regarding the biological process of the spheroid formation. Indeed, in this technique spheroids are formed by an aggregate of cells which create interactions between them because of the non-adhesive properties of the matrix. However, it exists more representative tumor models that could be performed using other spheroid generation techniques starting from a single cell that in turn forms the spheroid after proliferation. These other techniques might be representing a more representative tumor model compared to the 3D petri dish technique, with a proliferation closer to *in vivo* tumor. [2]

The discrepancy between volume estimations is due to the fact that the segmentation of spheroid images allows a better precision of the estimation as it takes into account the whole volume stack by stack compared to calculation using diameter volume formula. Therefore, ReViMS can be considered as more accurate for the estimation of volume of spheroids because all the differences in structure and size are taken into account thanks to the modeling of a 3D volume using the segmented images. In addition, the observation revealed a non-sphericity shape of spheroids and drug treatment could alter the shape of spheroid. [2]

We conclude that the volume must be calculated by ReViMS software to have the most accurate volume allowed by the segmentation treatment. For purpose of repeatability and simplicity of visualization and manipulation, spheroids with a theoretical diameter of 400 µm were generated in these experiments and should be used for further experiments of drug screening assay.

Paclitaxel concentration was based on literature about 2D HeLa cell culture and 3D cell culture of another cell type. The concentration was chosen to have a severe effect on spheroid while maintaining integrity. However, due to a manipulation error, spheroids were smaller than expected and the concentration of paclitaxel was destined for a higher size of spheroid and therefore was supposed to be a slightly too high for this size of spheroid. Further experiment is required to test this concentration with the good theoretical size of spheroid and a kinetic of concentration and time could be realized to get the most accurate results.

Once paclitaxel concentration will be optimized, the introduction of specific markers to study drug effects on spheroids should also be studied. For example, the treatment of spheroid with the combination of propidium iodide and annexin V could inform on the penetration of paclitaxel into spheroids. The paclitaxel is known to induce cell apoptosis [29] and annexin V allows to detect apoptotic cells. The use of this marker could reveal cells affected by paclitaxel and the penetration of paclitaxel into the spheroid. Indeed, we could see if the apoptosis is induced only for peripheral cells or also inside the spheroid. [31] We are not yet sure that paclitaxel penetrated into the spheroid or stayed at its surface. The use of propidium iodide/annexin V could verify this hypothesis. [32]

Moreover, another drug treatment could be carried out afterwards to verify the validity of the screening. 5-fluorouracil is one of the most widely used anti-tumor drug and its mechanism is known to affect the synthesis of DNA. This drug could be studied and used for a drug screening on other cell lines. [33] This experiment would allow to verify if our screening drug protocol can be transposed to other cell types and drugs.

ACKNOWLEDGMENTS

The authors are liable to Professor Elise Delage for continuous supervision, encouragement and valuable criticism of the protocols on the study and for LSFM learning. Leonard Raimbault and Estelle Zhang contributed to protocol and experiments in clearing techniques and spheroid generation. The assistance of Léonard Raimbault for the use of ReViMS software was helpful to carry out image processing. The assistance of Mrs Perdiz for spheroid generation, and Elise Delage for HeLa cell thawing and culture was greatly appreciated.

REFERENCES

[1] Duval, K., Grover, H., Han, L. H., Mou, Y., Pegoraro, A. F., Fredberg, J., & Chen, Z. (2017). Modeling physiological events in 2D vs. 3D cell culture. Physiology, 32(4), 266-277.

[2] Zanoni, M., Piccinini, F., Arienti, C., Zamagni, A., Santi, S., Polico, R., ... & Tesei, A. (2016). 3D tumor spheroid models for in vitro therapeutic screening: a systematic approach to enhance the biological relevance of data obtained. *Scientific reports*, *6*, 19103

[3] Breslin, S., & O'Driscoll, L. (2013). Three-dimensional cell culture: the missing link in drug discovery. *Drug discovery today*, *18*(5-6), 240-249.

[4] Pampaloni, F., Reynaud, E. G., & Stelzer, E. H. (2007). The third dimension bridges the gap between cell culture and live tissue. *Nature reviews Molecular cell biology*, *8*(10), 839.

[5] Kapałczyńska, M., Kolenda, T., Przybyła, W., Zajączkowska, M., Teresiak, A., Filas, V., ... & Lamperska, K. (2018). 2D and 3D cell cultures–a comparison of different types of cancer cell cultures. Archives of medical science: AMS, 14(4), 910.

[6] Ghosh S, Spagnoli GC, Martin I, et al. Three-dimensional culture of melanoma cells profoundly affects gene expression profile: a high-density oligonucleotide array study. J Cell Physiol. 2005; 204:522–31.

[7] Berthiaume F, Moghe PV, Toner M, Yarmush ML. Effect of extracellular matrix topology on cell structure, function, and physiological responsiveness: hepatocytes cultured in a sandwich configuration. FASEB J. 1996; 10:1471–84.

[8] Hamburger A, Salmon SE. Primary bioassay of human tumor stem cells. Science 1977; 197: 461-3.

[9] Piccinini, F., Tesei, A., Arienti, C., & Bevilacqua, A. (2015). Cancer multicellular spheroids: volume assessment from a single 2D projection. Computer methods and programs in biomedicine, 118(2), 95-106

[10] Huisken, J., & Stainier, D. Y. R. (2009). Selective plane illumination microscopy techniques in developmental biology. Development, 136(12), 1963-1975. https://doi.org/10.1242/dev.022426

[11] Reynaud, E. G., Kržič, U., Greger, K., & Stelzer, E. H. (2008). Light sheet-based fluorescence microscopy: more dimensions, more photons, and less photodamage. HFSP journal, 2(5), 266-275.

[12] Lim, J., Lee, H. K., Yu, W., & Ahmed, S. (2014). Light sheet fluorescence microscopy (LSFM): past, present and future. Analyst, 139(19), 4758-4768

[13] Sigma Aldrich. (2018). The 3D Petri Dish ® A New Cutting-Edge Culture Format.

[14] Mathews Griner, L. A., Zhang, X., Guha, R., McKnight, C., Goldlust, I. S., Lal-Nag, M., … Ferrer, M. (2016). Large-scale pharmacological profiling of 3D tumor models of cancer cells. Cell Death & Disease, 7(12), e2492–e2492. doi: 10.1038/cddis.2016.360

[15] Klingberg, A., Hasenberg, A., Ludwig-Portugall, I., Medyukhina, A., Männ, L., Brenzel, A., ... & Gunzer, M. (2017). Fully automated evaluation of total glomerular number and capillary tuft size in nephritic kidneys using lightsheet microscopy. Journal of the American Society of Nephrology, 28(2), 452-459.

[16] Richardson, D. S., & Lichtman, J. W. (2015). Clarifying tissue clearing. Cell, 162(2), 246-257

[17] Piccinini, F., Tesei, A., Zanoni, M., & Bevilacqua, A. (2017). ReViMS: Software tool for estimating the volumes of 3-D multicellular spheroids imaged using a light sheet fluorescence microscope. *BioTechniques*, *63*(5), 227-229.

[18] Gey, G. (1952). Tissue culture studies of the proliferative capacity of cervical carcinoma and normal epithelium. *Cancer Res.*, *12*, 264-265.

[21] Alix, E. (2010). Nouveaux fixateurs en anatomie pathologique.

[22] Haji-Karim, M., & Carisson, J. (1978). Proliferation and viability in cellular spheroids of human origin. Cancer research, 38(5), 1457-1464

[23] Becker, K., Jährling, N., Saghafi, S., Weiler, R., & Dodt, H. U. (2012). Chemical clearing and dehydration of GFP expressing mouse brains. *PloS one*, *7*(3), e33916.

[24] Richardson, D. S., & Lichtman, J. W. (2017). SnapShot: tissue clearing. Cell, 171(2), 496-496.

[25] Cancer therapy advisor, (2017), Cervical cancer treatments régiment, available on https://www.cancertherapyadvisor.com/gynecologic-cancer/cervical-cancer-treatment-regimens/article/218139/

[26] Schiff, P. B., & Horwitz, S. B. (1980). Taxol stabilizes microtubules in mouse fibroblast cells. Proceedings of the National Academy of Sciences of the United States of America, 77(3), 1561-1565

[27] Risinger, A. L., & Mooberry, S. L. (2011). Cellular studies reveal mechanistic differences between taccalonolide A and paclitaxel. *Cell Cycle*, *10*(13), 2162-2171.

[28] Maldonado, V., De Anda, J., & Meléndez-Zajgla, J. (1996). Paclitaxel-induced apoptosis in HeLa cells is serum dependent. Journal of biochemical toxicology, 11(4), 183-188.

[29] Yang, C. P., & Horwitz, S. (2017). Taxol®: the first microtubule stabilizing agent. International journal of molecular sciences, 18(8), 1733.

[30] Shi, W., Kwon, J., Huang, Y., Tan, J., Uhl, C. G., He, R., Liu, Y. (2018). Facile Tumor Spheroids Formation in Large Quantity with Controllable Size and High Uniformity. Scientific Reports, 8(1). https://doi.org/10.1038/s41598-018-25203-3

[31] Liao, J., Qian, F., Tchabo, N., Mhawech-Fauceglia, P., Beck, A., Qian, Z., ... & Odunsi, K. (2014). Ovarian cancer spheroid cells with stem cell-like properties contribute to tumor generation, metastasis and chemotherapy resistance through hypoxia-resistant metabolism. PloS one, 9(1), e84941

[32] Qu, Y., Cong, P., Lin, C., Deng, Y., Li-Ling, J., & Zhang, M. (2017). Inhibition of paclitaxel resistance and apoptosis induction by cucurbitacin B in ovarian carcinoma cells. *Oncology letters*, *14*(1), 145-152.

[33] Que, W. C., Huang, Y. F., Lin, X. Y., Lan, Y. Q., Gao, X. Y., Wang, X. L., ... & Zhong, D. T. (2018). Paclitaxel, 5-fluorouracil, and leucovorin combination chemotherapy as first-line treatment in patients with advanced gastric cancer. Anti-Cancer Drugs.

Calibration of chromatography columns for the characterization of peptones

Paul-Etienne Fontaine, Amélie Raby*
Sup'Biotech, Villejuif, France

*Corresponding author: amelie.raby@supbiotech.fr
Tutors: Chloé Lezin, Sarah Rakotoasimbola (Organotechnie)

Abstract – Peptones are commonly used today in many applications of biotechnologies studies, as in drugs development to make cell culture media, or fungal fermentation for enzymes production. Those characterization are nowadays done by HPLC but it is expensive. For the first steps in the development of new products it could save time and money to have another mean to characterize the ratios composition of peptones. In literature, chromatography of exclusion on a large range of molecular weights can be achieved by decomposing the separation of peptones in two sequential chromatography. Then quantification of the total amino nitrogen present in the sample of mix peptones and in our different sample of size separated peptones. In this article we will focus on the first part of the global process, which determines the standard curve of both of our chromatography, in order to know the molecular weight of the peptones in function of the elution's fractions of the exclusion chromatography.

Index Terms – Characterization, Chromatography, Molecular weight, Peptones, Separation

INTRODUCTION

Founded in 1902, Organotechnie produces peptones from different sources (Soy flour, Wheat gluten, Casein, Beef heart, ...) for the pharmaceutical industry.

Peptones are derived from the partial digestion (hydrolysis) of proteins [1]. They are a source of oligopeptides and free amino acids mainly used in culture medium as a source of nitrogen and as growth factors.

As of today, most compositions are not exactly referenced, and are described as the percentage of a class size of components (from 150 Da to 15 000 Da). Those compositions are determined by the Quality Control Lab of the company using HPLC. However, the price and time required by this technique makes the application for the R&D service complicated. In addition to this, the samples are denatured after HPLC, so no further characterization for each fraction can be made. That is why it was chosen to work with two chromatography [2].

The objective of this article is to determine the possibility of a standard curve determination for both of our chromatography, in order to proceed to a separation of peptones according to their molecular weight.

Following the obtained results in this research, other experiments should be done especially in the determination of the total amino nitrogen in the tested samples and in each fraction. This part won't be detailed in this article.

MATERIALS AND METHODS

In order to obtain the standard curve representing the molecular weight in function of the volume of elution, we used two kinds of chromatography [3][4].

Before the column preparation, a step of degazing the matrix is necessary to avoid any air bubble during the separation.

First, the Sephadex G10 (GE17-0010-01 Sigma), which allows a separation between 0 to 700 Daltons, filled in a column of 28 cm which we calibrated using small known molecular weighted molecules. The Dextran Blue (2MDa) will determine the front lines of the chromatography and was put in trace quantity; the potassium hexanocianoferrate II (370Da) has a yellow color, facilitating the visibility of the migration and was also added in trace quantity, the di-peptide Glycine-Glycine (150Da) and the amino acid Glycine (75Da). The last two are both uncolored and were added in a final solution of 30mg/ml of each. Those markers were selected due to their detectability by spectrophotometer and by eyes and their placement in the range MW analyzed by both columns.

TABLE I
MARKERS, MOLECULAR WEIGHTS AND ATTRIBUTION TO THE COLUMNS.

Markers	*Molecular Weight*	*Used in columns*
Glycine	75 Da	G10
Gly-Gly	150 Da	
Potassium hexacyanoferrate(III)	368.35 Da	
Bacitracin	1 422 Da	G50
Insuline Beta	3495 Da	

Lactalbumine	14.1 kDa	
Myoglobine	16.7 kDa	
Dextran Blue	2.10^6	Both

Secondly, the Sephadex G50 (G5050 Sigma), allows a separation of molecule from 1500 Daltons to 30 000 Daltons. The column was filled at 24 cm. For the calibration, the molecules used here had another molecular weight range. The Dextran Blue (2MDa) again to determine the front lines of the chromatography, was added in trace quantity. Myoglobin (16.7Da) with a red color was added with a concentration of 30mg/ml, Lactalbumine (14.1Da) and Bacitracin (1422Da) were both at a concentration of 30mg/ml. Insulin Beta Chain (3495.8 Da) was put in our solution with a final concentration of only 1mg/ml because we had to keep in mind its high price.

When both of our mix were made at the concentrations told above, we deposed 1 or 2 ml of each mix in the corresponding columns, and we waited until all the mix were absorbed by the Sephadex before adding Phosphate Buffer Saline 1X (PBS 1X) to proceed the elution. The volume before the Dextran blue elution was kept for both column in order to determine the Dead volume of our chromatography. To avoid the degradation of the matrices and cracks in the columns, we were careful of never let them dry. Then fractions were collected each 0.5ml in 70 fractions for the G10, and around 290 fractions for the G50.

The analysis of the fractions was made using a Spectrophotometer at 280nm for the fractions from the G50 column, and at 220nm for the G10 column.

Those optic density permitted us to draw the chromatograph of our chromatography which will allow us to create a standard curve of those matrices.

RESULTS

After several chromatography which failed due to our lack of knowledge about this technique, we finally managed to obtain a full chromatography from both of our columns.

The G10 chromatography shows 4 peaks representing our 4 known molecules. The Dextran Blue was eluted in first in the fraction number 5, which is logical because its molecular weight is around 2 millions Daltons and way bigger than the limit of the column. Then the Myoglobin was eluted in the fraction 25, which seems coherent with its molecular weight of 16700 Daltons. We were sure about those two molecules thanks to their colors. The last two molecules were the Insulin Beta Chain and the Bacitracin which were not detected at 280 nm so we decided to test at 220 nm if it was possible to detect them, and we obtained a peak at the fractions 52 representing the Insulin Beta Chain and a small ledge which we extrapolated to be the Bacitracin (FIG1).

Using this graph, we were able to determine the molecular weights of the eluted molecules in function of the fraction number. Using the known molecular weight and the fraction number we were able to create a standard curve. The range of our molecules were too wide to obtain a linear curve, to compensate this problem we decided to change the scale of the abscissa axis into a logarithmic one (FIG2) this logarhithmic transformation were made using the conversion system present in the Excel software. Our results are almost linear and we clearly obtained a linear trend. This validated our experiments and could allow us to collect the peptones at

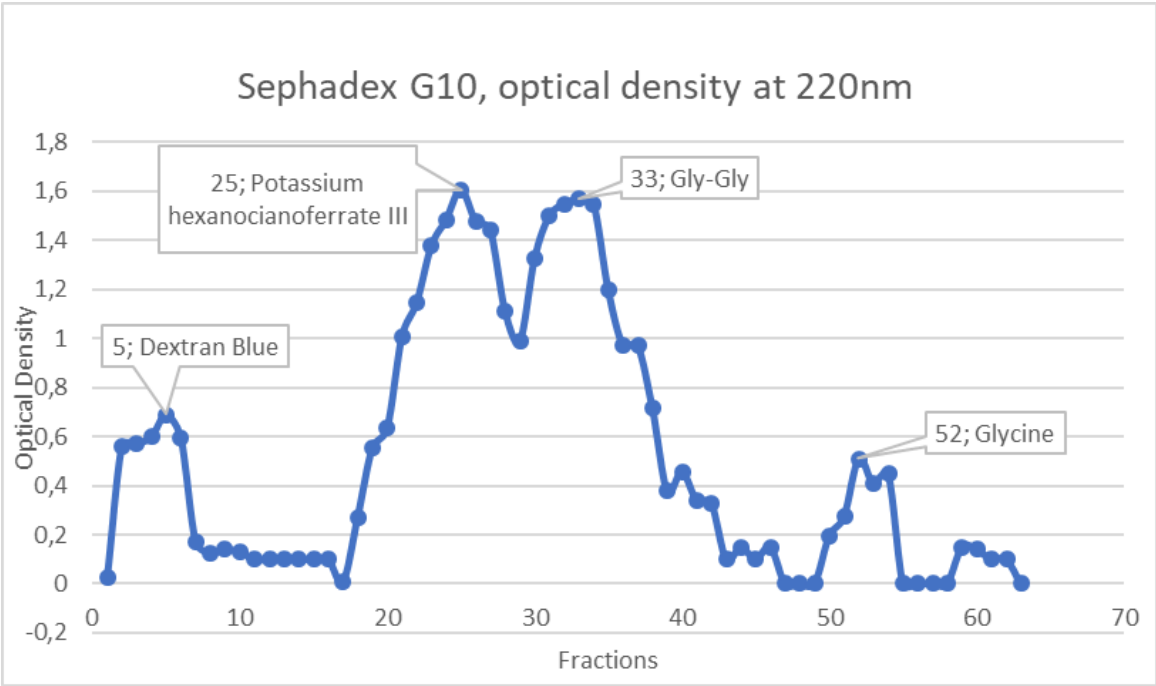

FIGURE 1
CHROMATOGRAPH REPRESENTING THE ELUTION FRACTIONS (ABSCISES) IN FUNCTION OF THE OPTICAL DENSITY (ORDINATE) OF THE COLUMN SEPHADEX G10

a specific molecular weight just by choosing the corresponding fraction on the standard curve.

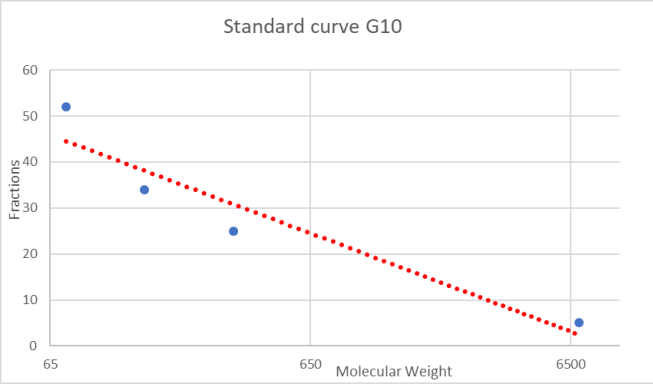

FIGURE 2
STANDARD CURVE OF THE COLUMN SEPHADEX G10, REPRESENTING THE CORRELATION BETWEEN ELUTION FRACTION (ORDINATE) AND MOLECULAR WEIGHT (ABSCISES) WITH A LOGARITHMIC SCALE

The graph of the optical density after the G50 chromatography reveals 4 peaks. On this graph 2 curves were drawn because the concentration of the Insulin Beta chain and the Bacitracin was too high for exploitable OD reading. A dilution was realized to have the second curve (orange) on those fractions. The first molecule to be eluted is Dextran Blue because of its high molecular weight. We could visualize the blue color in the collected fractions corresponding to the peak. Then the next molecule to be eluted is Myoglobin. This time again the red color was visible with the naked eye even if it was very faint. Those fractions correspond to the second peak on the blue curve. On the blue curve a slump is observed after the 50th fraction. The number reported after optical density lecture were outside of the exploitable range of 0-1 and the fractions concerned were diluted 1/10 to get back to readable and exploitable values, this dilution factor was decided because de optical density were around 10 time more important than the exploitable range of the spectrophotometer.

Using the same procedure as used for the G10 column, we extracted the data from the chromatograph and drew a standard curve representing the fractions corresponding to the molecular weight. We obtained an almost perfect linear correlation which is what we expected (FIG 4).

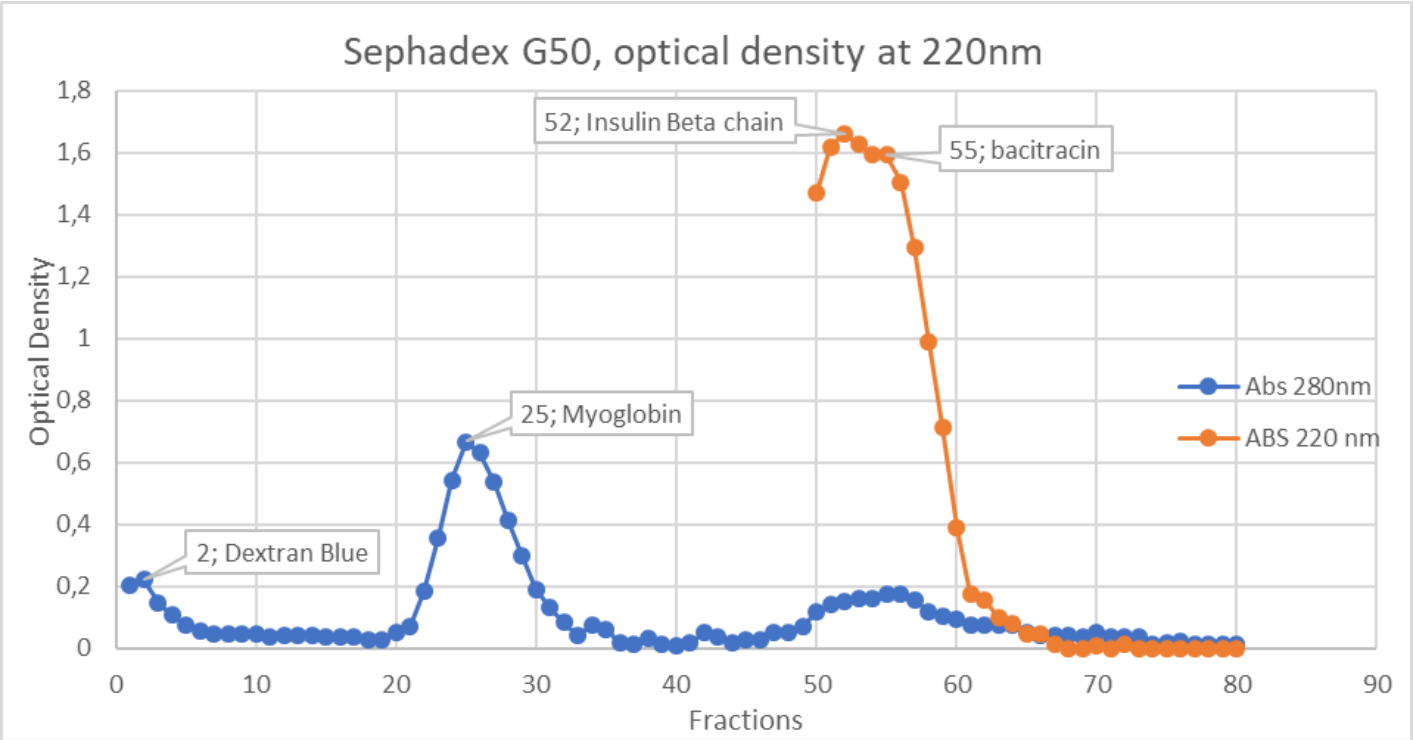

FIGURE 3
CHROMATOGRAPH REPRESENTING THE ELUTION FRACTIONS (ABSCISES) IN FUNCTION OF THE OPTICAL DENSITY (ORDINATE) OF THE COLUMN SEPHADEX G15

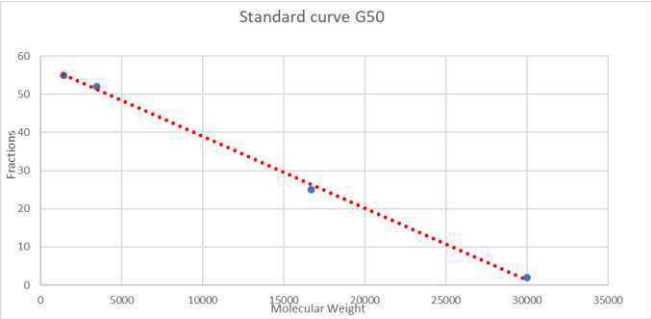

FIGURE 4
STANDARD CURVE OF THE COLUMN SEPHADEX G50, REPRESENTING THE CORRELATION BETWEEN ELUTION FRACTIONS (ORDINATE) AND MOLECULAR WEIGHTS (ABSCISES) WITH A LOGARITHMIC SCALE

DISCUSSION AND PERSPECTIVES

Our results are promising in the development of peptones' first characterization for research on new candidates' products. Yet several aspects are in need of further experiment to ensure that this method can be validated and used on a daily basis at Organotechnie Research and Development laboratory.

The people who will continue the project would have to do a calibration curve in the same conditions than our final experiment; then put in the system a sample of peptones known characteristics. A comparison with the characterizes sheet and the results of our method should be done. This validation would be the last step to the proof of concept of the proposed method.

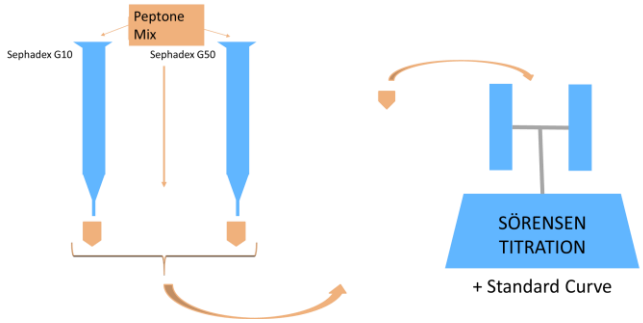

FIGURE 5
SCHEME OF THE GLOBAL PRINCIPLE TO VALIDATE OUR EXPERIMENTS

In the case of peptone samples, after the chromatography the samples will have to undergoes a Sorensen Titration [5] and not a standard DO lecture (FIG 5). This titration technique can measure the content of amino azote in a solution. This amino azote is the function present at the end of each peptone fragment and will represent the number of peptones. By calculating a yield between the amino azote in the different fractions and the total amino azote in the whole sample, a relation could be established to the usual characteristic sheet of the peptones.

Before its everyday use, the automatization of the method is already a problem that was discussed. Indeed, our method is time consuming. The use of an automated snail collector and a pump that would drop buffer at the top of the column in order to keep the column wet and to regulate the velocity of the column flow is still being discussed. With the same mindset, the OD measurement could be done through a micro-plate UV. This optimization can enhance the reproducibility and the precisions of the results and improve our method of peptones characterization.

ACKNOWLEDGMENT

Many thanks to our tutors at Organotechnie, Chloé Lezin and Sarah Rakotoasimbola and also a sincerely thank you to the tutors of the other groups Agnes Saint-Pol, Jaqueline Bert Franck Yates, Rafika Jarray and Valentina Gligorijevic who answered our everyday questions in the laboratory and guided us in our project.

REFERENCES

[1] V. K. Pasupuleti and A. L. Demain, Eds., *Protein Hydrolysates in Biotechnology*. Dordrecht: Springer Netherlands, 2010.

[2] P. Hong, S. Koza, and E. S. P. Bouvier, "Size-Exclusion Chromatography for the Analysis of Protein Biotherapeutics and their Aggregates.," *J. Liq. Chromatogr. Relat. Technol.*, vol. 35, no. 20, pp. 2923–2950, Nov. 2012.

[3] F. Touraine, G. Brulé, J. Maubois, and rr Maubois, "Séparation chromatographique de peptides issus de l'hydrolyse enzymatique de protéines de lactosérum et de caséines Séparation chromatographique de peptides issus de l'hydrolyse enzymatique de protéines de lactosérum et de caséines *," 1987.

[4] I. Lascu, "Chromatographie d'exclusion par la taille Size Exclusion Chromatography (SEC)," *http://lascu.free.fr/*. [Online]. Available: http://lascu.free.fr/Purification/Volume 3_SEC_2017.pdf. [Accessed: 15-Dec-2018].

[5] W. H. Taylor, "Formol titration: an evaluation of its various modifications," *Analyst*, vol. 82, no. 976, p. 488, Jan. 1957.

Laboratoire partenarial Sup'Biotech
CEA- Service d'Etude des Prions et Infections Atypiques (SEPIA)
Bâtiment 60 – 1er étage

Vous êtes intéressé par l'imagerie en 3D ?

Notre microscope à feuillet de lumière n'attend que vous !

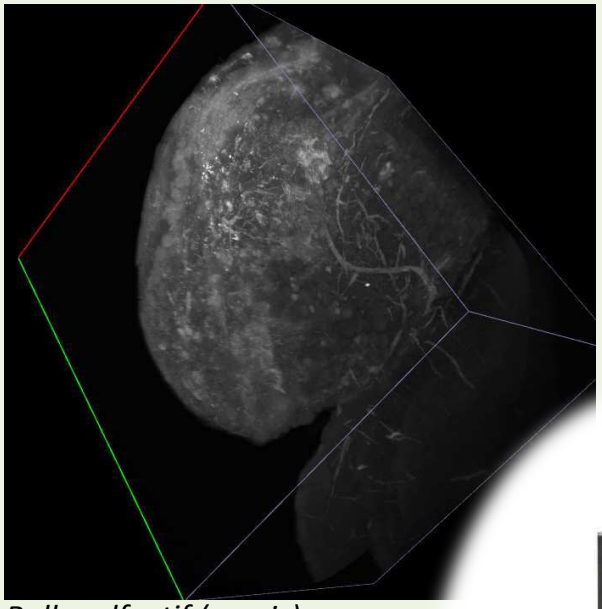

Bulbe olfactif (souris)

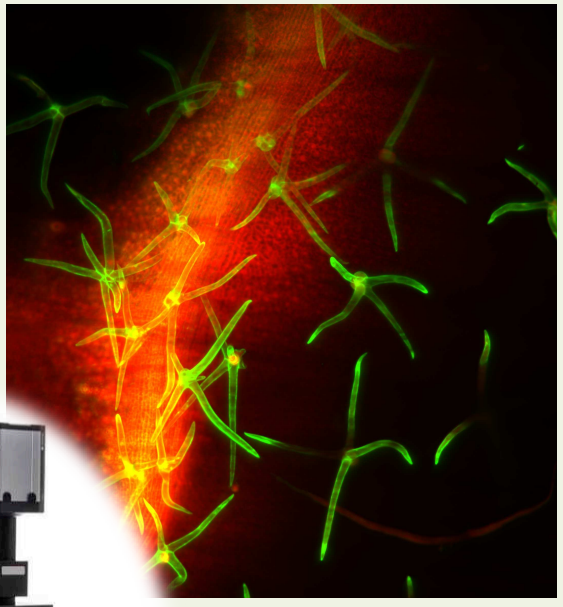

Trichomes de lierre

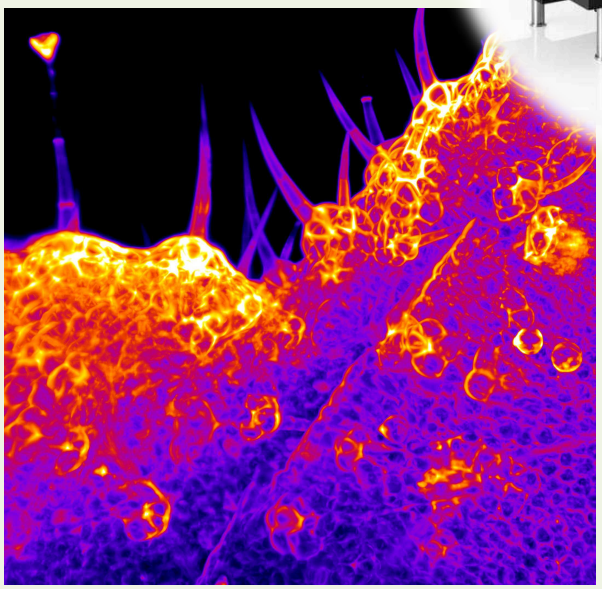

Epiderme de géranium)

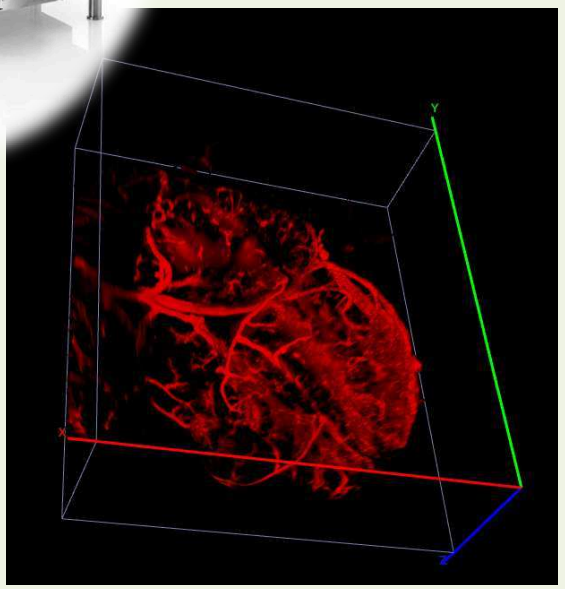

Vasculature du cerveau (souris)

Notre site internet: **http://recherche.supbiotech.fr/imagerie3D**

Pour tout renseignement, écrivez-nous!
elise.delage@supbiotech.fr

SUP biotech
PARIS

Sup'Biotech Projects Journal

Sup'Biotech
Ecole d'ingénieurs
66, rue Guy Moquet
94800 Villejuif

Service recherche
http://recherche.supbiotech.fr

Service des laboratoires d'enseignement
estelle.mogensen@supbiotech.fr